

SECTION 6

UCB REPORTS

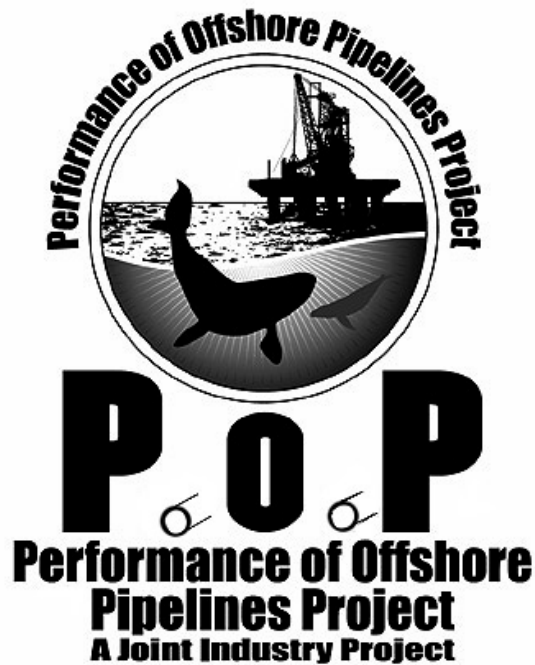
INDEX – UCB REPORTS

- Report 1 - Analyses Of Experimental Databases On The Burst Pressure of Corroded Pipelines - May 2002
- Report 2 - Burst Pressure Analyses Before Field Test - November 9, 2001
- Report 3 - Spring 2001 Report
- Report 4 - POP Project Meeting - March 2, 2001
- Report 5 - Fall 2000 Report - January 2001
- Report 6 - Performance Of Offshore Pipelines (POP) Project - UCB MTMG Tasks

SUB SECTION 6

REPORT 1

Analyses Of Experimental Databases On The Burst Pressure Of Corroded Pipelines May 2002



***ANALYSES OF EXPERIMENTAL DATABASES
ON THE BURST PRESSURE OF CORRODED
PIPELINES***

Performance of Offshore Pipelines (POP)

by

Professor Robert Bea

Graduate Student Researcher Elizabeth Schreiber

Marine Technology & Management Group

Department of Civil & Environmental Engineering

University of California Berkeley

May 2002

Table of Contents

1	Introduction	6
1.1	Laboratory Test Database	6
1.2	Model Bias	6
1.3	Approach	6
2	Remaining Strength Criteria	7
2.1	Classes of Defects	7
2.2	Two categories of remaining strength criteria for defects	7
3	When is Repair Necessary?	8
4	Risks	8
5	Fitness for Purpose	9
5.1	Procedure	9
6	Background Information on New Analytical Methods	10
6.1	British Standard	10
6.1.1	Purpose	10
6.1.2	Corrosion Flaws detected	10
6.1.3	Limitations	11
6.1.4	Factors of Safety	11
6.1.5	Safe working pressure calculation	12
6.1.5.1	Single Flaws	12
6.1.5.2	Interaction between flaws	12
6.2	API 579	13
6.2.1	Local Metal Loss	13
6.2.2	Limitations	13
6.2.3	Data Required	13
6.2.4	Level 1 Assessment	14
6.2.4.1	Procedure	14
6.2.5	Level 2 Assessment	14
6.2.5.1	Procedure	14
6.2.6	Level 3 Assessment	15

6.2.6.1	Procedure	15
6.3	Rstreng (Remaining strength of corroded pipe)	16
6.3.1	Background	16
6.3.2	Criterion	16
6.3.3	Software Applicability	16
6.3.4	Advantages of Rstreng over B31G	17
6.3.5	Rstreng Assessment	18
7	Background on Existing Analytical Models	19
7.1	ASME B31-G	19
7.1.1	Equation	19
7.1.2	Limitations	19
7.1.3	Use	20
7.2	Det Norske Veritas RP-F101, Corroded Pipelines, 1999	20
7.2.1	Equation	20
7.2.2	Limitations	21
7.2.3	Use	21
7.3	ABS Formulation	21
7.3.1	Equation	21
7.3.2	Use	22
7.4	RAM PIPE #1 (SMYS)	22
7.4.1	Equation	22
7.4.2	Use	23
7.5	RAM PIPE #2 (SMTS)	23
7.5.1	Equation	23
7.5.2	Use	23
7.6	RAM PIPE #3 (UTS)	24
7.6.1	Equation	24
7.6.2	Illustration	24
8	Bias Definition	25
8.1	Bias Equation	25
9	Populations	26

<u>10</u>	<u>Working with the Database</u>	27
<u>10.1</u>	<u>Existing Database</u>	27
<u>10.2</u>	<u>Recent Additions to the database</u>	28
<u>10.3</u>	<u>Information contained in the Database</u>	28
<u>11</u>	<u>Procedure for Analysis</u>	29
<u>12</u>	<u>Results & Conclusions from Entire Database Analysis</u>	30
<u>13</u>	<u>Results & Conclusions from Natural Corrosion</u>	31
<u>13.1</u>	<u>Varying d/t ratios</u>	32
<u>13.2</u>	<u>Varying L/w ratios and d/t in a certain range</u>	32
<u>14</u>	<u>Results & Conclusions from Machined Corrosion</u>	32
<u>14.1</u>	<u>Varying d/t ratios</u>	33
<u>14.2</u>	<u>Varying L/w ratios and d/t in a certain range</u>	33
<u>15</u>	<u>Cumulative Distribution Plots</u>	33
<u>16</u>	<u>General Conclusions/Observations</u>	35
<u>17</u>	<u>References</u>	36
<u>18</u>	<u>Appendix</u>	37
<u>18.1</u>	<u>Appendix A</u>	37
<u>18.2</u>	<u>Appendix B</u>	38
<u>18.3</u>	<u>Appendix C</u>	39
<u>18.4</u>	<u>Appendix D</u>	40
<u>18.5</u>	<u>Appendix E</u>	41
<u>18.6</u>	<u>Appendix F</u>	42
<u>18.7</u>	<u>Appendix G</u>	43
<u>18.8</u>	<u>Appendix H</u>	44
<u>18.9</u>	<u>Appendix I</u>	45
<u>18.10</u>	<u>Appendix J</u>	46
<u>18.11</u>	<u>Appendix K</u>	47
<u>18.12</u>	<u>Appendix L</u>	48
<u>18.13</u>	<u>Appendix M</u>	49
<u>18.14</u>	<u>Appendix N</u>	50
<u>18.15</u>	<u>Appendix O</u>	51

<u>18.16</u>	<u>Appendix P</u>	52
<u>18.17</u>	<u>Appendix Q</u>	53
<u>18.18</u>	<u>Appendix R</u>	54

1 Introduction

1.1 Laboratory Test Database

The MTMG test database is composed of 151 burst pressure tests on corroded pipelines. These data points were collected in conglomeration with the AGA, NOVA, British Gas, DNV, Petrobras and the University of Waterloo. 47 of those tests were used to develop criterion for the B31G formulation. The other 86 were pipe sections removed from in service, corroded pipe.

DNV conducted 12 tests that involved machined defects, internal pressure and bending and axial loading. These tests were also added to the existing database and used in our analysis. Also, 7 tests done by Petrobras that involved induced defects were added to the database as well.

1.2 Model Bias

Bias is the measure of predicted versus actual burst pressures. For each of the tests we will exam, a mean bias will be determined as well as a median and coefficient of variation of the bias. A statistical distribution model will be created to illustrate the ‘best fit’ model.

1.3 Approach

First, all the test data will be analyzed. Then, natural corrosion and machined corrosion features will be analyzed separately. All 7 prediction models will be used. Then machined and natural features will be analyzed for different ranges of feature characteristics of d/t of the following:

1. 0.0 to 0.4
2. 0.4 to 0.8
3. 0.8 to 1.0

Similarly, the database will be analyzed with different L/W ranges as follows:

1. 0 to 2
2. 2 to 4
3. 4 and greater

This accounts for a total of 15 sets of analysis done using 7 prediction models.

2 Remaining Strength Criteria

In the paper written by Stephens and Francini, it presents an overview of how some criteria in corrosion models may appear to be excessively conservative. However, in the Rstreng model, the authors point out that some of the conservatism has been taken out. Rstreng is useful and may eliminate some unnecessary repairs.

2.1 Classes of Defects

In the past, corrosion defects have been assumed to have failed in plastic collapse. It is this criteria that has been at the source of some of the conservatism in corrosion models. More recently, it has been discovered that the strength of defects is controlled not through failure due to plastic collapse, but instead by the material ultimate strength. This results in a lower value of the flow stress than previously thought. The new criteria for models such as Rstreng is now based on the ultimate tensile strength. This has seemed to work well in pipes that are of moderate to high toughness. However, there are problems that can be encountered when testing defects in pipe that are tested below the brittle-ductile transition temperatures. Sometimes this proves to be unreliable and not conservative enough.

2.2 Two categories of remaining strength criteria for defects

There are now two classifications of remaining strength criteria. The first classification is for empirically calibrated criteria. This criteria has been adjusted to be conservative. The second type of classification is for plastic collapse criteria. This is used for moderate to high toughness pipe and can not be applied to low toughness pipe. This criteria is based on ultimate strength.

Reference: Stephens and Francini

3 When is Repair Necessary?

Corrosion features must be replaced when they cause the pipeline to operate below a safe level and no longer can produce a reliable operation. Hydro testing criteria defines the minimum factor of safety as:

Factor of Safety = Test Pressure/Operating Pressure

For a pipeline, this should be 72% of SMYS. This factor of safety is independent of the pipeline geometry, material properties and operating conditions.

As in most situations, there is not always necessarily a concrete answer on when the pipeline needs repair. Sometimes, methods may indicate that repair is necessary but actually, it may be able to be in service for a longer period of time. However, these guidelines give us a measure of when repairs are necessary. Combined with experience and engineering judgment, a decision on repair can be made.

4 Risks

To be effective, a pipeline must be operated safely and efficiently. There are four major classifications of risks that need to be analyzed for pipeline systems. They are as follows:

1. Safety
2. Security of supply
3. Cost effectiveness
4. Regulations

Safety must be analyzed in order to ensure that the system doesn't pose a threat to the surrounding area and population.

The security of supply is important to ensure that the system delivers its product continuously. The owner and the customer must be satisfied.

The cost must be such that it is attractive to the market. It must not be too high as to risk losing business in the future.

Regulations are very important. They must be followed and met. There must be an operator who assures the regulations are being met.

Reference: Cosham and Kirkwood

5 Fitness for Purpose

The fitness for purpose method required engineers to explore outside of the engineering codes. There is a procedure in which Cosham and Kirkwood describes that should be followed to assess fitness for purpose.

5.1 Procedure

1. Appraisal

- Is it really there or could it go away?
- Is it a defect or a mess?

- Can I do it?

2. Assessment

- Can fitness for purpose methods solve it?

3. Safety factors and probabilistic aspects

- What safety margins are needed?

4. Consequence

-What are the consequences of getting it wrong?

5. Reporting

-Who needs to know, and what details are needed?

Reference: Cosham and Kirkwood

6 Background Information on New Analytical Methods

6.1 *British Standard*

6.1.1 Purpose

The British Standard is a method, which gives us a way to measure the acceptability of loss in wall thickness caused by either internal or external corrosion. The calculated safe working pressure produced in this method was tested through finite element analysis and other small-scale testing. This method has been used for pipes that have been designed to a recognized code.

6.1.2 Corrosion Flaws detected

The assessment of the following corrosion flaws can be modeled using the British Standard:

1. internal corrosion
2. external corrosion
3. corrosion in the parent material
4. corrosion in or adjacent to longitudinal and circumferential welds
5. colonies of interacting corrosion flaws

Longitudinal and circumferential flaws can be applied to this procedure as well as long as there is no significant weld flaw present that may interact with the corrosion flaw and a brittle fracture is not likely.

6.1.3 Limitations

The following are limitations to the British Standard

1. materials with specified minimum yield strengths exceeding 550N/mm^2
2. values of $\sigma_y/\sigma_u > .9$
3. loading other than internal pressure above atmospheric
4. cyclic loading
5. sharp flaws
6. combined corrosion and cracks
7. corrosion in association with mechanical damage
8. metal loss flaws attributable to mechanical damage
9. fabrication flaws in welds
10. environmentally induced cracking
11. flaws in depths greater than 85% of the original wall thickness
12. corrosion at regions of stress concentration such as nozzles

The procedure is also not applicable when brittle fracture occurs. The following are examples of such a situation:

1. any material that has been shown to have a full-scale initiation transition temperature above the operating temperature
2. material of thickness 13mm and greater
3. flaws in mechanical joints
4. flaws in bond lines of flash welded pipe
5. lap welded pipe

6.1.4 Factors of Safety

The factors of safety used to determine a safe working pressure are:

1. a modeling factors, f_{c1}
2. an original design factor, f_{c2}

These two factors are multiplied to determine a total factor of safety, f_c .

6.1.5 Safe working pressure calculation

6.1.5.1 Single Flaws

The failure pressure of a pipe is calculated by:

$$P_o = 2B_o_{-u} / (D - B_o)$$

The length of the corrosion factor is:

$$Q_c = \sqrt{(1 + .31(l_c / \sqrt{DB_o}))^2}$$

The reserve strength factor is:

$$R_s = (1 - d_c / B_o) / (1 - d_c / B_o Q_c)$$

The failure pressure is calculated by:

$$P_f = P_o \times R_s$$

The safe working pressure is:

$$P_{sw} = f_c \times P_f$$

6.1.5.2 Interaction between flaws

Single flaw equations no longer apply when there is interaction between flaws. A flaw can be treated as isolated if it meets the following criteria:

1. its depth is less than 20% of the wall thickness
2. the circumferential spacing between adjacent flaws exceeds the angle given by:

$$\theta > 360 (3/\pi) \sqrt{(B_o/D)}$$

3. the axial spacing between adjacent flaws exceeds the value given by:

$$s > 2 \sqrt{(DB_o)}$$

The calculation of failures pressures for each flaw or composite as a single flaw is:

$$P_i = P_o [(-d_i/B_o) / (-d_i/B_o Q_i)]$$

Where $Q = \sqrt{(1 + .31(l_i / \sqrt{DB_o}))^2}$

The combined length of the corrosion flaws is:

$$L_{nm} = l_m + \sum (l_i + s_i)$$

The failure pressure is:

$$P_{nm} = P_o [(1 - d_{nm}/B_o) / (1 - d_{nm}/B_o Q_{nm})]$$

Where $Q_{nm} = \sqrt{(1 + .31(l_{nm}/\sqrt{DB_o})^2)}$

The safe working is calculated as:

$$P_{sw} = f_c \times P_f$$

The failure pressure is considered to be the pressure that causes the averaged stress in the specimen to be equal to the material's tensile strength from an uniaxial tensile test.

Errors could occur when using this model due to the application of incorrect constraints or using the wrong elements from analysis.

(Reference for the above section: Annex G of the British Standard Code)

6.2 API 579

This is an analytical method that determines the Fitness-For-Service for pressurized pipe resulting in metal loss in wall thickness due to corrosion. The thickness data is needed for analysis and assessment.

6.2.1 Local Metal Loss

Local metal loss can occur inside or outside of the element. Flaws characterized by local metal loss are:

1. Locally Thin Area-metal loss on the surface of the component
2. Groove-like flaw-grooves or gouges

6.2.2 Limitations

Limitations to the API analysis method apply if the following are not met:

1. The original design was not in accordance to code
2. The component is operating in the creep zone
3. The material doesn't have sufficient material toughness
4. The component is not in a cyclic service
5. The component does not have crack-like flaws

6.2.3 Data Required

To use the API analysis method, the following data is needed:

1. Thickness profiles of the region of local metal loss
2. Flaw dimensions

3. Flaw-To-Major Structural Discontinuity Spacing
4. Vessel Geometry Data
5. Materials Property Data

6.2.4 Level 1 Assessment

The level 1 assessment is used to in the situation where there is local metal loss and there is internal pressure.

6.2.4.1 Procedure

1. Determine critical thickness profiles:
 - a. D , inside diameter
 - b. FCA, Future corrosion allowance
 - c. G_r , radius at the base of the groove
 - d. L_{msd} , distance from the edge of the region of local metal loss
 - e. MAWP, maximum allowable working pressure
 - f. MFH, maximum fill height of the tank
 - g. RSF_a , allowable remaining strength factor
2. Determine required minimum thickness
3. Determine minimum measured thickness
4. Check limiting flaw criteria

6.2.5 Level 2 Assessment

Level 2 assessment targets the remaining strength factor. It identifies the weakest element.

6.2.5.1 Procedure

1. Determine critical thickness profiles
2. Calculate minimum thickness required
3. Determine the minimum measured thickness
4. Check the limiting flaw size criteria
5. Determine the remaining strength factor

6. Evaluate longitudinal extent of the flaw

6.2.6 Level 3 Assessment

Level 3 assess the remaining life due to metal loss. The remaining life approach can be used if the region of local metal loss is characterized by a single thickness.

6.2.6.1 Procedure

To determine remaining life, you can use an iterative approach.

$$RSF \leq RSF_a$$

$$R_t \leq t_{mm} - (C_{rate} \times \text{time}) / t_{min}$$

For a groove-like flaw use:

$$s \leq s + C_{rate}^s \times \text{time}$$

$$c \leq c + C_{rate}^c \times \text{time}$$

Where:

C_{rate} = anticipated future corrosion rate

C_{rate}^s = estimated rate of change of the length of the region of local metal loss

C_{rate}^c = estimated rate of change in the length of the region of local metal loss

c = circumferential length of the region of local metal loss

RSF = computed remaining strength factor

RSF_a = allowable remaining strength factor

R_t = remaining thickness ratio

s = longitudinal length of the region of the local metal loss

t_{min} = the minimum required thickness for the component

t_{mm} = the minimum remaining thickness determined at the time of inspection

time = time in the future

The remaining life determined using the thickness based approach can only be utilized if the region of the local metal loss is characterized by a single thickness.

Reference: Section 5-Assessment of Local Metal Loss, API guidelines

6.3 Rstreng (Remaining strength of corroded pipe)

6.3.1 Background

Rstreng was initially released in 1989. Over the years, the software has been developed to become more user friendly. The Rstreng analytical method provides a more accurate method of prediction than the B31G approach it was based upon. Rstreng uses the effective area method to assess the actual shape of the corrosion defect. The defect area for this calculation is assumed to be .85dL. Rstreng has been validated against 86 burst pressure tests. Any shape can be assessed. The defect can be a single or composite defect interaction. Rstreng was developed as by the American Gas Association.

6.3.2 Criterion

The probability of failure is calculated as:

$$Pf = 2t/D (\sigma_{yield} + 10,000)[1 - .85(d/t)/1 - .85(d/t)M_{t2}^{-1}]$$

$$\text{For } L^2/Dt < 50 : M_{t2} = \sqrt{(1 + .6275 L^2/Dt (.003375) L^4/D^2/t^2)}$$

The Rstreng software computes the failure pressure based on 16 possible defect geometries and reports the lowest failure prediction as the result.

Reference: Kiefner and Vieth 1989

6.3.3 Software Applicability

Rstreng was developed to eliminate the excess conservatism that is incorporated in the B31G equation. This software hopefully will eliminate unnecessary pipe replacements. Rstreng permits metal loss of a greater size to remain in service at the maximum

operating pressure. This criterion will require less pressure reduction to maintain an adequate margin of safety.

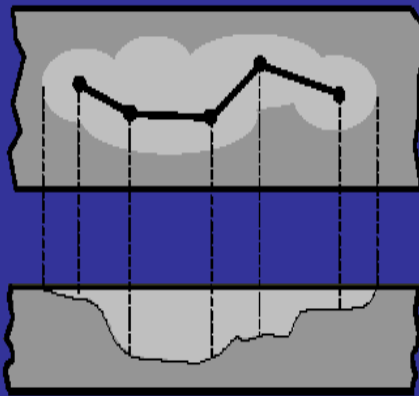
6.3.4 Advantages of Rstreng over B31G

1. Rstreng was developed to eliminate excess conservatism
2. Rstreng permits the determination of metal loss that can safely remain in service at the maximum operating pressure

6.3.5 Rstreng Assessment

Detailed RSTRENG Assessment

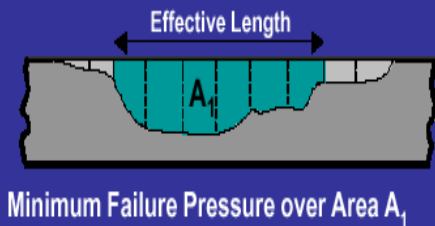
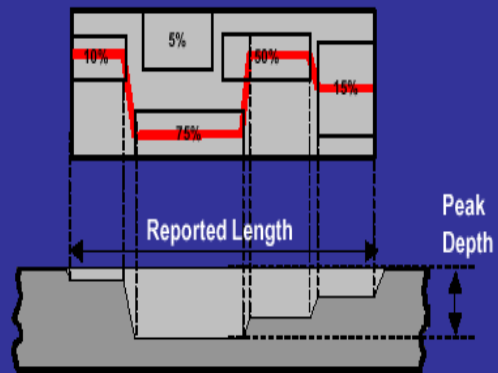
Field Measurements



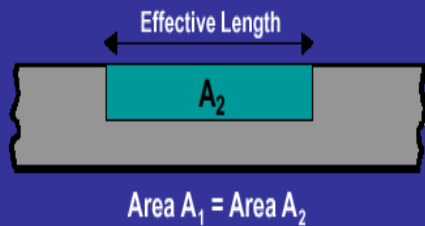
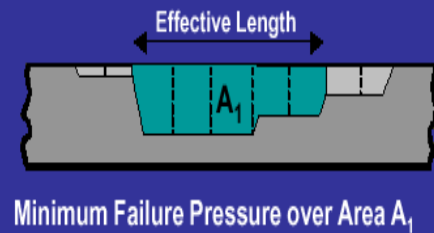
Corrosion
Plan

Project
Depth Profile

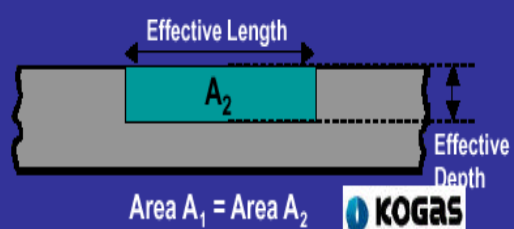
Inspection Data



Calculate
Minimum
Failure
Pressure



Effective
Dimensions



7 Background on Existing Analytical Models

7.1 ASME B31-G

Using the equation below, ASME B31-G is used for finding the remaining strength of corroded pipelines.

7.1.1 Equation

$$P \leq 1.1P' \left[\frac{1 - \frac{2}{3} \left(\frac{d}{t} \right)}{1 - \frac{2}{3} \left(\frac{d}{t \sqrt{A^2 + 1}} \right)} \right] \quad \text{for } A = .893 \left(\frac{L_m}{\sqrt{Dt}} \right) \leq 4$$

Where:

L_m = measured longitudinal extent of the corroded area, inches

D = nominal outside diameter of the pipe, inches

t = nominal wall thickness of the pipe, inches

d = measured depth of the corroded area

P = the greater of either the established MAOP or $P = SMYS \cdot 2t \cdot F / D$

(F is the design factor, usually equal to .72)

P' = safe maximum pressure

7.1.2 Limitations

There are a few limitations to using the B31-G equation for analysis. The limitations are:

1. Carbon or high strength low alloy steels must be used
2. Applicable to areas of smooth contours only
3. Do not use to find remaining strength of girth, longitudinal weld, or heat affected zones
4. For pipe to remain in service, pipe must be able to maintain structural integrity under internal pressure
5. Does not predict leaks

6. Does not predict rupture failures

7.1.3 Use

The B31-G formulation is best used to model smooth pipeline corrosion defects. It is also important to note that although the design factor listed above is usually .72, we did not limit F to .72 to obtain our results.

7.2 Det Norske Veritas RP-F101, Corroded Pipelines, 1999

This technique is used to evaluate corrosion defects due to internal pressure loading and longitudinal compressive stresses.

7.2.1 Equation

$$P_f = \frac{2 \cdot t \cdot UTS(1 - (d/t))}{(D - t) \left(1 - \frac{(d/t)}{Q} \right)}$$

Where Q is:

$$Q = \sqrt{1 + .31 \left(\frac{1}{\sqrt{D \cdot t}} \right)^2}$$

P_f = failure pressure of the corroded pipe

t = uncorroded, measured, pipe wall thickness

d = depth of corroded region

D = nominal outside diameter

Q = length correction factor

UTS = ultimate tensile strength

7.2.2 Limitations

The limitations of the DNV equation are:

1. Materials other than carbon line pipe steel
2. Grades of line pipe over X80
3. Cyclic loading
4. Sharp defects
5. Combined corrosion and cracking
6. Combined corrosion and mechanical damage
7. Metal loss due to gouges
8. Fabrication defects in welds
9. Defects greater than 85% of the original wall thickness

The guidelines for DNV RP-F101 are based on a data set of over 70 burst tests.

7.2.3 Use

The major difference distinction in the DNV formulation is the use of the Ultimate Tensile Strength (UTS).

7.3 *ABS Formulation*

7.3.1 Equation

$$P_b = \eta \text{ SMYS } (t - t_c) / R_o$$

Where:

$$R_o = (D - t) / 2$$

SMYS - specified minimum yield strength

η - utilization factor = 1.0

t - pipe nominal wall thickness

t_c - pipe corrosion thickness

D - pipe nominal outer diameter

7.3.2 Use

It is important to note that although η is equal to 1.0 above, this factor is dependent on the reliability you want to obtain.

7.4 RAM PIPE #1 (SMYS)

The RAM PIPE equation was developed at the University of California, Berkeley. It calculates burst pressures for corroded pipelines. Unlike the previous equations, it is important to note that RAM Pipe is not dependent on the length characteristic in its formulation.

7.4.1 Equation

$$P_{bd} = \frac{3.2 \cdot t_{nom} \cdot SMYS}{D_o \cdot SCF_C} = \frac{2.4 \cdot t_{nom} \cdot SMTS}{D_o \cdot SCF_C}$$

Where:

t_{nom} = nominal pipe wall thickness

D_o = mean pipeline diameter (D-t)

SMYS = Specified Minimum Yield Strength of pipeline steel

SCF_C = Stress Concentration Factor for corrosion features, defined by:

$$SCF_C = 1 + 2 \cdot (d/R)^5$$

7.4.2 Use

When using the RAM pipe formulation, the factor of 3.2 in the above equation is present as a measure of unbiasing to the median tensile strength of the pipeline. Also, the SCF factor is the effect of corrosion due to the sharpness of the pipe.

7.5 RAM PIPE #2 (SMTS)

This formulation uses the tensile strength as opposed to #1's yield strength.

7.5.1 Equation

$$p_B = (1.2 \text{ SMTS} / \text{SCF}) (t / R)$$

$$\text{SCF} = 1 + 2(tc/R)^{0.5}$$

Where:

t_c = the depth of the feature

R = the radius of the round pipe at the crack

Note: The factor has been decreased from formulation #1

7.5.2 Use

This formulation is used for conditioning SCF with the effects of the feature.

7.6 RAM PIPE #3 (UTS)

7.6.1 Equation

$$p_B = (UTS / SCF)(t / R)$$

$$SCF = 1 + 2 (tc/R)^{0.5}$$

UTS = mean longitudinal

7.6.2 Illustration

tc, t, and R can be shown are illustrated in Figure 1 below.

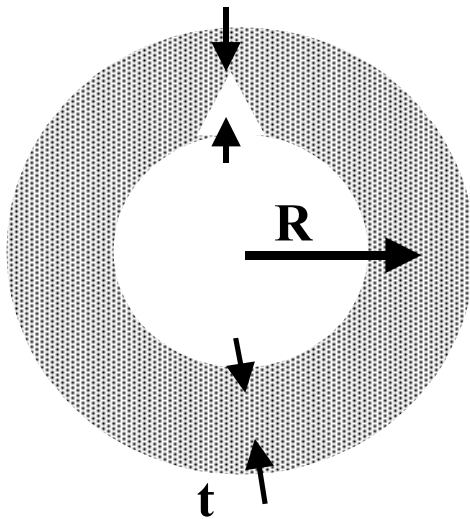


Figure 1

8 Bias Definition

The bias is not a single number. It is a series of numbers. The bias provides us with some insight on variability. It can be better understood in Figure 2 below.

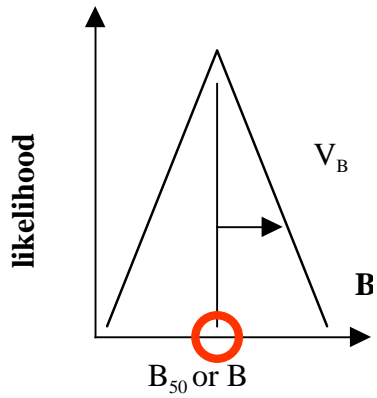


Figure 2.

8.1 Bias Equation

$$\text{Bias} = \text{Measured } P_b / \text{Predicted } P_b$$

9 Populations

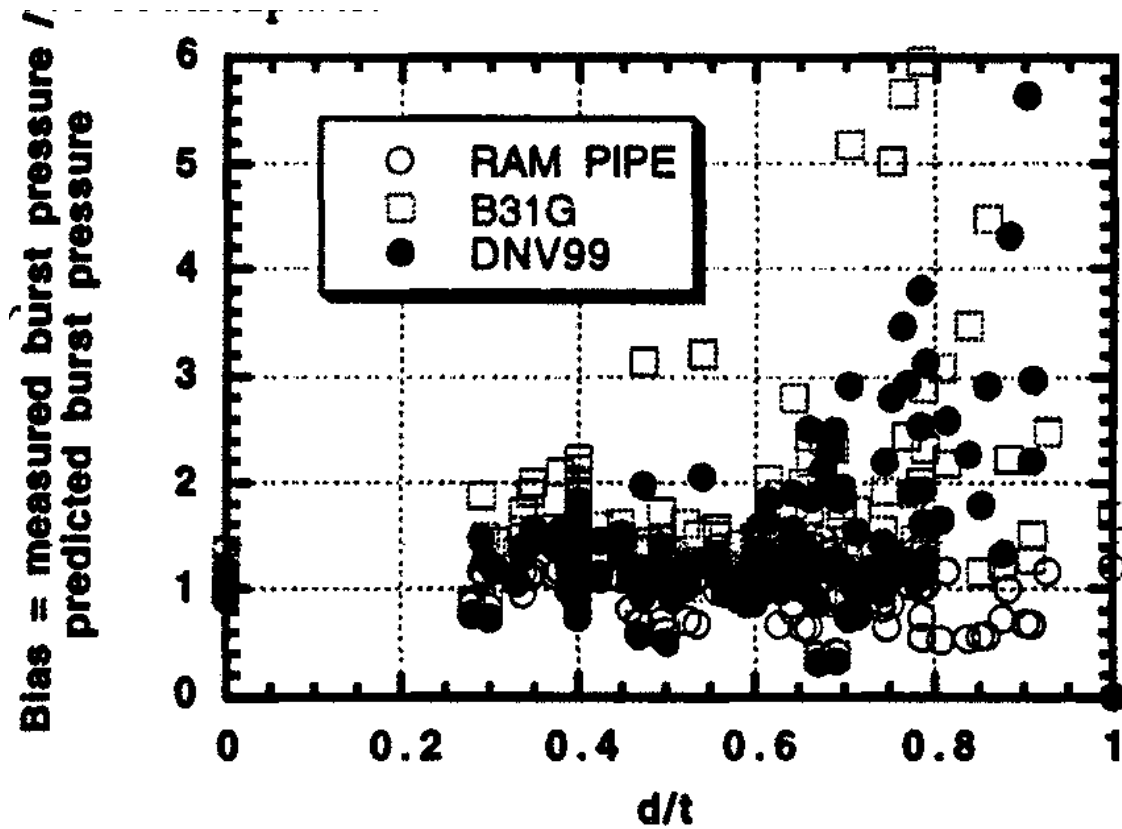


Figure 3

Figure 3 illustrates why the grouping of the populations are divided the way they were chosen. As seen above, in the section 0 to 0.2, there are very few data points. Not a significant amount to divide the population at this point. Similarly, the scatter is scarce at the right side of the graph between 0.8 to 1. The best accumulation of data that is illustrated above are in the sections 0.2 to 0.4, 0.4 to 0.6, and 0.6 to 0.8. This is the reasoning behind the population divisions of d/t .

10 Working with the Database

10.1 Existing Database

The database we are using was developed by the Marine Technology and Management Group. The information contained in the database came from:

1. The American Gas Association
2. NOVA Pipeline Corporation
3. British Gas
4. The University of Waterloo
5. DNV
6. Petrobas

The database is composed of 151 burst pressure tests on corroded pipelines.

The American Gas Association's contribution to the database came from a series of 86 burst pressure tests. 47 of those tests were full scale and went toward B31G criterion. The remaining tests were tests on pipe containing corrosion and removed from the field.

NOVA conducted 2 series of burst tests. The purpose of this was to see the applicability of the B31G criterion to long longitudinal and spiral defects. The characteristics of these pipes are shown below in the table.

Steel Grade	Diameter	Wall Thickness
414 (X60)	4064 mm	50.8 mm

Machined grooves were used to simulate the longitudinal and spiral defects. The test series were broken down into 2 groups as shown below:

Test group	Simulated defect width	Simulated defect depth	Width to thickness ratio (w/t)	Depth to thickness ratio (d/t)

#1: 13 tests	203mm	20.3mm	4	0.4
--------------	-------	--------	---	-----

Test Group	Items tested
#2: 7 tests	Tested varying w/t and d/t ratios

British Gas conducted 5 burst tests on vessels and 4 on pipe rings. The characteristics were as follows:

Test	Diameter	Wall thickness	Grade	Depth
Rings	914mm	22mm	API 5L X60	-----
Vessel	508mm	102mm	X52	.4t

On the ring tests, 7 of the nine were machined internally.

The University of Waterloo conducted 13 burst tests containing internal corrosion pits and 8 burst tests containing circumferentially aligned pits and 8 containing longitudinal aligned pits.

10.2 Recent Additions to the database

DNV contributed data from 12 full scale burst tests containing:

1. machined defects
2. internal pressure
3. bending loads
4. axial loads

Two of these tests involved internal pressure. This data is an add on to the existing database. In addition, Petrobas published 7 small scale tests that were also added this semester to the existing database

10.3 Information contained in the Database

The database contains the following information:

1. Specimen Number
2. Diameter, D

3. Thickness, t
4. Diameter to thickness ratio, D/t
5. Yield stress
6. Specified minimum yield stress
7. Defect Type
8. Defect depth
9. Defect width
10. Burst pressure
11. Specified minimum tensile stress
12. Angle
13. depth to thickness ratio, d/t
14. L^2 / Dt

11 Procedure for Analysis

The data was divided into 5 groups:

1. Entire database
2. Natural corrosion with varying d/t ratios
3. Natural corrosion with varying l/w ratios and d/t confined within a range
4. Machined corrosion with varying d/t ratios
5. Machined corrosion with varying l/w ratios and d/t confined within a range

When analyzing the entire database, I calculated burst pressures that resulted in using the British Standard, API, B-31G, DNV, ABS, Ram Pipe, and Rstreng methods. I then graphed the predicted burst pressure found by each method versus the measured burst pressure given in the database. I then graphed all the methods on the same graph against a 45 degree line so it could be visually inspected in Appendix A which method had a grouping closest to a bias equal to 1.0.

The natural corrosion was then separated into a designated spreadsheet where the data was analyzed according to varying d/t ratios. The data was arranged in ascending order so that it was easily visible where the specified d/t grouping started and ended. The data was grouped into d/t between 0 to .4, d/t between .4 to .8, and d/t between .8 to 1.0. Each of these groups were graphed in an attempt to see which method was best suitable in different d/t ranges. The results can be seen in Appendix B, C, and D respectively. Similarly, the same procedure was done using the machined corrosion data. The d/t range between 0 to .4 for machined corrosion can be seen in Appendix E, d/t between .4-.8 can be seen in Appendix F, and d/t between .8 to 1.0 can be seen in Appendix G.

Natural corrosion was also analyzed by varying l/w ratios and confined d/t to be set between .2 to .8. The data was arranged so that d/t values that fell outside the designated range were not used. Then, l/w ratios were arranged in ascending order so that the groupings of 0 to 2, 2-4, and 4-10 could easily be recognizable. The predicted versus measured was once again graphed within each of the above categories to evaluate which method was the best measure in each of the ranges. The results for l/w between 0 to 2 can be seen in Appendix H, between 2-4 in Appendix I, and between 4-10 in Appendix J. Similarly, the same procedure was done using the machined data and those can be found in Appendix K, Appendix L, and Appendix M respectively.

12 Results & Conclusions from Entire Database Analysis

The analysis of the entire database was not broken down into varying groups of d/t or l/w ranges as the other analysis sections were. We included all of the data. None was truncated and found the following results shown below in the table below.

The mean is sum of all the data divided by the number of data in the set. The median is the middlemost point in a set of data. The standard deviation is the square root of the variance. The variance is a measure of how spread out a distribution is.

Method	British Standard	API	B31-G	DNV	ABS	Ram Pipe	Rstreng
Variance	.38	.55	.04	.38	.99	.03	.11
Standard Deviation	.62	.74	.21	.62	.99	.18	.33
Bias (median)	1.09	1.22	.99	1.09	1.96	.95	1.01
Bias (mean)	1.31	1.48	1.03	1.31	2.31	.93	1.12

As a measure of which method best fits the data given in the database, we can compare which method had a mean bias closest to 1.0. For all the data given, the B31-G method produced a result closest to 1.0. The Ram Pipe formulation was the second best method used when comparing mean and median biases. However, if you want the formulation that least variance, Ram Pipe would be the one to use followed closely by B31-G.

13 Results & Conclusions from Natural Corrosion

The bias calculation for all of the data that resulted from natural corrosion is shown below.

Method	British Standard	API	B31-G	DNV	ABS	Ram Pipe	Rstreng
Variance	.09	.17	.02	.09	.47	.14	.19
Standard Deviation	.30	.41	.15	.30	.69	.14	.44
Bias (median)	.98	1.13	.87	.98	2.05	.92	1.23
Bias (mean)	1.02	1.21	.90	1.02	2.14	.92	1.30

For the overall natural corrosion results shown above, the B31-G formulation produced the least amount of variance. Overall, the British Standard and DNV formulations produced biases closest to 1.0.

13.1 Varying d/t ratios

Appendix E and F show d/t's ranging from 0 to .4 and .4 to .8. In both of those ranges, Ram pipe seems to be the best model.

In the range of .8 to 1.0, B31-G seems to be the best model. This is shown in Appendix G.

13.2 Varying L/w ratios and d/t in a certain range

Appendix H shows that Ram Pipe is best used in the range of l/w between 0 to 2.

B31-G appears to be the best model for the range of l/w between 2-4 and 4-10 as shown in Appendix I and J respectively.

14 Results & Conclusions from Machined Corrosion

The bias calculation for all of the data that resulted from machined corrosion is shown below.

Method	British Standard	API	B31-G	DNV	ABS	Ram Pipe	Rstreng
Variance	.43	.62	.03	.43	1.09	.03	.61
Standard Deviation	.65	.79	.18	.65	1.04	.17	.78
Bias (mean)	1.41	1.55	1.10	1.41	2.42	.94	1.60
Bias (median)	1.16	1.27	1.09	1.16	1.95	1.02	1.34

Overall, for machined corrosion, Ram Pipe produced the least amount of variance as well as having a mean and median bias closest to 1.0

14.1 Varying d/t ratios

Ram Pipe is the best method used in all the divisions of d/t. In the range of d/t between .4 to .8, DNV and B.S approach the accuracy of Ram Pipe.

14.2 Varying L/w ratios and d/t in a certain range

Appendix K shows the results of l/w between 0 to 2. It appears as though Ram Pipe is the best model used.

Appendix L and M show the range of l/w between 2-4 and 4-10. B31-G is the best model for this data range.

15 Cumulative Distribution Plots

The cumulative distribution plots illustrate the bias versus the percentile in which that bias number falls. To complete these plots, I rank ordered the bias results. The highest bias number became rank #1. Then, I used the equation:

$$\text{rank}/(N+1)$$

Where, N = the total number of points in the set

Then, I determined what percentile the data point fell in.

For example:

$$\text{Max Bias} = 3.0$$

$$\text{Rank} = 1$$

$$\text{Number of Bias data points in the set} = 99$$

$$\text{Rank}/(N+1) = 1/(99+1) = .01$$

$$1-.01 = .99$$

Therefore, a bias equal to 3.0 would correspond to a percentile of 97%.

It is important to note that there are some high and low values in the bias calculations. These extreme values could result the large range of depth data that was given in the database. There were values of depths of corrosion that were extreme and could have impacted the calculation of predicted burst pressure which, would in turn impact the bias calculation resulting in highs and lows.

The cumulative distribution plots can be seen in Appendix N-R.

16 General Conclusions/Observations

British Standard and DNV produce the same results.

All methods, in all ranges appear to be best modeled by the Ram Pipe equation or B31-G. The standard deviations of the bias for all the methods were averaged and are shown in the table below.

Method	British Standard	API	B31-G	DNV	ABS	Ram Pipe	Rstreng
Standard Deviation	.47	.60	.31	.47	.94	.16	.61

The least deviation from the mean is shown in the Ram Pipe equation.

It is important to note that there are some high and low values in the bias calculations. These extreme values could result the large range of depth data that was given in the database. There were values of depths of corrosion that were extreme and could have impacted the calculation of predicted burst pressure which, would in turn impact the bias calculation resulting in highs and lows.

17 References

A. Cosham and Dr. M.G. Kirkwood. Best Practice in Pipeline Defect Assessment- An Industry Initiative. 1999.

American Petroleum Institute. API 579 First Addition, Washington D.C. Jan. 2000

BSI. British Standard 7910. London. December 2000

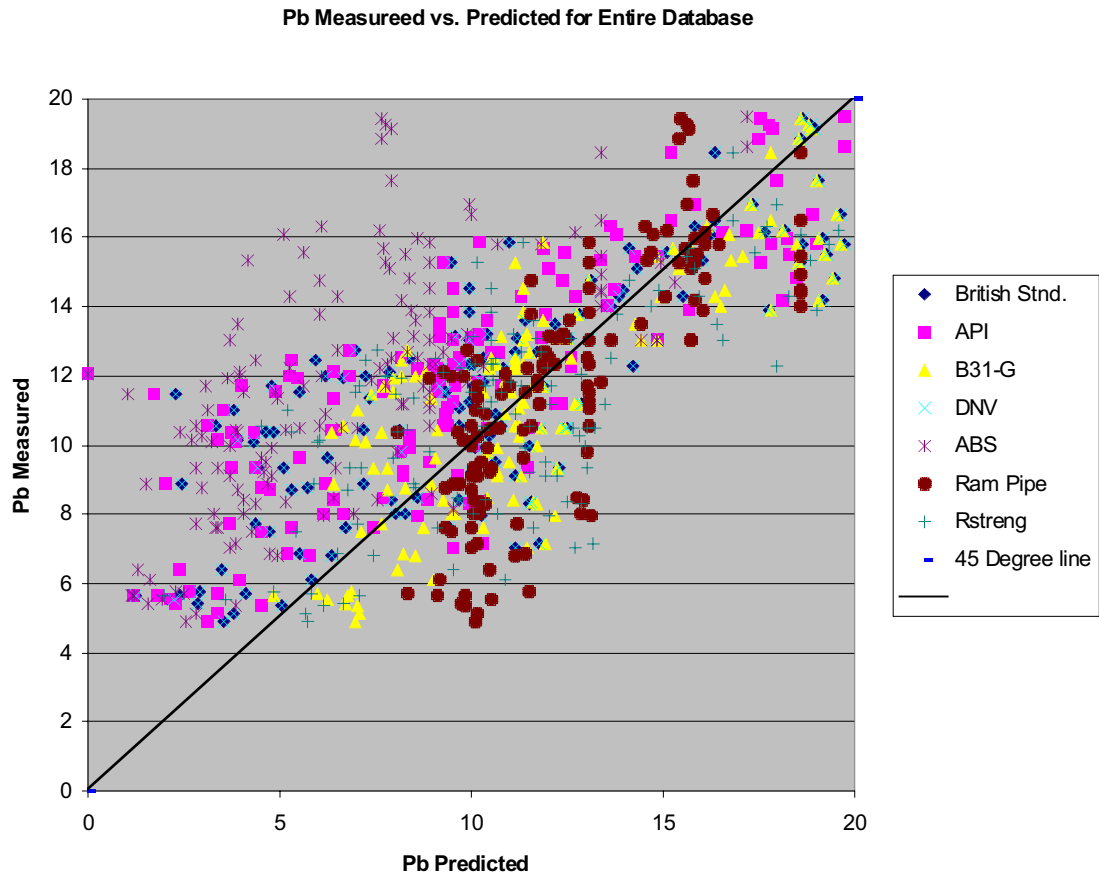
Denny R. Stephens and Robert B. Francini. A Review and evaluation of remaining strength criteria for corrosion defects in transmission pipelines. 2000.

RAM Pipe Database. Dr. Tao Xu and Professor Robert Bea

Rstreng Software for Windows. Technical Toolboxes. Version 3.0. Jan 2002.

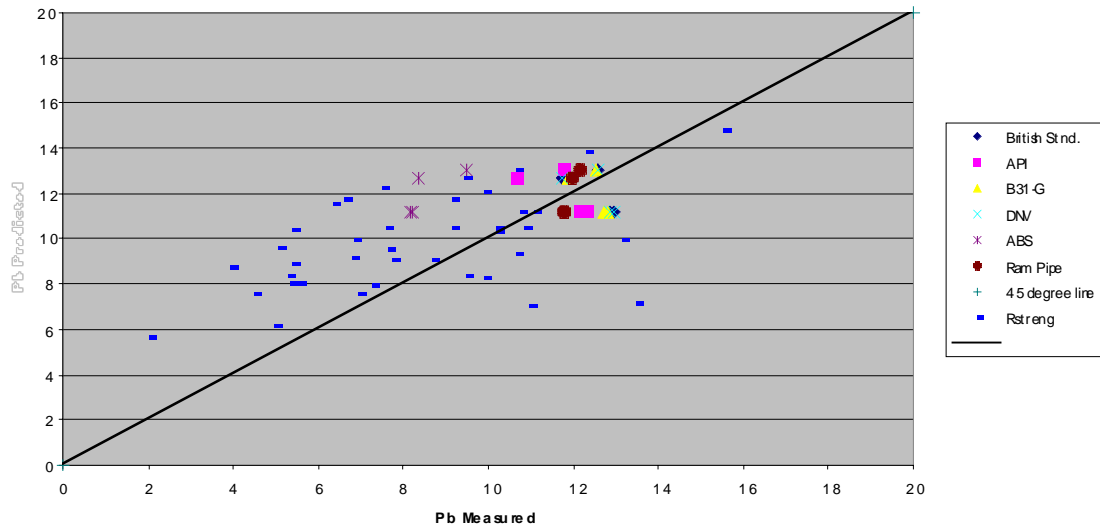
18 Appendix

18.1 Appendix A



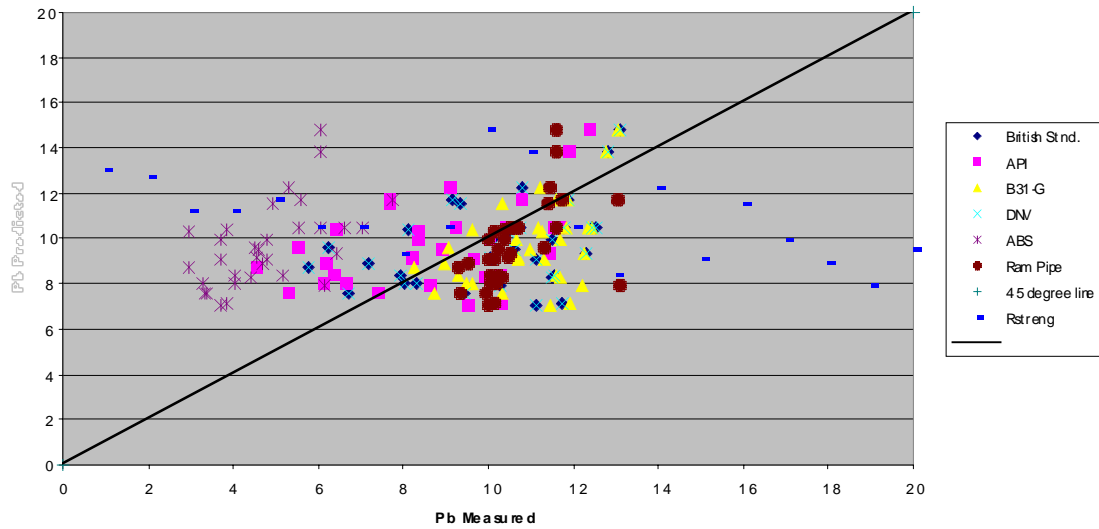
18.2 Appendix B

Natural Corrosion: Pb predicted vs. Measured corresponding to d/t between 0-.4



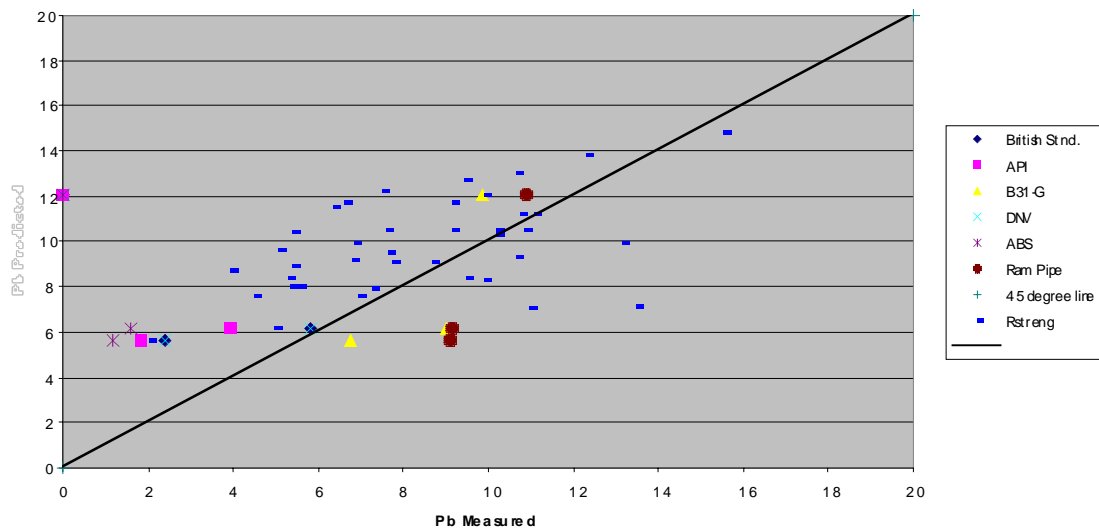
18.3 Appendix C

Natural Corrosion: Pb predicted vs. Measured corresponding to d/t between .4-.8



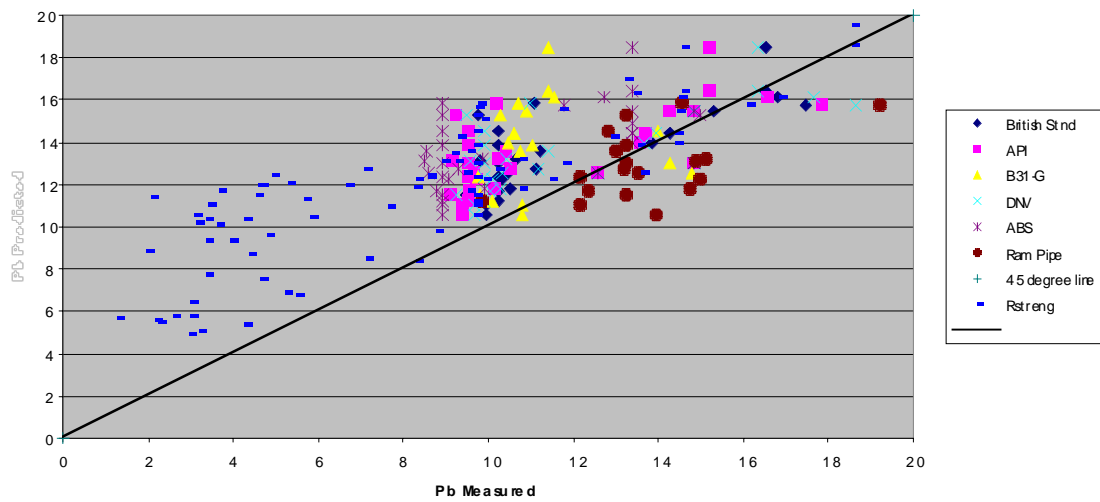
18.4 Appendix D

Natural Corrosion: Pb predicted vs. Measured corresponding to d/t between .8-1



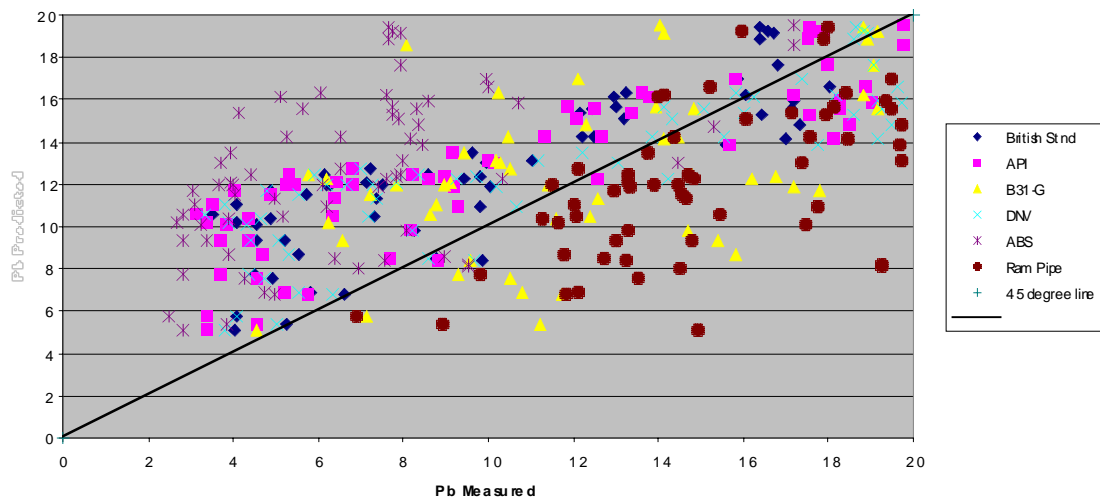
18.5 Appendix E

Machined Corrosion: Pb predicted vs. Measured corresponding to d/t between 0-.4



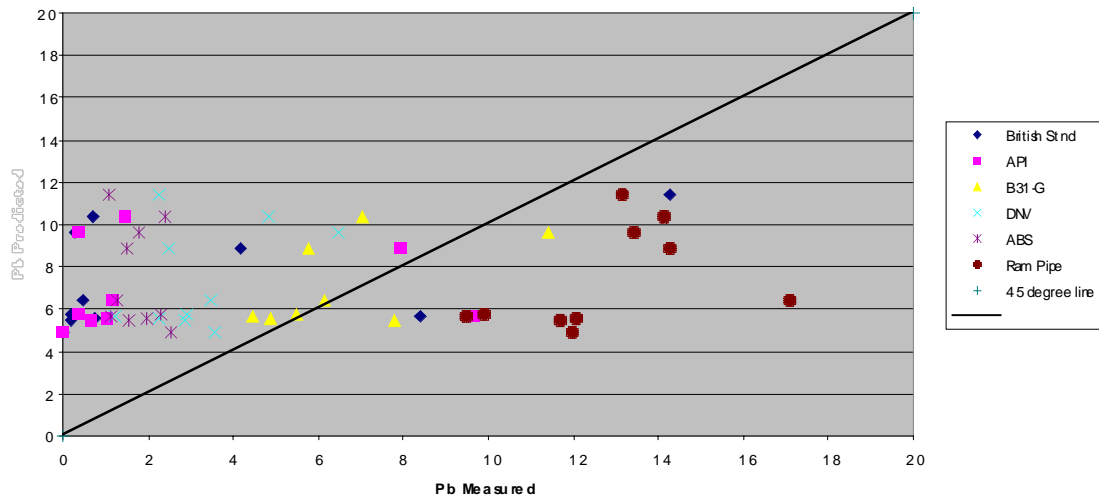
18.6 Appendix F

Machined Corrosion: Pb predicted vs. Measured corresponding to d/t between .4-.8



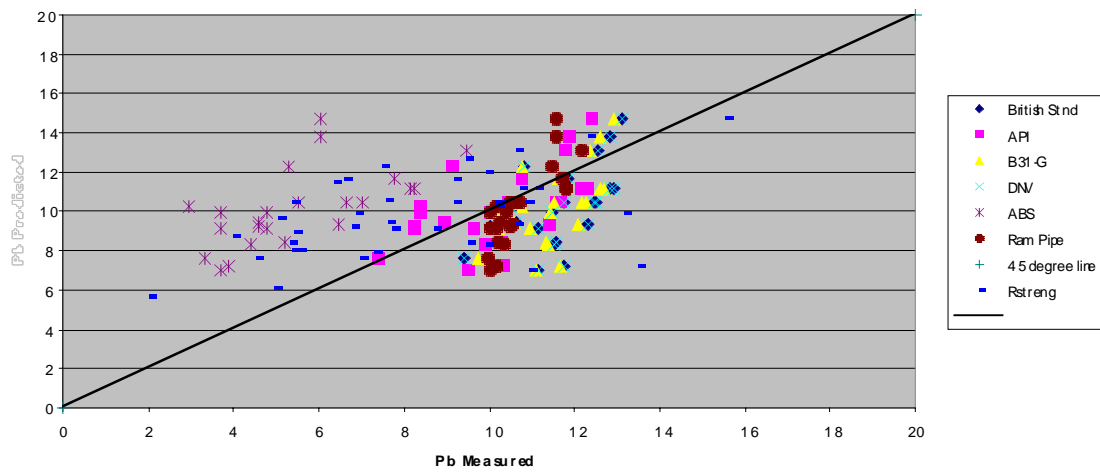
18.7 Appendix G

Machined Corrosion: Pb predicted vs. Measured corresponding to d/t between .4-.8



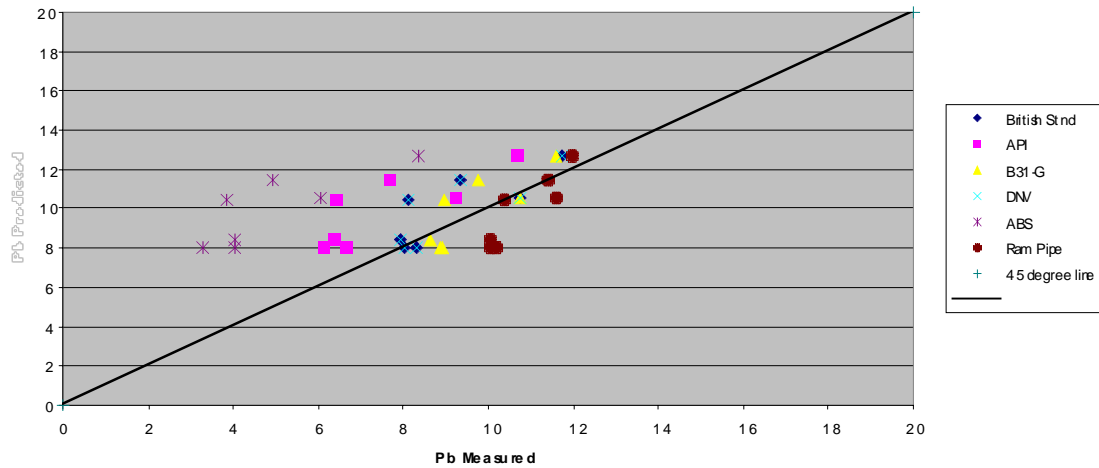
18.8 Appendix H

Natural Corrosion: Pb predicted vs. Measured corresponding to L/W between 0-2
and d/t between the range of .2-.8



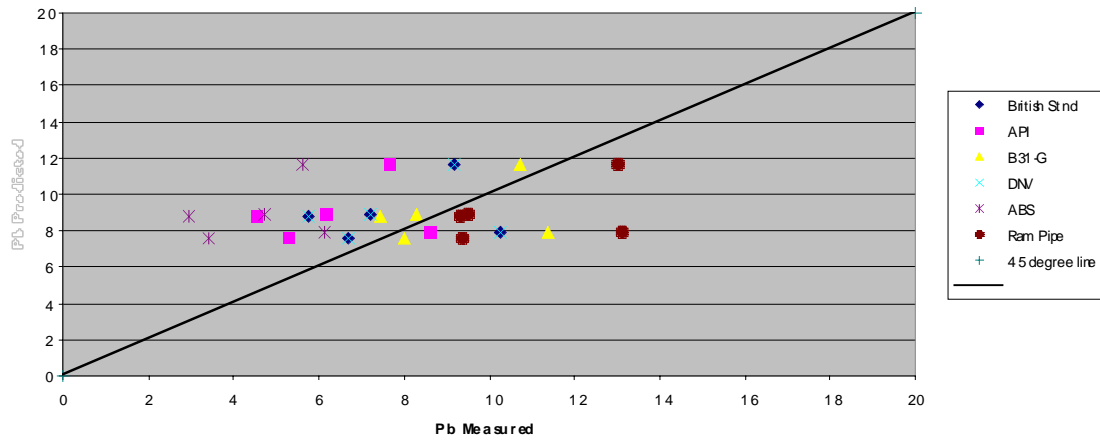
18.9 Appendix I

Natural Corrosion: Pb predicted vs. Measured corresponding to L/W between 2-4
and d/t between the range of .2-.8



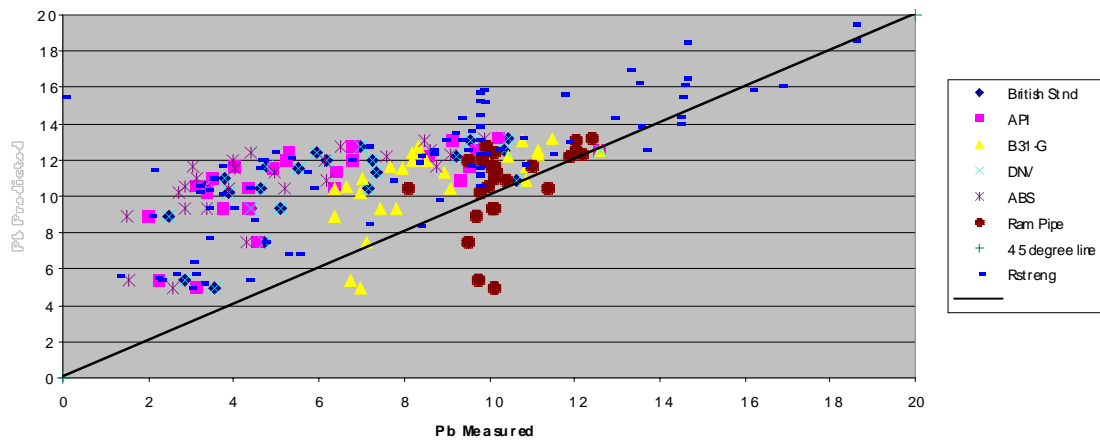
18.10 Appendix J

Natural Corrosion: Pb predicted vs. Measured corresponding to L/W between 4-10
and d/t between the range of .2-.8



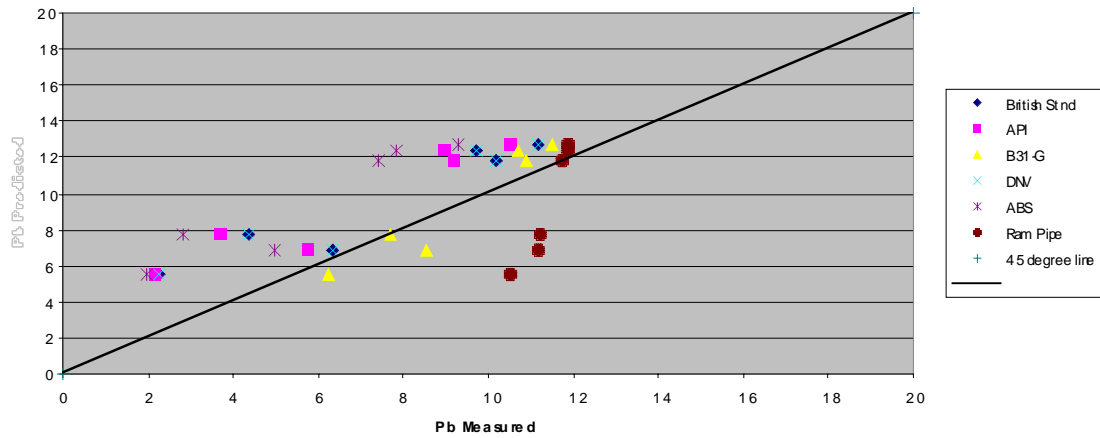
18.11 Appendix K

Machined Corrosion: Pb predicted vs. Measured corresponding to L/W between
0-2
and d/t between the range of .2-.8



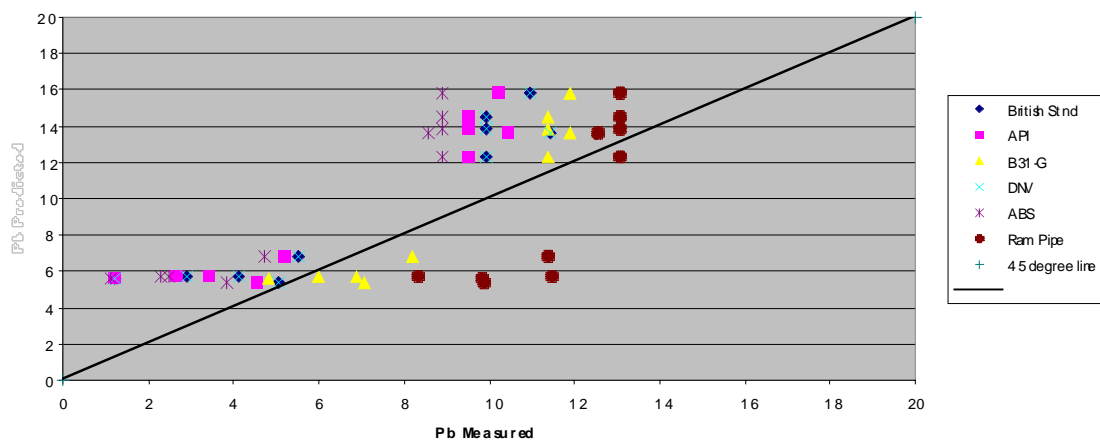
18.12Appendix L

Machined Corrosion: Pb predicted vs. Measured corresponding to L/W between
2-4
and d/t between the range of .2-.8



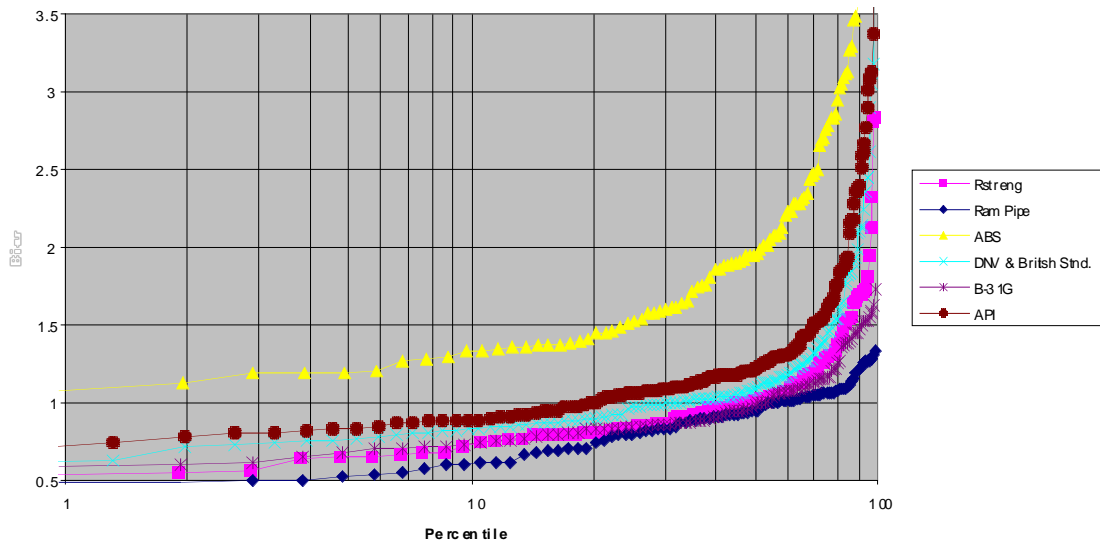
18.13 Appendix M

Machined Corrosion: Pb predicted vs. Measured corresponding to L/W between 4-10 and d/t between the range of .2-.8



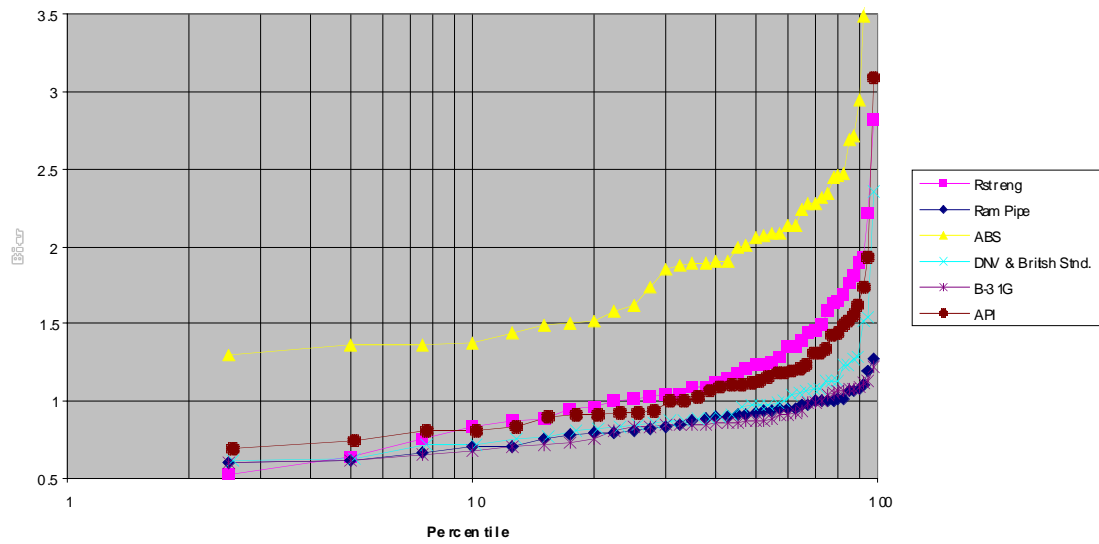
18.14 Appendix N

Cumulative Distribution of the Bias - Entire Database



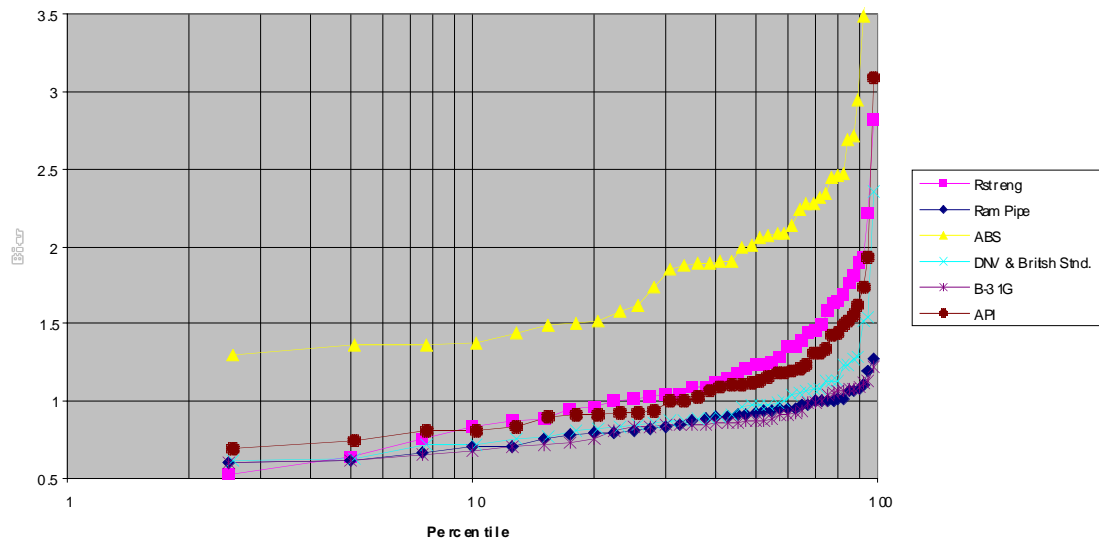
18.15 Appendix O

Cummulative Distribution of the Bias - Natural Corrosion varying d/t



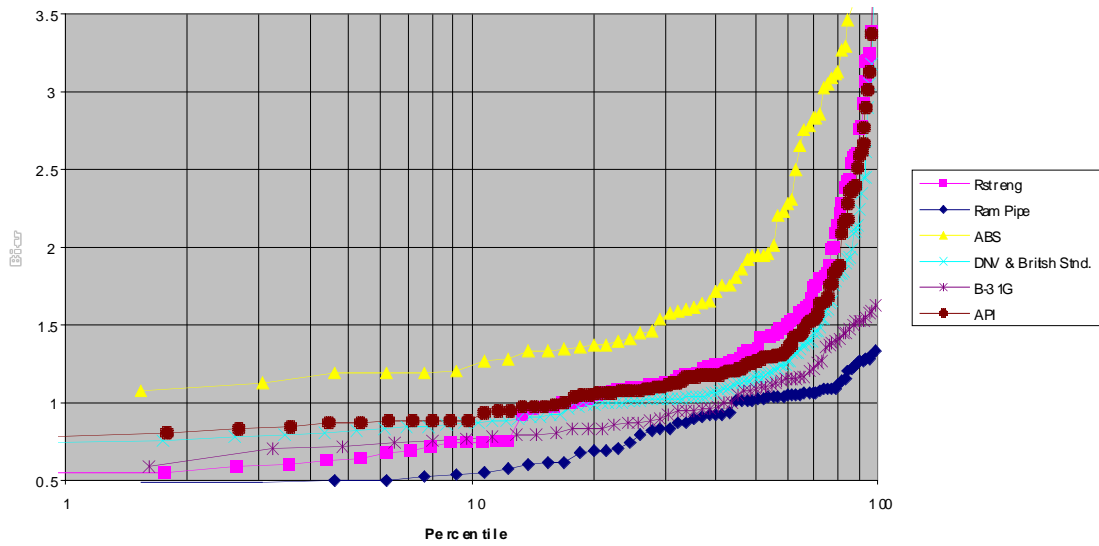
18.16 Appendix P

Cummulative Distribution of the Bias - Natural Corrosion varying L/W



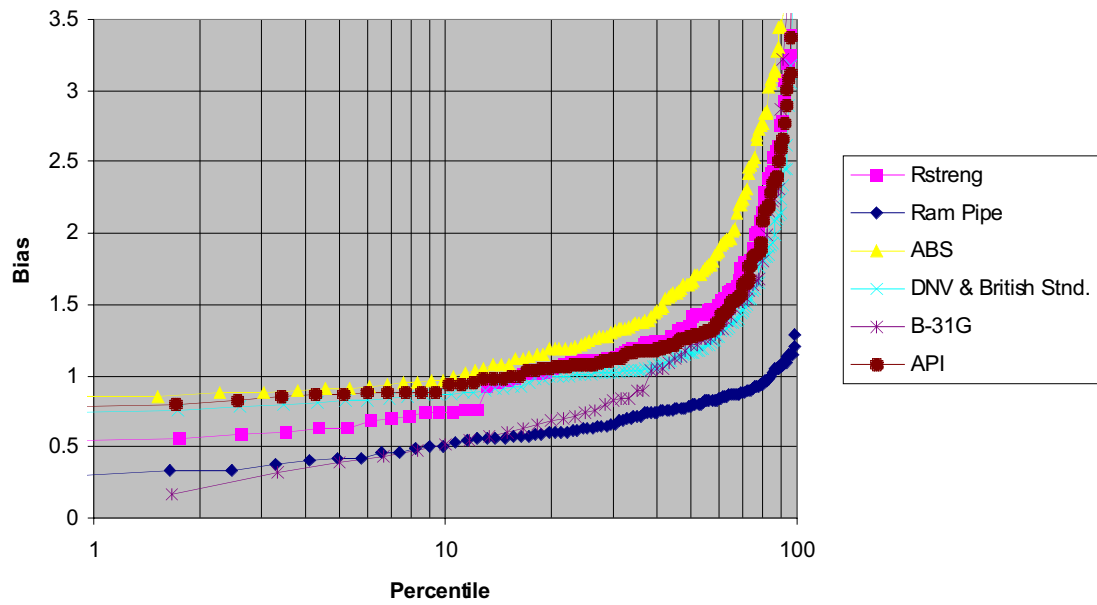
18.17 Appendix Q

Cummulative Distribution of the Bias - Machined Corrosion varying d/t



18.18 Appendix R

Cummulative Distribution of the Bias - Machined Corrosion varying L/W



OMAE 2002/PIPE-28322

REAL-TIME RELIABILITY ASSESSMENT & MANAGEMENT OF MARINE PIPELINES

Robert Bea
University of California at Berkeley
Berkeley, California USA

Charles Smith and Bob Smith
U.S. Minerals Management Service
Herndon, Virginia USA

Johannes Rosenmoeller, Thomas Beuker, and Bryce Brown
ROSEN Pipeline Inspection
Lingen, Germany and Houston, Texas, USA

ABSTRACT

In-line instrumentation information processing procedures have been developed and implemented to permit 'real-time' assessment of the reliability characteristics of marine pipelines. The objective of this work is to provide pipeline engineers, owners and operators with additional useful information that can help determine what should be done to help maintain pipelines.

This paper describes the real-time RAM (reliability assessment and management) procedures that have been developed and verified with results from laboratory and field tests to determine the burst pressures of pipelines. These procedures address the detection and accuracy characteristics of results from in-line or 'smart pig' instrumentation, evaluation of the implications of non-detection, and the accuracy of alternative methods that can be used to evaluate the burst pressures of corroded and dented – gouged pipelines.

In addition, processes are described have been developed to permit use of the information accumulated from in-line instrumentation (pipeline integrity information databases) to make evaluations of the burst pressure characteristics of pipelines that have not or can not be instrumented.

Both of these processes are illustrated with applications to two example pipelines; one for which in-line instrumentation results are available and one for which such information is not available.

Keywords: Pipelines, Reliability, Instrumentation

INTRODUCTION

Pipeline in-line instrumentation has become a primary means for gathering detailed data on the current condition of pipelines. It would be very desirable for the pipeline owner, operator, and regulator to have a highly automated process to enable preliminary assessment of the reliability of the pipeline in its current and projected future conditions (Fig. 1)

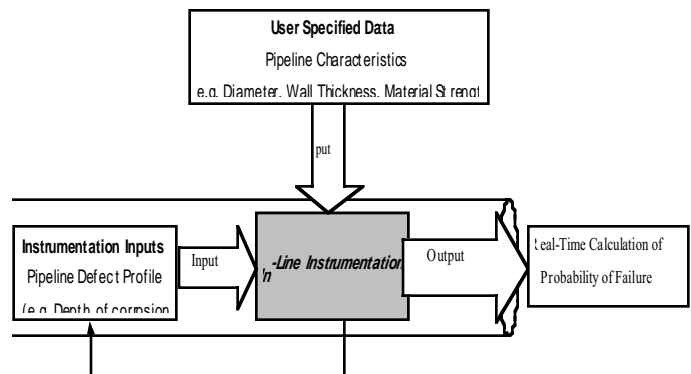


Fig. 1: Real-Time RAM process

Pipeline in-line instrumentation data can provide a large amount of data on damage and defects (features) in a pipeline. This data must be properly interpreted before the features can be characterized. The detection of features varies as a function of

the size and geometry of the features, the in-line instrumentation used, and the characteristics and condition of the pipeline. Given results from in-line instrumentation, it is desirable to develop a rapid and realistic evaluation of the effects of the detected features on the pipeline integrity. This evaluation requires and analysis of how the detected features might affect the ability of the pipeline to maintain containment.

RELIABILITY FORMULATION

The Reliability Assessment and Management (RAM) formulation used in this development is based on a probabilistic approach based on Lognormal distributions for both pipeline demand and capacity distributions. Such distributions have been shown to provide good approximations to the ‘best-fit’ distributions, particularly when the tails of the Lognormal distributions are fitted to the region of the distributions that have the greatest influence on the probability of failure. The Lognormal formulation for the probability of failure (Pf) is:

$$Pf = 1 - \Phi \left[\frac{\ln \left(\frac{R_{50}}{S_{50}} \right)}{\sigma_{\ln RS}} \right] = 1 - \Phi[\beta]$$

Φ is the Cumulative Normal Distribution for the quantity $[\bullet]$. R_{50} is the median capacity. S_{50} is the median demand. The ratio of R_{50} to S_{50} is known as the median or central Factor of Safety (FS_{50}). $\sigma_{\ln RS}$ is the standard deviation of the logarithms of the capacity (R) and demand (S):

$$\sigma_{\ln RS} = \sqrt{\sigma_{\ln R}^2 + \sigma_{\ln S}^2}$$

$\sigma_{\ln R}$ is the standard deviation of the capacity and $\sigma_{\ln S}$ is the standard deviation of the demand. For coefficients of variation ($V_X = \text{ratio of standard deviation to mean value of variable } X$) less than about 0.5, the coefficient of variation of a variable is approximately equal to the standard deviation of the logarithm of the variable. The quantity in brackets is defined as the Safety Index (β). The Safety Index β is related approximately to Pf as $1 \leq \beta \leq 3$:

$$Pf \approx 0.475 \exp -(\beta)^{1.6}$$

The results of this development are summarized in Fig. 2. The probability of failure (loss of containment) is shown as a function of the central factor of safety (FS_{50}) and the total uncertainty in the pipeline demands and capacities (σ). Note that the probability of failure can be determined from two fundamental parameters: the central factor of safety ($FS_{50} = R_{50}/S_{50}$) and the total uncertainty in the demands and capacities ($\sigma_{\ln RS} = \sigma$).

TIME DEPENDENT RELIABILITY

When a pipeline is subjected to active corrosion processes, the probability of failure is a time dependent function that is dependent on the corroded thickness of the pipeline (t_{ci}/e). The corroded thickness is dependent on the rate of corrosion and the time that the pipeline or riser is exposed to corrosion.

Insight into the change in the uncertainty associated with the pipeline capacity associated with the loss of wall thickness due to corrosion, can be developed by the following:

$$\bar{t} \ominus \bar{t} - \bar{d}$$

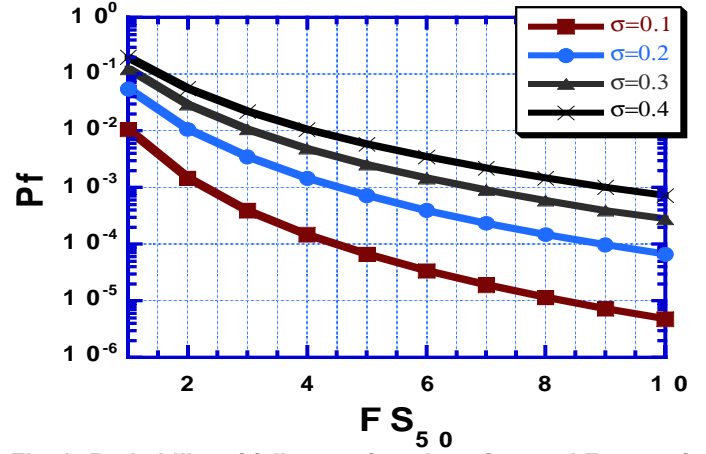


Fig. 2: Probability of failure as function of central Factor of Safety and total uncertainty

t' is the wall thickness after the corrosion, t is the wall thickness before corrosion, and d is the maximum depth of the corrosion loss. Bars over the variables indicate mean values.

Based on First Order – Second Moment methods, the standard deviation of the wall thickness after corrosion can be expressed as:

$$\sigma_{t \ominus} = \sqrt{\sigma_t^2 + \sigma_d^2}$$

The Coefficient of Variation ($COV = V$) can be expressed as:

$$V_{t \ominus} = \frac{\sigma_{t \ominus}}{\bar{t} \ominus} = \frac{\sqrt{(V_t \bar{t})^2 + (V_d \bar{d})^2}}{\bar{t} - \bar{d}}$$

A representative value for the COV of t would be 2%. A representative value for the COV of d would be $V_d = 40\%$. Fig. 3 summarizes the foregoing developments for a 16-in. (406 mm) diameter pipeline with an initial wall thickness of $t = 0.5$ in. (17 mm) that has an average rate of corrosion of 10 mpy (0.010 in. / yr, 0.25 mm / yr). The dashed line shows the results for the uncertainties associated with the wall thickness. The solid line shows the results for the uncertainties that include those of the wall thickness, the prediction of the corrosion burst pressure, and the variabilities in the maximum operating pressure.

At the time of installation, the pipeline wall thickness COV is equal to 2%. But, as time develops, the uncertainties associated with the wall thickness increase due to the large uncertainties associated with the corrosion rate – maximum depth of corrosion. The solid line that reflects all of the uncertainties converges with the dashed line that represents the uncertainties in the remaining wall thickness, until at a time of about 20 years, the total uncertainty is about the same as that of

the remaining wall thickness ($Vt-d \approx 25\%$). As more time develops, there is a dramatic increase in the COV associated with the remaining wall thickness. These uncertainties are dominated by the uncertainties attributed to the corrosion processes.

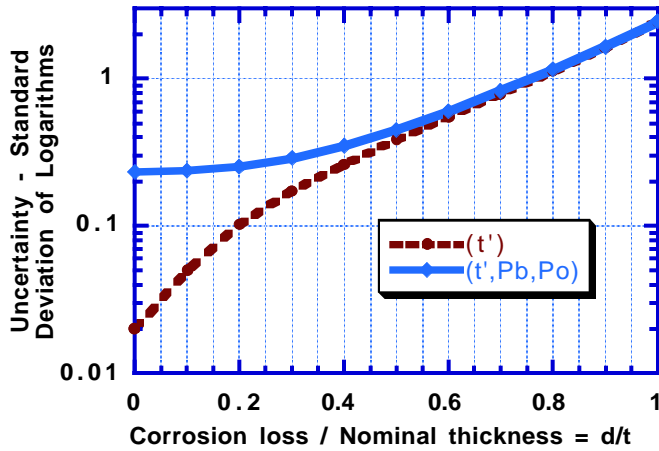


Fig. 3: Uncertainty in pipeline wall thickness and burst pressure capacity as a function of the normalized loss in pipeline wall thickness

These observations have important ramifications on the probabilities of failure – loss of containment of the pipeline. After the ‘life’ of the pipeline is exceeded (e.g. 20 to 25 years), one can expect there to be a rapid and dramatic increase in the uncertainties associated with the corrosion processes. In addition, there will be the continued losses in wall thickness. Combined, these two factors will result in a dramatic increase in the probability of failure of a pipeline.

Fig. 4 summarizes example results for a 16-in. (406 mm) diameter, 0.5 in (13 mm) wall thickness pipeline that has a maximum operating pressure (MOP) of 5,000 psi (34.5 Mpa). The COV associated with the MOP is 10%. The pipeline is operated at the maximum pressure, and at 60% of the maximum operating pressure for a life of 0 to 50 years. The average corrosion rate was taken as 10 mills per year (mpy). For the 60% pressured line, during the first 20 years, the annual probability of failure rises from $1E-7$ to $5E-3$ per year. After 20 years, the annual probability of failure rises very quickly to values in the range of 0.1 to 1. Perhaps, this helps explain why the observed pipeline failure rates associated with corrosion in the Gulf of Mexico are in the range of $1E-3$ per year.

TRUNCATED DEMAND & CAPACITY DISTRIBUTIONS

Real-time RAM analytical models have been developed to allow determination of the effects of user specified truncations in pipeline demands, capacities; separately or combined.

The effect of pressure testing is to effectively ‘truncate’ the probability distribution of the pipeline burst pressure capacity below the test pressure (Fig. 5). Pressure testing is a form of ‘proof testing’ that can result in an effective increase in the reliability of the pipeline.

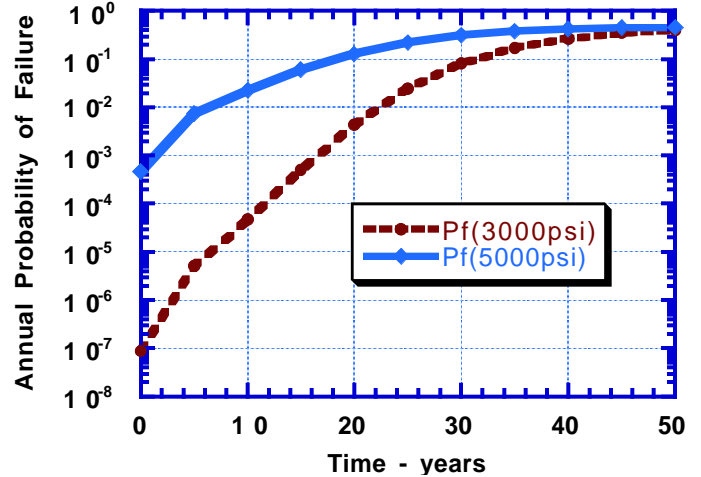


Fig. 4: Example pipeline failure rates as function of exposure to corrosion

There can be a similar effect on the operating pressure demands if there are pressure relief or control mechanisms maintained in the pipeline. Such pressure relief or control equipment can act to effectively truncate or limit the probabilities of developing very high unanticipated operating pressures (due to surges, slugging, or blockage of the pipeline).

Pipeline capacity before testing

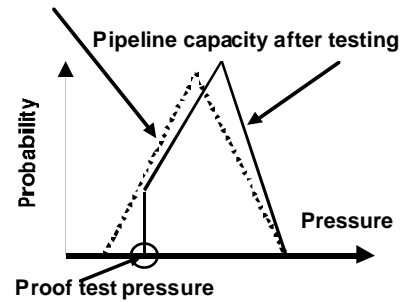


Fig. 5: Effects of proof testing on pipeline capacity distribution

This raises the issues associated with pressure testing and pressure controls on the computed probabilities of failure. It is important to note that such distribution truncation considerations have been omitted from all pipeline reliability based studies and developments that have been reviewed during the past 10 years of research on this topic.

Fig. 6 summarizes the results of pipeline proof testing on the pipeline Safety Index (the probability of loss of containment is $Plc \approx 10^{-6}$) as a function of the ‘level’ of the proof testing pressure factor, K:

$$K = \ln(Xp / p_b) / \sigma_{\ln p_b}$$

where Xp / p_b is the ratio of the test pressure to the median burst pressure capacity of the pipeline (test pressure deterministic, burst pressure capacity Lognormally distributed) and is the standard deviation of the Logarithms of the pipeline burst pressure capacities. These results have been generated for

the case where the uncertainty associated with the maximum operating / incidental pressures is equal to the uncertainty of the pipeline burst pressures and for Safety Indices in the range of $\beta = 3$ to $\beta = 4.5$.

For example, if the median burst pressure of the pipeline were 2,000 psi and this had a Coefficient of Variation of 10 %, there was a factor of safety on this burst pressure of 2 ($f = 0.5$) (maximum operating pressure = 1,000 psi), and the pipeline was tested to a pressure of 1.25 times the maximum operating pressure ($X_p = 1,250$ psi), the proof testing factor $K = -4.7$. The results in Fig. 6, indicate that this level of proof testing is not effective in changing the pipeline reliability. Even if the pipeline were tested to a pressure that was 1.5 times the operating pressure, the change in the Safety Index would be less than 5 %.

If the test pressure were increased to 75% of the median burst pressure, the Safety Index would be increased by about 25 %. For a Safety Index of $\beta = 3.0$ ($P_f = 1E-3$), these results indicate a $\beta = 3.75$ ($P_f = 1E-4$) after proof testing.

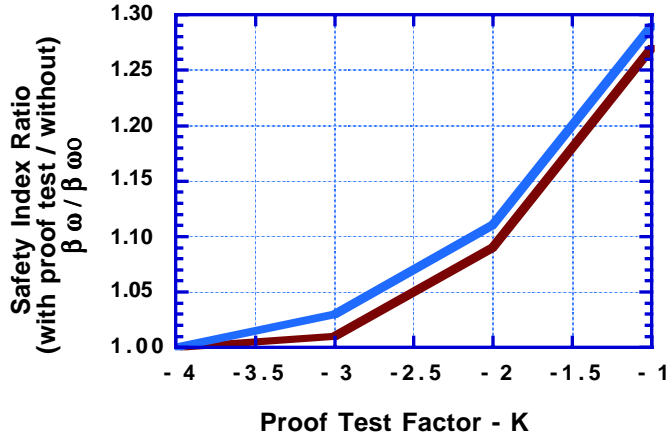


Fig. 6: Effects of proof testing on pipeline reliability

Very high levels of proof testing are required before there is any substantial improvement in the pipeline reliability. These results indicate that conventional pressure testing may not be very effective at increasing the burst pressure reliability characteristics. Such testing may be effective at disclosing accidental flaws incorporated into the pipeline (e.g. poor welding).

PROBABILITIES OF DETECTION

Fig. 7 shows results from inline Magnetic Flux Leakage (MFL) instrumentation of a 20-in (508 mm) diameter gas line in the Bay of Campeche (Pig C) [1]. The measured and corrected corrosion expressed as a percentage of the wall thickness is shown.

Fig. 8 summarizes data for two inline MFL instruments in which the in-line data on corrosion defect depths were compared with the corrosion defect depths determined from direct measurements on recovered sections of the pipeline that was in-line instrumented. For this particular condition, both in-line instruments tend to under estimate the corrosion depth. The uncertainties associated with the measured depths ranged from 35% (for 50 mils depths) to 25% (for 200 mils depths). The

corrected wall thickness shown in Fig. 7 was based on these data.

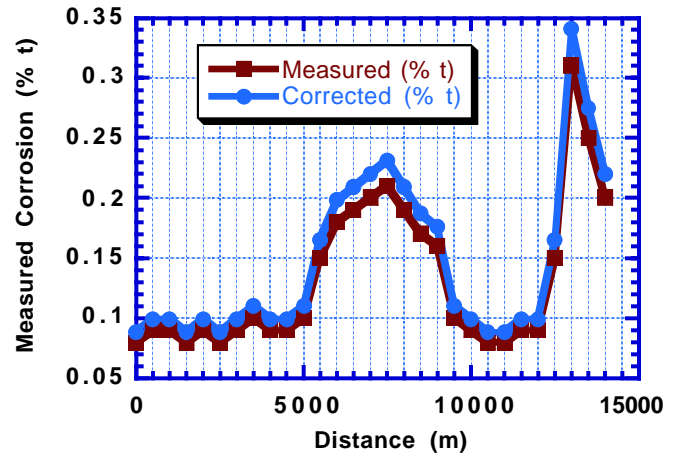


Fig. 7: Measured and corrected corrosion readings

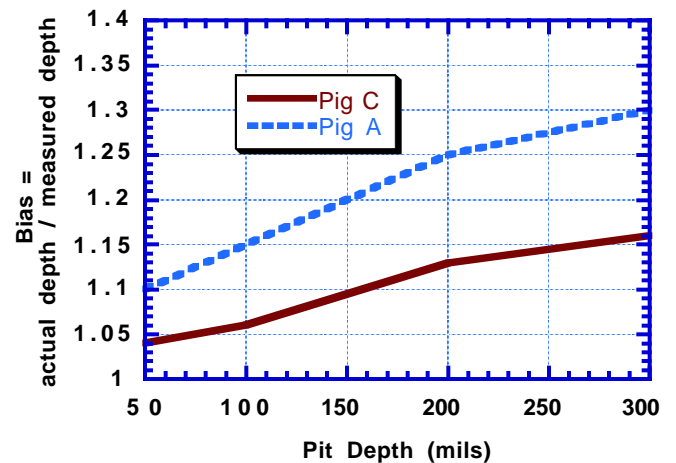


Fig. 8: Bias in measured corrosion depths

Based on using results from inline instrumentation, the probability of failure can be expressed as:

$$P_f = P_{f_D} + P_{f_{ND}}$$

where P_{f_D} is the probability of failure associated with the detected flaws and $P_{f_{ND}}$ is the probability of failure associated with the non-detected flaws. It is important to recognize that making evaluations of corrosion rates and wall thicknesses from the recordings have significant uncertainties. Fig. 9 shows a comparison of the Probability of Detection (POD) of corrosion depths (in mils, 50 mils = 1.27 mm) developed by three different inline MFL instruments. This information was based on comparing measured results from sections of a pipeline that were repeatedly in-line instrumented and then retrieved and the directly measured corrosion depths determined. These are results from three similar MFL in-line instruments. However, there are significant differences in the POD. This indicates an important need to standardize in-line instrumentation and data interpretation.

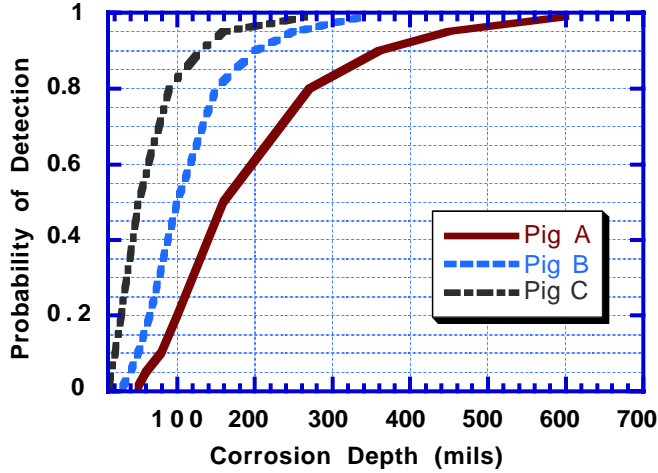


Fig. 9: Probability of detection curves for three in-line instruments

The probability of failure associated with the detected depth of corrosion can be expressed as:

$$P_{fD} = 1 - \Phi\left\{\frac{\ln(p_{B50}/p_{O50})}{[(\sigma_{pB}^2 + \sigma_{pO}^2)^{0.5}]}\right\}$$

where p_{B50} is the 50th percentile (median) burst pressure, p_{O50} is the 50th percentile maximum operating pressure, σ_{pB} is the standard deviation of the logarithms of the burst pressure, and σ_{pO} is the standard deviation of the logarithms of the maximum operating pressures. The pipeline burst pressure is determined from the RAM PIPE formulation:

$$P_{bd} = 3.2 t \text{ SMYS} / D_o \text{ SCF}$$

$$\text{SCF} = 1 + 2 (d / R)^{0.5}$$

where P_{bd} is the burst pressure capacity of the corroded pipeline, t is the nominal wall thickness (including the corrosion allowance), D_o is the mean diameter ($D-t$), D is the pipeline outside diameter, SMYS is the specified minimum yield strength, and SCF is a stress concentration factor that is a function of the depth of corrosion, d ($d \leq t$), and the pipeline radius, R .

The median of the burst pressure is determined from the medians of the variables. The uncertainty in the burst pressure is determined from the standard deviations of all of the variables:

$$\sigma_{\ln p_{B50}}^2 = \sigma_{\ln S}^2 + \sigma_{\ln t}^2 + \sigma_{\ln t_c}^2 + \sigma_{\ln D}^2$$

The probability of a corrosion depth, X , exceeding a lower limit of corrosion depth detectability, x_o , is:

$$P[X \geq x_o | ND] =$$

$$P[X > x_o] P[ND | X \geq x_o] / P[ND]$$

$P[X \geq x_o | ND]$ is the probability of no detection given $X \geq x_o$. $P[X > x_o]$ is the probability that the corrosion depth is greater than the lower limit of detectability. $P[ND | X \geq x_o]$ is the probability of non detection given a flaw depth. $P[ND]$ is the probability of non detection across the range of flaw depths where:

$$P[ND] = 1 - P[D]$$

and:

$$P[ND] = \sum P[ND | X > x_o] P[X > x_o]$$

The probability of failure for non-detected flaws is the convolution of:

$$P_{fND} = \sum [P_f | X > x_o] P[X \geq x_o | ND]$$

Fig. 24 shows the probabilities of burst failure (detected and non-detected) of the pipeline. The majority of the pipeline has probabilities of failure of about $1 \text{ E-}2$ per year. However, there are two sections that have substantially higher probabilities of failure. One section is a low section in the pipeline where water can accumulate and the other is in the riser section that is subjected to higher temperatures and external corrosion. The probabilities of failure for these two sections are $1.7 \text{ E-}2$ and $2.9 \text{ E-}2$ per year, respectively. These two sections of the pipeline would be candidates for replacement.

ANALYTICAL MODEL BIAS

One of the most important parts of a reliability assessment is the evaluation of the Bias that is associated with various analytical models to determine the capacity of a pipeline. In this development, Bias is defined as the ratio of the true or measured (actual) loss of containment (LOC) pressure capacity of a pipeline to the predicted or nominal (e.g. code or guideline based) capacity:

$$\text{Bias} = B_x = \frac{\text{True}}{\text{Predicted}} = \frac{\text{Measured}}{\text{Nominal}}$$

It is important to note that the measured value determined from a laboratory experiment is not necessarily equal to the true or actual value that would be present in the field setting. Laboratory experiments involve ‘compromises’ that can lead to important differences between the true or actual pipeline capacity and that measured in the laboratory. For example, the end closure plates used on laboratory test specimens of pipelines will introduce axial stresses that can act to increase the LOC pressure capacity relative to a segment of the pipeline in the field in which there would not be any significant axial stresses.

One important example of the potential differences between the true pipeline capacity and the experimentally determined pipeline capacity regards laboratory experiments that are used to determine the burst pressure capacity of corroded pipelines. To facilitate the laboratory experiments (controlled parameter variations), the corroded features frequently are machined into the pipeline specimen. This machining process can lead to important differences between actual corroded features and those machined into the specimens; stress concentrations can be very different; residual stresses imparted by the machining process can be very different; and there can be metallurgical changes caused by the machining process. Thus, laboratory results must be carefully regarded and it must be understood that such experiments can themselves introduce Bias into the assessment of pipeline reliability.

Another important example regards true or ‘measured’ results that are based on results from analytical models. Such

an approach has been used to generate 'data' used in several recent major reliability based code and guideline developments. The general approach is to use a few high quality physical laboratory tests to validate or calibrate the analytical model. Then the analytical model is used to generate results with the model's parameters being varied to develop experimental data. One colleague has called these "visual experiments." The primary problems with this approach concern how the model's parameters are varied (e.g. recognition of parameter correlations recognized and definition of the parametric ranges), and the abilities of the model to incorporate all of the important physical aspects (e.g. residual stresses, material nonlinearity). The use of analytical models introduces additional uncertainties and these additional uncertainties should not be omitted. In one recent case, the analytical models have been calibrated based on machined pipeline test sample results. Thus, the analytical models have 'carried over' the inherent Bias incorporated into the physical laboratory tests.

In this study, a differentiation has been made between physical laboratory test data and analytical test data. Further, differentiation has been made between physical laboratory test data on specimens from the field and those that are machined or involve simulated damage and defects. Earlier studies performed on these databases have clearly indicated potentially important differences between physical and analytical test data based Biases and differences between 'natural' and simulated defects and damage.

Burst Capacities of Corroded Pipelines

A test database consisting of 151 burst pressure tests on corroded pipelines was assembled from tests performed by the American Gas Association [2], NOVA [3], British Gas [4], and the University of Waterloo [5]. The Pipeline Research Committee of the American Gas Association published a report on the research to reduce the excessive conservatism of the B31G criterion (Kiefner, et al, 1989)[2] Eightysix (86) test data were included in the AGA test data. The first 47 tests were used to develop the B31G criterion, and were full scale tests conducted at Battelle Memorial Institute. The other 39 tests were also full scale and were tests on pipe sections removed from service and containing real corrosion.

Two series of burst tests of large diameter pipelines were conducted by NOVA during 1986 and 1988 to investigate the applicability of the B31G criterion to long longitudinal corrosion defects and long spiral corrosion defects [3]. These pipes were made of grade 414 (X60) steel with an outside diameter of 4064 mm and a wall thickness of 50.8 mm. Longitudinal and spiral corrosion defects were simulated with machined grooves on the outside of the pipe. The first series of tests, a total of 13 pipes, were burst. The simulated corrosion defects were 203 mm wide and 20.3 mm deep producing a width to thickness ratio (W/t) of 4 and a depth to thickness ratio (d/t) of 0.4. Various lengths and orientations of the grooves were studied. Angles of 20, 30, 45 and 90 degrees from the circumferential direction, referred to as the spiral angle, were used. In some tests, two adjacent grooves were used to indicate interaction effects. The second series of tests, a total of seven pipes, were burst. The defect geometries tested were

longitudinal defects, circumferential defects, and corrosion patches of varying W/t and d/t. A corrosion patch refers to a region where the corrosion covers a relatively large area of pipe and the longitudinal and circumferential dimensions were comparable. In some of the pipes, two defects of different sizes were introduced and kept far enough apart to eliminate any interaction.

Hopkins and Jones (1992) [4] conducted five vessel burst tests and four pipe ring tests. The pipe diameter were 508 mm. The wall thickness was 102 mm. The pipe was made of X52. The defect depth was 40% of the wall thickness. Jones et al (1992) also conducted nine pressurized ring tests. Seven of the nine were machined internally over 20% of the circumference, the reduced wall thickness simulating smooth corrosion. All specimens were cut from a single pipe of Grade API 5L X60 with the diameter of 914 mm and wall thickness of 22 mm.

As part of a research project performed at the University of Waterloo, 13 burst tests of pipes containing internal corrosion pits were reported by Chouchaoui, et al [5]. In addition, Chouchaoui et al reported the 8 burst tests of pipes containing circumferentially aligned pits and the 8 burst tests of pipes containing longitudinally aligned pits.

The laboratory test database was used to determine the Bias in the DNV RP F-101 [6], B31G [7], and RAM PIPE [8] formulations were used to determine the burst pressure bias (measured burst pressure divided by predicted burst pressure). The results for the 151 physical tests are summarized in Fig. 10 and Fig. 11. These tests included specimens that had corrosion depth to thickness ratios in the range of 0 to 1 (Fig. 11). The statistical results from the data summarized in Fig. 10 are summarized in Table 1.

Table 1: Bias statistics for three burst pressure formulations (d/t = 0 to 1)

Formulation	B mean	B ₅₀	V _B %
DNV 99	1.46	1.22	56
B 31 G	1.71	1.48	54
RAM PIPE	1.01	1.03	22

The RAM PIPE formulation has the median Bias closest to unity and the lowest COV of the Bias. The DNV formulation has a lower Bias than B31G, but the COV of the Bias is about the same as for B31G. The B31G mean Bias and COV in Table 1 compares with values of 1.74 and 54 %, respectively, found by Bai, et al [9]. The burst pressure test data were reanalyzed to include only those tests for d/t = 0.3 to 0.8. The bias statistics were relatively insensitive to this partitioning of the data.

A last step in the analysis of the physical test database was to analyze the Bias statistics based on only naturally corroded specimens. The results are summarized in Fig. 12 and Table 2. The Bias statistics for the DNV and B31G formulations were affected substantially. The results indicate that the machined specimens develop lower burst pressures than their naturally corroded counterparts. Even though the feature depth and area might be the same for machined and natural features, the differences caused by the stress concentrations, residual stresses, and metallurgical effects cause important differences.

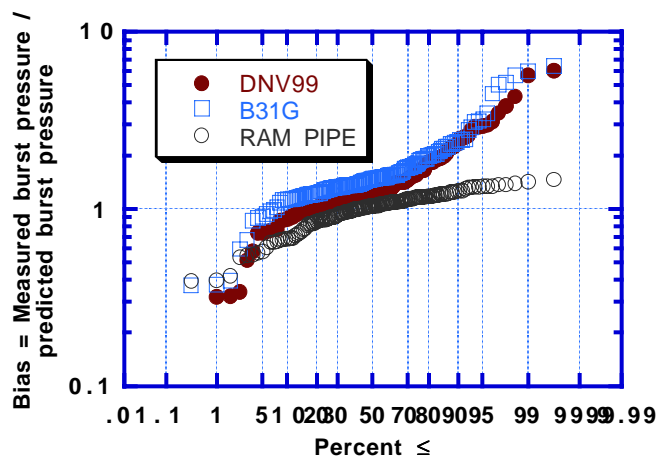


Fig. 10: Bias in burst pressure formulations (Lognormal probability scales)

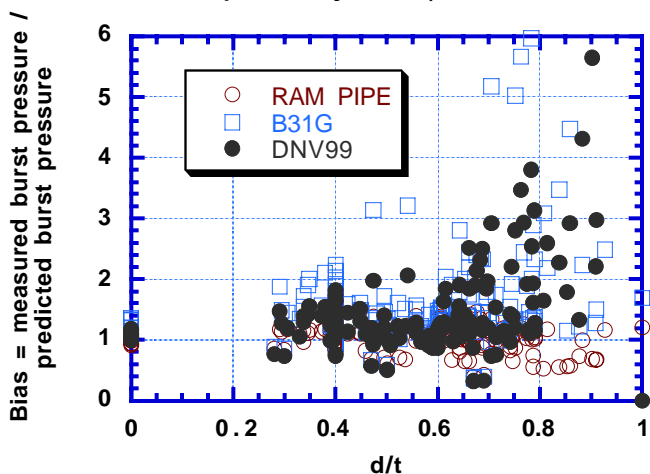


Fig. 11: Bias in burst pressure formulations as function of corrosion depth to wall thickness ratio (d/t)

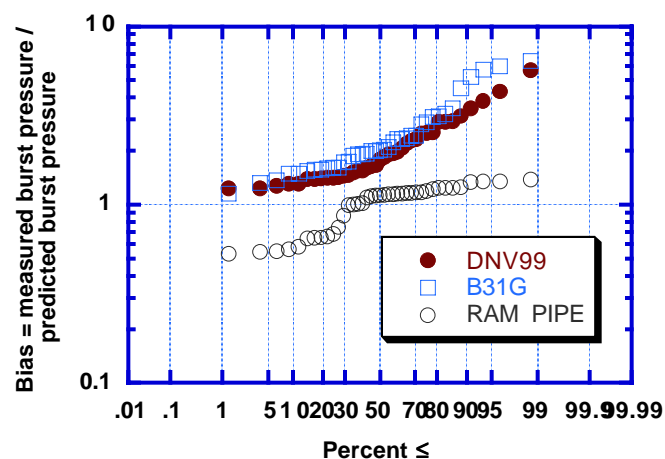


Fig. 12: Bias in burst pressure formulations for naturally corroded test specimens (Lognormal probability scales)

Table 2. Bias statistics for three burst pressure formulations – naturally corroded tests

Formulation	B mean	B ₅₀	V _B %
DNV 99	2.10	1.83	46
B 31 G	2.51	2.01	52
RAM PIPE	1.00	1.10	26

Burst Capacities of Dented & Gouged Pipelines

A database on dented and gouged pipeline tests consisting of 121 tests was assembled from test data published by Battelle Research Corp. and British Gas [10-16]. This database was organized by the sequence of denting and gouging and type of test performed. Study of this test data led to the following observations:

- Plain denting with smooth shoulders has no significant effect on burst pressures. Smooth shoulder denting is not accompanied by macro or microcracking and the dent is re-formed under increasing internal pressures.
- Denting with sharp shoulders can cause macro and micro cracking which can have some effects on burst pressures and on fatigue life (if there are significant sources of cyclic pressures – straining). The degree of macro and micro cracking will be a function of the depth of gouging. Generally, given pressure formed gouging, there will be distortion of the metal and cracking below the primary gouge that is about one half of the depth of the primary gouge.
- Gouging can cause macro and micro cracking in addition to the visible gouging and these can have significant effects on burst pressures. In laboratory tests, frequently gouging has been simulated by cutting grooves in the pipe. These grooves can be expected to have less macro and micro cracking beneath the test gouge feature.
- The combination of gouging and denting can have very significant effects on burst pressures. The effects of combined gouging and denting is very dependent on the history of how the gouging and denting have been developed. Different combinations have been used in developing laboratory data. In some cases, the pipe is gouged, dented, and pressured to failure. In other cases, the pipe is dented and gouged simultaneously, and then pressured to failure. In a few cases, the pipe is gouged, pressured, and then dented until the pipeline loses containment. These different histories of denting and gouging have important effects on the propagation of macro and micro cracks developed during the gouging and denting. It will be very difficult for a single formulation to be able to adequately address all of the possible combinations of histories and types of gouging and denting.
- Gouging is normally accompanied by denting a pipeline under pressure. If the pipeline does not lose containment, the reassessment issue is one of determining what the reliability of the pipeline segment is given the observed denting and gouging. Addressing this problem requires an understanding of how the pipeline would be expected to perform under increasing pressure demands (loss of containment due to pressure) or under continuing

cyclic strains (introduced by external or internal sources). In the case of loss of containment due to pressure, the dent is re-formed under the increasing pressure and the gouge is propagated during the re-forming. Cracks developed on the shoulders of the dents can also be expected to propagate during the re-forming.

The analyses of the laboratory test database on the loss of containment pressure of dented and gouged pipelines was based on:

$$P_{bd} = (2 \text{ SMTS} / \text{SCF}_{DG}) (t / D)$$

where SCF_{DG} is the Stress Concentration Factor for the combined dent and gouge. Two methods were to evaluate the SCF associated with gouging and denting. The first method (Method 1) was based on separate SCF for the gouging and the dent reformation propagation:

$$\text{SCF}_G = (1 - d/t)^{-1}$$

$$\text{SCF}_D = 1 + 0.2 (H/t)^3$$

$$\text{SCF}_{DG} = [(1 - d/t)^{-1}] [1 + 0.2 (H/t)^3]$$

The second method (Method 2) was based on a single SCF that incorporated the gouge formation and propagation:

$$\text{SCF}_{DG} = \{[1 - (d/t) - [16 H/D(1-d/t)]\}^{-1}$$

Fig. 13 summarizes results from analysis of the test database. The dent depths (H) to diameter ratios were in the range $H/D = 1.0\%$ to 3.6% . The gouge defects had depths (h) to wall thickness ratios that were $h/t = 25\%$.

Results of the analyses indicate Method 1 has a median Bias of $B_{50} = 1.2$ and a COV of the Bias of $V_B = 33\%$. Method 2 has a $B_{50} = 1.3$ and $V_B = 25\%$.

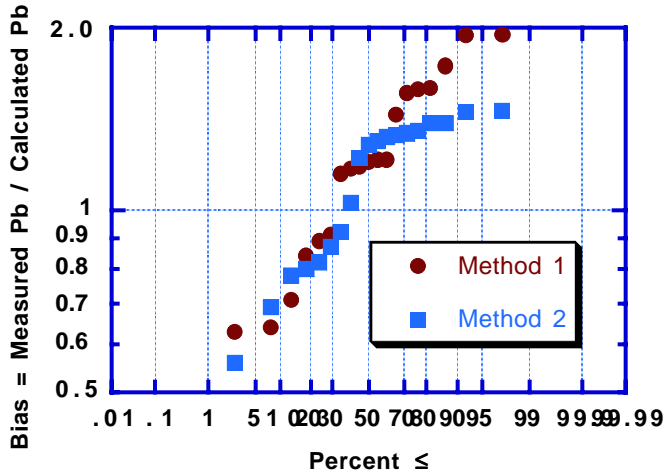


Fig. 13: Analysis of test database on pipelines with dents and gouges

SYSTEMS AND SEGMENTS

In development of the formulation for the probability of failure, it is important to discriminate between pipeline 'segments' and 'systems'. A pipeline system can be

decomposed into sub-systems of a series segments. A series segment is one in which the failure of one of the segments leads to the failure of the system.

A series (weak-link) system fails when any single element fails. In probabilistic terms, the probability of failure of a series system can be expressed in terms of the unions (\cup) of the probabilities of failure of its N elements as [17]:

$$P_{f_{\text{system}}} = (P_{f1}) \cup (P_{f2}) \cup \dots (P_{fN})$$

For a series system comprised of N elements, if the elements have the same strengths and the failures of the elements are independent ($\rho = 0$), then the probability of failure of the system can be expressed as:

$$P_{f_{\text{system}}} = 1 - (1 - P_{fi})^N$$

If P_{fi} is small, as is usual, then approximately:

$$P_{f_{\text{system}}} \approx N P_{fi}$$

If the N segments of the pipeline are independent and have different failure probabilities:

$$P_{f_{\text{system}}} = 1 - \prod_{i=1}^N (1 - P_{fi})$$

If the segments are perfectly correlated then:

$$P_{f_{\text{system}}} = \text{maximum} (P_{fi})$$

There can be a variety of ways in which correlations can be developed in elements and between the segments that comprise a pipeline system. Important sources of correlations include:

- segment to segment strength characteristics correlations, and
- segment to segment failure mode correlations.

The correlation coefficient, ρ , expresses how strongly the magnitudes of two paired variables, X and Y , are related to each other. The correlation coefficient ranges between positive and negative unity ($-1 \leq \rho \leq +1$). If $\rho = 1$, they are perfectly correlated, so that knowing X allows one to make perfect predictions of Y . If $\rho = 0$, they have no correlation, or are 'independent,' so that the occurrence of X has no affect on the occurrence of Y and the magnitude of X is not related to the magnitude of Y . Independent random variables are uncorrelated, but uncorrelated random variables (magnitudes not related) are not in general independent (their occurrences can be related) [17].

Frequently, the correlation coefficient can be quickly and accurately estimated by plotting the variables on a scattergram that shows the results of measurements or analyses of the magnitudes of the two variables. Two strongly positively correlated variables will plot with data points that closely lie along a line that indicates as one variable increases the other variable increases. Two strongly negatively correlated variables will plot with data points that closely lie along a line that indicates as one variable increases, the other variable decreases. If the plot does not indicate any systematic variation in the variables, the general conclusion is that the correlation is very low or close to zero.

In general, samples of paired pipeline segments are strongly positively correlated; tensile strengths, collapse pressures, and burst pressures show very high degrees of correlation (Figs. 14-16) [18]. These test data were taken from samples of delivered pipeline joints and were not intentionally paired from the same plate or runs of steel. High degrees of correlation of pipe properties were also found by Jaio, et al (1997) for samples of the same pipe steel plate.

These results have important implications regarding the relationship between the reliability of a pipeline system and the reliability of the pipeline system elements and segments. The probability of failure of the pipeline system will be characterized by the probability of failure of the most likely to fail element – segment that comprises the system.

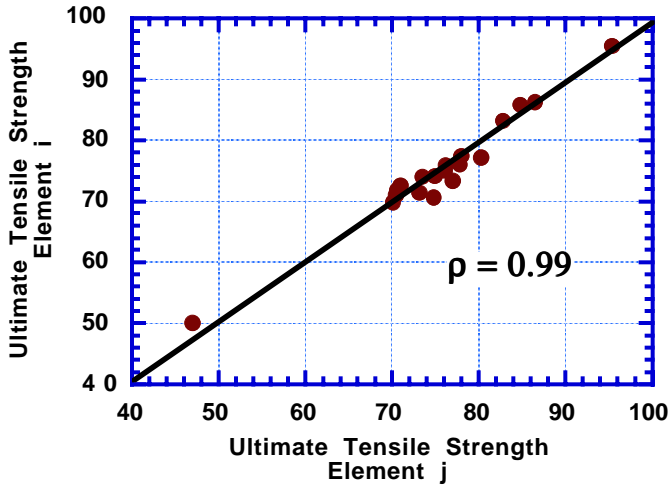


Fig. 14: Correlation of measured ultimate tensile strengths of paired pipeline steel samples from adjacent pipeline segments

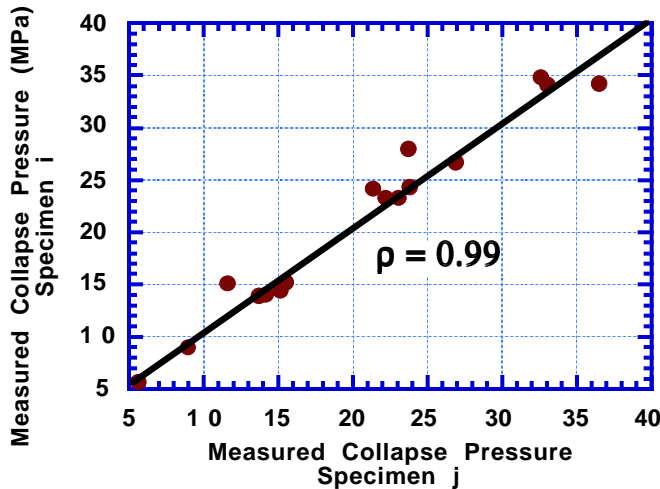


Fig. 15: Correlation of measured collapse strengths of paired steel pipeline samples from adjacent pipeline segments

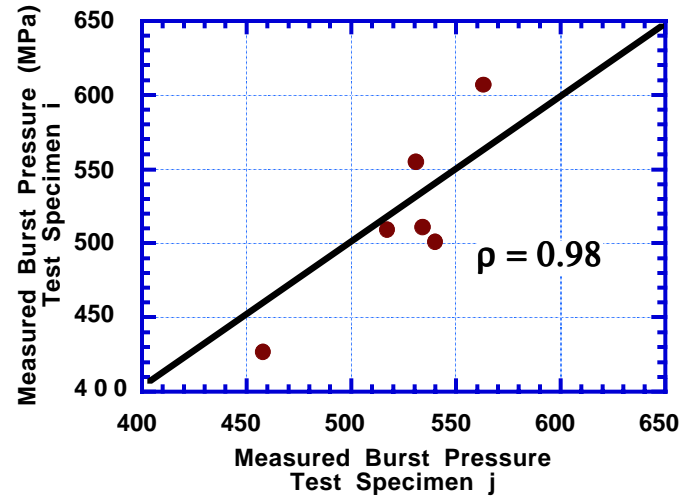


Fig. 16: Correlation of measured burst strengths of paired steel pipeline samples from adjacent pipeline segments

Correlations can also be developed between the failure modes. A useful expression to determine the approximate correlation coefficient between the probabilities of failure of a system's components (or correlation of failure modes) is:

$$\rho_{fm} \approx \frac{V_S^2}{V_R^2 + V_S^2}$$

where V_S^2 and V_R^2 are the squared coefficients of variation of the demand (S) and capacity (R), respectively. It is often the case for pipeline systems that the coefficients of variation of the demands are equal to or larger than those of the capacity. Thus, the correlation of the probabilities of the failure of the system's segments can be very large, and there is a high degree of correlation between the system's failure modes. Again, this indicates that the probability of failure of the system can be determined by the probability of failure of the system's most likely to fail segment.

CONCLUSIONS

A practical formulation has been developed to allow 'real-time' assessments of pipeline likelihoods of LOC (probabilities of failure). This development as involved developing analytical models to evaluate time effects, Biases introduced by different models used to evaluate the LOC pressures, and system versus segment probabilities of failure. Laboratory test data has been used to provide the important parameters for these analytical models.

The real-time RAM formulation is a Level 2 approach in the general pipeline Inspection, Maintenance, and Repair process proposed by Bea, et al [19]. This formulation is consistent with the Risk Based Inspection process proposed by Bjornoy, et al [20]. Verification of the real-time RAM LOC analytical models with field hydro-test to failure data is the subject of a companion paper [21].

The ability to develop real-time estimates of the probabilities of LOC can provide the pipeline owner / operator, pipeline engineers, and regulators with useful additional

information to help guide their decisions regarding pipeline maintenance.

ACKNOWLEDGMENTS

The authors would like to acknowledge the support to perform this research and the permission to publish these results provided by the U.S. Minerals Management Service and Rosen Inspection Inc. The authors also would like to acknowledge the analytical and computational assistance provided by University of California Berkeley Graduate Student Researchers Sang Kim, Angus McLelland, and Ziad Nakat.

REFERENCES

- [1] Lara, L., Matias, J., Heredia, E., and Valle, O., 1998, *Transitory Criteria for Design and Evaluation of Submarine Pipelines in the Bay of Campeche*, First Meeting Report, Instituto Mexicano de Petroleo, Mexico, DF.
- [2] Kiefner, J. F., et al, 1989, *A Modified Criterion for Evaluating the Remaining Strength of Corroded Pipe*, RSTRENG, Project PR 3-805 Pipeline Research Committee, American Gas Association, Houston, TX.
- [3] Mok, D.H.B, Pick, R.J., Glover, A.G. and Hoff, R., 1991, "Bursting of Line Pipe with Long External Corrosion," *International Journal of Pressure Vessel & Piping*, Vol. 46, Applied Science Publishers Ltd, UK., pp 159-216.
- [4] Hopkins, P., and Jones, D.G, 1992, "A Study of the Behavior of Long and Complex-Shaped Corrosion in transmission Pipelines," *Proceedings of the Offshore Mechanics and Arctic Engineering Conference*, Pipeline Symposium, American society of Mechanical Engineers, New York, NY, pp 230-240.
- [5] Chouchaoui, B. A., et al (1992) "Burst Pressure Prediction of Line Pipe Containing Single Corrosion Pits using the Finite Element Methods", *Proceedings 13th International Offshore Mechanics and Arctic Engineering*, Pipeline Symposium, American Society of Mechanical Engineers, New York, NY, pp 11-19.
- [6] Det Norske Veritas, 2000, *Corroded Pipelines, Recommended Practice RP-F101*, Hovik, Norway.
- [7] American Society of Mechanical Engineers (ASME), 1993, *Manual for Determining the Remaining Strength of Corroded Pipelines*, Supplement to ANSI / ASME B31G Code for Pressure Piping, New York, NY.
- [8] Bea, R. G., 2000, "Reliability, Corrosion, and Burst Pressure Capacities of Pipelines," *Proceedings Offshore Mechanics and Arctic Engineering Conference, Safety and Reliability Symposium*, American Society of Mechanical Engineers, New York, NY, pp 1-11.
- [9] Bai, Y., Xu, T., and Bea, R.G., 1997, "Reliability-Based Design & Requalification Criteria for Longitudinally Corroded Pipelines," *Proceedings of the Seventh International Offshore and Polar Engineering Conference*, International Society of Offshore and Polar Engineers, Golden, CO, pp 1-12.
- [10] Kiefner, J.F., Maxey, W.A., Eiber, R.J., and Duffy, A.R., 1973, "Failure Stress Levels of Flaws in Pressurized Cylinders," *Progress in Flaw Growth and Fracture Toughness Testing*, ASTM STP 536, American Society for Testing and Materials, New York, NY, pp 120-135.
- [11] Eiber, R., et al 1981, *The Effects of Dents on the Failure Characteristics of Line Pipe*, Battelle Columbus Report to AGA, NG-18, AGA Catalog No. L51403, Columbus, OH.
- [12] Stephens, D.R., Olson, R.J., and Rosenfeld, M.J., 1991, *Topical Report on Pipeline Monitoring – Limit State Criteria*, Report to Line Pipe Research Supervisory Committee, American Gas Association, Columbus, OH.
- [13] Hopkins, P., 1990, *A Full Scale Evaluation of the Behaviour of Dents and Defects in Linepipe for the European Pipeline Research Group*, British Gas ERS Report R. 4516, British Gas Research & Technology, Newcastle upon Tyne, UK.
- [14] Hopkins, P., Jones, D. G., and Clyne, A.J.m 1989, *The Significance of Dents in Transmission Pipelines*, British Gas plc, Research & Technology, Engineering Research Station, Newcastle upon Tyne, UK.
- [15] Shannon, R.W.E., 1974, "The Failure Behaviour of Line Pipe Defects," *International Journal of Pressure Vessels & Piping*, Applied Science Publishers Ltd, UK.
- [16] Jones, D.G., 1981, *The Significance of Mechanical Damage in Pipelines*, British Gas Corporation, Research & Technology, Engineering Research Station, Newcastle upon Tyne, UK.
- [17] Madsen, H.O., Krenk, S., and Lind, N.C., 1986, *Methods of Structural Safety*, Prentice Hall Inc., Englewood Cliffs, NJ.
- [18] Bea, R. G., Xu, T., Mousselli, A., Bai, Y., and Orsamolu, W., 1998, *RAM PIPE Project, Risk Assessment and Management Based Allowable Stress Design & Load and Resistance Factor Design Stress Criteria & Guidelines for Design and Requalification of Pipelines and Risers in the Bay of Campeche, Mexico*, Phase 1, Reports 1 through 6, Reports to Petroleos Mexicanos and Instituto Mexicano de Petroleo, Mexico DF.
- [19] Bea, R. G., Farkas, B, Smith, C., Rosenmoller, J., Valdes, V., and Valle, O., 1999, "Assessment of Pipeline Suitability for Service," *Proceedings 9th International Offshore and Polar Engineering Conference & Exhibition*, Society of Offshore and Polar Engineers, Golden, CO., pp 347-354.
- [20] Bjornoy, O.H., Jahre-Nilsen, C., Marley, M.J., and Williamson, R., 2001, "RBI Planning for Pipelines, Principles and Benefits," *Proceedings of the Offshore Mechanics and Arctic Engineering Conference*, Pipeline Symposium, OMAE/01-PIPE4007, American Society of Mechanical Engineers, New York, NY., 1-6
- [21] Bea, R. G., Smith, C., Smith, R., Rosenmoeller, J., and Beuker, T., 2002, "Analysis of Field Data from the Performance of Offshore Pipelines (POP) Project," *Proceedings of the Offshore Mechanics and Arctic Engineering Conference, Pipeline Symposium*, OMAE/02-PIPE28323, American Society of Mechanical Engineers, New York, NY, pp 1-XX.

OMAE 2002/PIPE-28323

ANALYSIS OF FIELD DATA FROM THE PERFORMANCE OF OFFSHORE PIPELINES (POP) PROJECT

Robert Bea
University of California at Berkeley
Berkeley, California USA

Charles Smith and Bob Smith
U.S. Minerals Management Service
Herndon, Virginia USA

Johannes Rosenmoeller, Thomas Beuker, and Bryce Brown
ROSEN Pipeline Inspection
Lingen, Germany and Houston, Texas, USA

ABSTRACT

The Performance of Offshore Pipelines (POP) joint industry – government agency sponsored project was conceived to test pipelines in the field to allow verification of procedures used to analyze their potential loss of containment characteristics. This paper summarizes a series of analyses performed to predict the loss of containment (LOC) characteristics of one pipeline in the Gulf of Mexico. The oil pipeline tested had been in service for 22 years and was scheduled for removal. The pipeline was in-line instrumented, and then hydro-tested to failure. The failure section and other sections of the pipeline that had indicated significant corrosion features were retrieved and the geometric and material properties of the failure section and the other sections determined. LOC pressure forecasts were done in three stages: 1) before field testing, 2) after in-line instrumentation was performed and the data analyzed, and 3) after geometry measurements and materials testing. The LOC pressure and location determined during the field test were not released to the analysts until after all of the forecasts were completed and documented. This paper summarizes the results from the analyses of the field and laboratory test results to forecast the LOC pressure and compares the forecasts with the hydro-test results.

Keywords: Pipelines, Hydro-Test, Corrosion, Burst Pressures, Loss of Containment

INTRODUCTION

For offshore pipelines, the major cause of loss containment is corrosion [1-3]. Analytical methods used to predict the loss of containment (LOC) for corroded pipelines have been calibrated / verified based primarily on results from laboratory tests, and lately, based on results from numerical experiments [4-7]. The majority of the laboratory tests have been performed on pipeline specimens in which corrosion features were simulated with machined features [4, 6]. Recently, results from laboratory tests performed on specimens with machined features have been used to calibrate finite element analysis (FEA) models that have been used to perform ‘numerical experiments’ [5, 8]. Data from these numerical experiments have been used to develop statistical characterizations important to reliability based analysis of LOC pressures [4, 9].

There are important concerns about the Biases (actual LOC pressure / predicted or nominal LOC pressure) introduced by both laboratory tests and numerical tests [7]. Laboratory test concerns center on the machined features (shapes, residual stresses, metallurgical effects) and ‘end boundary condition effects’. Numerical test concerns how they have been calibrated, how the parametric variations are performed (e. g. treatment of parameter correlations), the characteristics used for the parametric statistical characterizations, and the omission of the uncertainties introduced by the FEA model itself.

Input for analytical model predictions of LOC pressure come from a variety of sources. Basic characteristics on the pipeline (e.g. diameter, wall thickness, material properties,

maintenance, product, operating pressures) come from the pipeline owner / operator. But, often for smaller and older pipelines, only the most fundamental information (e.g. diameter, material) is available and the other information must be gathered from a variety of other sources – or assumed. Sometimes, for larger diameter pipelines in-line instrumentation data is available or can be gathered. But, there are important questions regarding the detection of features and the accuracy and reliability of the interpreted data, particularly when the data has been gathered at different times using different in-line instrumentation and interpretation processes. For many pipelines, in-line instrumentation data is not available or can not be developed and LOC analysis must be based on indirect information on the condition and characteristics of the pipeline. All of these factors involve significant uncertainties resulting in similar uncertainties in the forecast LOC pressures.

For these and related reasons, a testing program was undertaken in which pipelines that had been in service and that were about to be removed from service would be hydro-tested to failure. The effort was identified as the POP (Performance of Offshore Pipelines) joint industry – government – classification society sponsored project. The project was organized and managed by Winmar Consulting Services in Houston, Texas during the period 1999-2001.

This paper summarizes a series of analyses performed to predict the LOC characteristics of one pipeline in the Gulf of Mexico (GOM). The oil pipeline (identified as Line 25) had been in service for 22 years and was scheduled for removal. The pipeline was first surveyed in the field to confirm the fundamental characteristics of the pipeline (diameter, wall thickness). The pipeline was then in-line instrumented ('smart pigged'), and then hydro-tested to failure - LOC. The failure section was retrieved and several other sections that had indicated significant corrosion features and the geometric and material properties of the failure and other sections determined.

The analytical effort involved a series of 'blind' forecasts to predict the pressure at which the pipeline would burst or lose containment. LOC pressure forecasts were done in three stages: 1) before field testing, 2) after in-line instrumentation and data analysis, and 3) after geometry measurements and materials testing. The LOC pressure and location determined during the field test were not released to the analysts until after all of the forecasts were completed and documented. The analytical strategy was to make the LOC predictions based on progressively more information from the field testing and to avoid influence of the knowledge of the pressure test results on the analytical predictions.

BURST PRESSURE ANALYTICAL MODELS

Four analytical models to predict the LOC pressure were used: ASME B31G, DNV RP101, ABS 2001, and RAM PIPE [10-13]. Both deterministic and probabilistic analyses were performed. The probabilistic analyses recognized Biases (Type 2 or model uncertainties) and variabilities (Type 1 or natural – inherent uncertainties) associated with the predicted LOC pressures. For the deterministic forecasts, all 'design factors'

explicitly included in the LOC analytical models were set at unity.

The analytical formulations to forecast the LOC pressures are summarized in Appendix A. Recently, two of these analytical models (B31G, DNV RP101) were used in a study of laboratory and numerical FEA data on burst pressures of corroded pipelines [14]. As a part of the POP project, this database was reanalyzed using these two models and the RAM PIPE model [15]. In the POP project analyses, the numerical FEA 'test' data included in the database were excluded and only physical laboratory tests were included. Table 1 summarizes the results from both sets of analyses. The results are summarized in terms of the statistical measures of the Bias where Bias is defined as the ratio of the test LOC pressure to the predicted pressure. Three statistical characteristics are used: the mean (\bar{B} = average) and median (B_{50} = 50th percentile) Bias and the coefficient of variation of the Bias (V_B = ratio of standard deviation of B to mean value of B). These characteristics reflect the central tendency and variability - uncertainty associated with the analytical models. The 'best' model would be one that had the mean / median bias closest to unity and the lowest coefficient of variation of the Bias.

It is important to note the magnitudes of these statistical characteristics of the model Bias and how the Bias varies depending on what is included or excluded from the 'test' database. The acknowledged large positive (conservative) central tendency Bias associated with B31G is evident in all of these results. Note also the large uncertainties associated with the results from the analytical predictions. Also note that the RAM PIPE model has the lowest central tendency Bias and the lowest coefficient of variation of the Bias.

Similar results have been found in parallel studies of Bias associated with the three predictive methods [7, 16, 17]. In these studies, the analysis of Bias was founded solely on a database of laboratory test results (151 tests) developed at the University of California at Berkeley (UCB). The Bias was determined for the entire database that included both machined and natural corrosion features (Table 2). The Bias was also determined for the database that included results for only specimens with natural corrosion features (Table 3).

It is apparent that there is an important difference in the results that include and exclude machined corrosion features. Comparison of the mean and median Biases in Tables 2 and 3 show that the machined corrosion features are introducing 'stress effects' that lower the laboratory test burst pressures. Again, the RAM PIPE has the central tendency Bias closest to unity and the lowest coefficient of variation of the Bias of the three models. The DNV model has a lower central tendency Bias than B31G and a comparable coefficient of variation of the Bias. The DNV model is able to eliminate some of the conservative Bias in the B31G model, but is not able to significantly impact the Type 3 model uncertainty (coefficient of variation of the Bias). These Bias uncertainties are significantly greater than those used in development of the DNV guidelines [4, 5, 9].

The probabilistic analyses performed during the POP project included these characterizations of Bias associated with the analytical models. The ABS 2001 model was not included

in these analyses because it has been published only relatively recently.

Table 1: Analytical model bias based on numerical FEA and laboratory burst pressure database developed by MSL [14]

	B31G		DNV		RAM PIPE	
	MSL	POP	MSL	POP	MSL	POP
\bar{B}	1.49	1.53	1.78	1.73	NA	0.91
B_{50}	1.40	1.52	1.72	1.48	NA	1.0
$V_B \%$	23	36	15	57	NA	34

Table 2: Analytical model bias based on numerical FEA and laboratory burst pressure database developed by UCB [7]

Formulation	B mean	B median	$V_B \%$
DNV	1.46	1.22	56
B31G	1.71	1.48	54
RAM PIPE	1.01	1.03	22

Table 3: Analytical model bias based on laboratory burst pressure database developed by UCB [7]

Formulation	B mean	B median	$V_B \%$
DNV	2.10	1.83	46
B31G	2.51	2.01	52
RAM PIPE	1.00	1.10	26

PIPELINE 25

Pipeline 25 had a nominal diameter of 8.625 inches, a nominal wall thickness of 0.5 inches and was made of API Grade B steel with a specified minimum yield strength (SMYS) of 42 ksi and a specified minimum tensile strength of 60 ksi. The pipeline was used to transfer treated oil from one platform (B) in 98 feet of water to another production platform (A) in the same water depth located 9,200 feet from Platform B.

Table 4 summarizes the results from each of the four LOC pressure models for the intact (no defects) pipeline. There are substantial differences in the forecasts LOC pressures even for the case of the pipeline with no defects. The RAM PIPE model results in the largest LOC pressures for the no defect condition. Comparison of the RAM PIPE LOC pressure model with laboratory test data on pipelines without defects indicates that it has a median Bias close to unity and a coefficient of variation of the Bias of about 20% [7].

Table 4: LOC pressures for Line 25 without defects

Method	Pb - psi
B31G	4,900
DNV	7,400
ABS	5,200
RAM PIPE	8,300

HYDRO-TEST RESULTS

The results from the hydro-test will be given at this point to facilitate discussion of the analytical forecast results. The pipeline failed at a point 6,793 feet from the pig launcher on Platform B. The pipeline failed at a hydro-test pressure of 6,794 psi.

FIRST ROUND ANALYSIS

The first sequence of predictions were made with the four LOC models before the pipeline was tested. This required the use of a model to predict the corrosion defects that could be present in the pipeline; no other damage or defects were known to exist along the length of the pipeline. The analytical models were used to make two types of predictions: deterministic and probabilistic. The probabilistic models incorporated the uncertainties associated with the prediction of corrosion and prediction of the burst pressures.

The analytical model that was used was one based on results from a study of pipeline corrosion data from GOM pipelines [3]:

$$tc = \alpha_i \cdot v_i \cdot (L_s - L_p)$$

where tc is the wall loss due to corrosion, α is a corrosion protection or inhibition efficiency factor v is an average corrosion rate (based on the transported product), L_s is the service period, and L_p is the initial period before corrosion is initiated. Based on the historic data that was available on this pipeline, the following values were used: $\alpha = 3$, $v = 3.94E-3$ inches per year, $L_p = 10$ years, and $L_s = 22$ years. The result indicated an expected maximum wall loss of 0.15 inches or 30% of the thickness. The uncertainty associated with this forecast wall thickness loss was 30% (coefficient of variation). For those models that required an area of corrosion in addition to the depth of corrosion, corrosion features that had areas of 1.0 square inches (lengths and widths of 1 inch) were assumed (corrosion pits); all of the analytical models are insensitive to features with these areas (Fig. 1).

Table 5 summarizes the results for the forecast corrosion condition. Results are given for both the LOC pressure and a prediction Bias (B_{pb}). The prediction Bias (B_{pb}) is the ratio of the measured maximum LOC pressure for Line 25 (6,794 psi) to the predicted LOC pressure. It is reiterated that at the time these forecasts were developed, the results from the field tests were not available to the analysts.

The DNV and RAM PIPE methods have the Bias closest to unity while the B31G and ABS methods have much larger Biases.

Table 5: First Round LOC pressure Biases

Method	B_{pb}
B31G	1.35
DNV	0.97
ABS	1.79
RAM PIPE	1.19

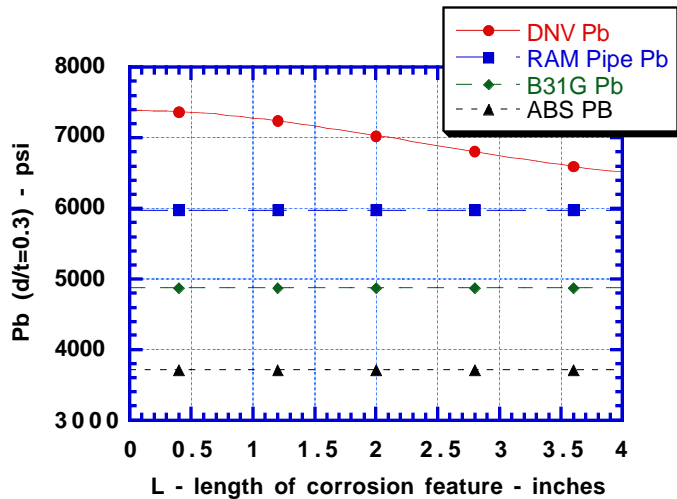


Fig. 1: Forecast LOC pressures (Pb) for different lengths (same widths) of corrosion features with maximum depth of corrosion of 30% of wall thickness

SECOND ROUND ANALYSIS

The second sequence of predictions were made with the four LOC models based on results from the in-line test data. The in-line tests were performed and analyzed by ROSEN USA personnel based in Houston, Texas with assistance provided by ROSEN Technology & Research Center in Lingen, Germany. The tests were performed using one of ROSEN's advanced MFL (magnetic flux leakage) in-line 'smart pigs'. Scraper pigs were used to thoroughly clean the line before the MFL tool was run. The test results were analyzed using ROSEN's standardized interpretation guidelines applied by a trained and experienced interpreter.

The results in terms of feature depths reported as percentage of the line wall thickness are summarized in Fig. 2. The different types of features and their lengths and widths also were identified (Fig. 3). Distances are identified from the pig launcher on Platform B to the pig receiver on Platform A.

The minimum wall thickness segments (about 50% wall loss) of the pipeline are adjacent to the risers; within about 1000 feet of Platform B and 500 feet of Platform A. The features are all relatively small with lengths and widths in the range of 1 to 2 inches. The feature (corrosion) depth in the failed section was identified as 22%, the width as 1.5 inches, and the length as 0.5 inches. Even though there were reported features that had much greater depths and areas, the pipeline did not fail at these points. Note the feature characteristics in the range of 100 to 200 feet from the Platform B launcher. These features (corrosion) have depths in the range of 45% to 50% of the wall thickness. This section of the pipeline was retrieved after the hydro-test had been completed and these in-line instrumentation results will be compared with what was measured on the retrieved section of the pipeline.

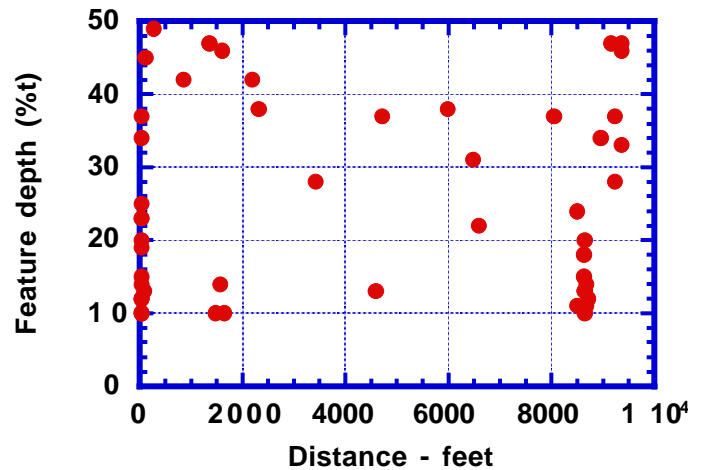


Fig. 2: Reported feature depths from interpretation of Rosen MFL in-line instrumentation data

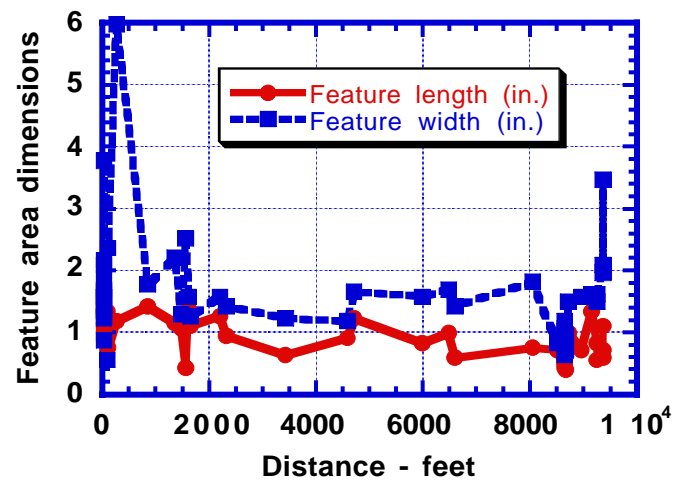


Fig. 3: Feature lengths and widths from interpretation of MFL in-line instrumentation data

Figure 4 summarizes the results from the second round analyses for the RAM PIPE formulation in terms of the forecast LOC pressure (Pb). Two forecasts are shown, one for the RAM PIPE as formulated and one that included a median Bias (1.1) identified from the analyses of laboratory test data summarized earlier (Table 3 for natural corrosion features). The lowest burst pressures are forecast to be in the range of 6,000 psi to 7,000 psi. These low burst pressures are associated with the minimum wall thickness segments of the pipeline. The forecast burst pressure in the failed section was in the range of 6,400 psi to 7,200 psi. These pressures bracketed the measured LOC pressure of 6,794 psi.

The probabilities of failure (2) for given internal pressures along the length of the pipeline based on the RAM PIPE forecasts are summarized in Fig. 5. The results indicate that there is about a 50% probability of LOC at a pressure of 5,200 psi and more than a 90% probability of LOC at a pressure of 7,700 psi. The total uncertainty used in these probabilistic analyses ranged between 22% and 27%. No Bias and

uncertainty were attributed to the input parameters other than the Type 2 Bias associated with the analytical model.

Fig. 6 summarizes the deterministic results for all of the four analytical models based on the input derived from the in-line instrumentation data results. The lowest LOC pressures are those from the B31G and ABS models. The highest LOC pressures are from the DNV and RAM PIPE models. The highest minimum pressures are about 7,500 psi and the lowest minimum pressures are about 2,500 psi. The forecast LOC pressures in the failure section (at 6,793 feet) range from about 4,000 psi to 7,500 psi.

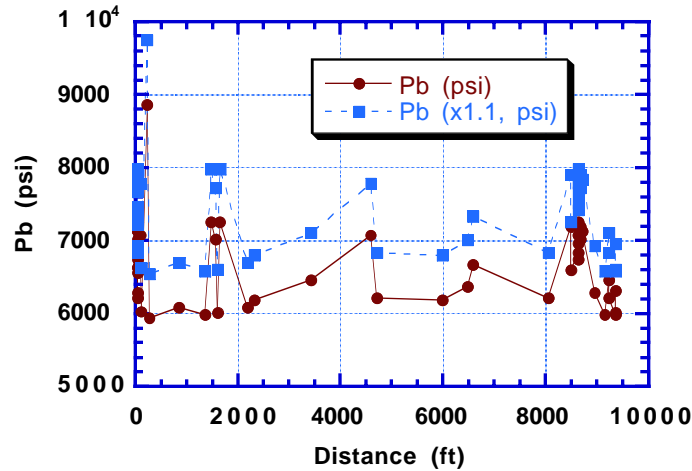


Fig. 4: Second round RAM PIPE based LOC pressures

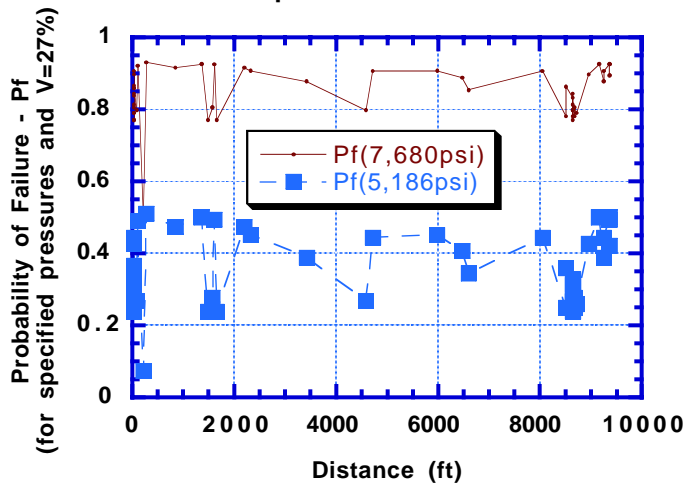


Fig. 5: Second round RAM PIPE based probability of LOC results

Table 6 summarizes the field test Bias (measured LOC pressure / predicted LOC pressure at the failed section) from the second stage analyses. The RAM PIPE method has the Bias closest to unity, followed by the DNV method. The B31G and ABS methods have much larger Biases.

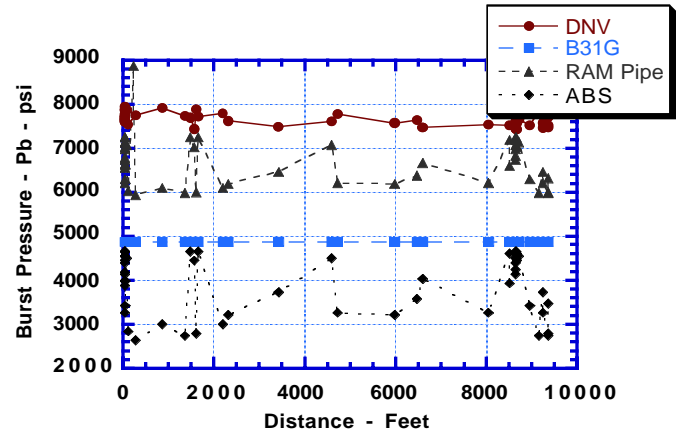


Fig. 6: Second round LOC pressures

Table 6: First Round LOC pressure Biases

Method	B_{Ph}
B31G	1.39
DNV	0.90
ABS	1.84
RAM PIPE	1.02

THIRD ROUND ANALYSIS

The third sequence of predictions were made with the four LOC models based on the results from the in-line test data and the results from the laboratory tests performed on the section of pipeline that had ruptured. In addition, sections of the pipeline between 98 feet (end of riser tube turn) and 224 feet from the Platform B pig launcher were retrieved because the in-line instrumentation had indicated severe corrosion features in this segment (Figs. 2 and 3).

The laboratory tests were performed and analyzed by Stress Engineering Services Inc. of Houston, Texas [18]. The tests included detailed measurements of the diameters, wall thicknesses, and material properties including longitudinal and transverse coupon tensile stress-strain tests from the retrieved sections of the pipeline.

A picture of the ruptured section of the pipeline is shown in Fig. 7. The fracture initiation site is indicated on the photograph. Based on detailed examinations of the fracture surfaces and failed section, the failure originated at an inclusion (lamination) in the pipe wall. Once rupture was initiated it propagated along the pipe axis in both directions until it reached 'thicker' material where the fracture bifurcated at both ends of the crack. The features on the fracture walls indicated a brittle crack propagation.

There was very little corrosion in the vicinity of the failed section. There was obvious thinning of the pipeline wall due to the pressure induced expansion (Fig. 8). The measured maximum (D1) and minimum (D2) diameters in the section of pipe that was retrieved are summarized in Fig. 9. The measured wall thicknesses in this same section of pipe are summarized in Fig. 10 (taken 90 degrees apart around circumference). Note that there were adjacent sections that experienced much greater expansions and wall thinning as a result of the hydrotesting.

The wall thickness of the sections that did not rupture coupled with the expanded diameters of these sections indicated that there was essentially no loss of material due to corrosion (volume of material constant).

Materials tests on this section of the pipeline (Table 7) indicated significantly lower tensile strengths than were found from other segments of the pipeline that were retrieved. All of the tensile tests indicated both yield and tensile strengths that substantially exceeded the nominal properties.

Other sections of the pipeline had apparently been expanded significantly during the hydro-test but failed to loose containment before this section of the pipeline failed. The maximum reduced wall thickness in the corroded section of the pipeline retrieved from the pipeline near Platform B indicated a maximum wall thickness loss of 33%. This correlated with a maximum wall thickness loss of 33% to 45% based on the in-line instrumentation data interpretation.

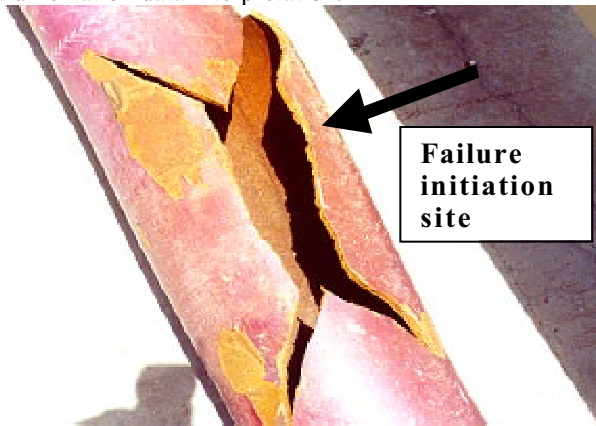


Fig. 7: Failed section of pipeline 25

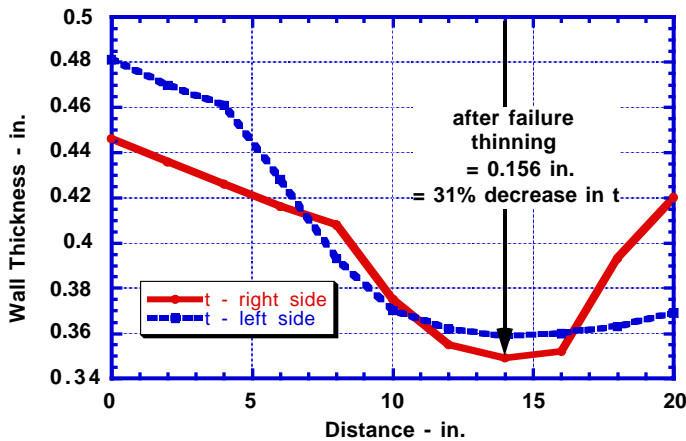


Fig. 8: Profiles of wall thickness along length of failed section

Table 8 summarizes the Biases from the third round of forecasts based on the measured mean values of the yield and tensile strengths for the failed section and for the non-failed section. The range of Bias is due to the range in the measured strengths. The DNV and RAM PIPE forecasts have comparable Biases; both close to unity. The B31G and ABS forecasts have comparable Biases that are much larger than unity.

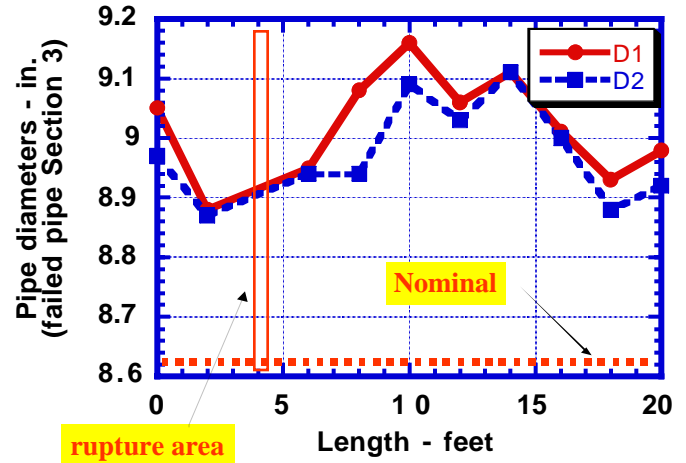


Fig. 9: Maximum and minimum diameters of failure section

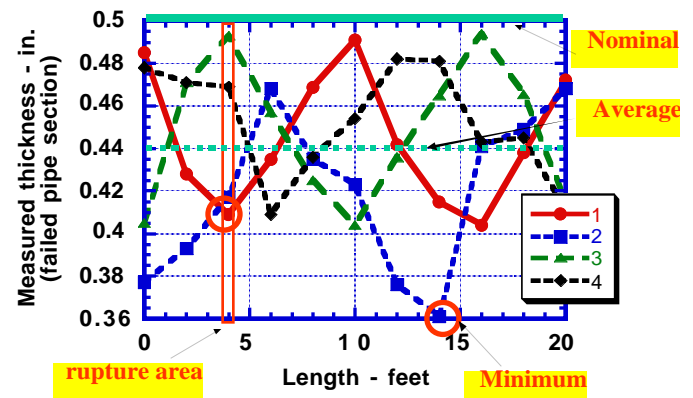


Fig. 10: Wall thickness of failed section at 'clock' positions (1 = 12 o'clock)

Table 7: Summary of material characteristics of failure section and non-failed section of pipeline 25

	Yield Strength E = 2%, psi	Ultimate Tensile Strength, psi
Longitudinal Failed section	53,600	71,600
Non failed section	47,200	80,000
Transverse Failed section	60,100	69,400

Table 8: Third Round LOC pressure Biases

Method	B _{Pb}
B31G	1.28-1.45
DNV	0.81-0.91
ABS	1.21-1.38
RAM PIPE	0.98-0.98

SUMMARY

A summary of the results for the three rounds of forecasts is given in Table 9. The DNV and RAM PIPE forecasts consistently have the Biases closest to unity. The ABS and B31G consistently have the Biases that are much larger than unity.

The Biases summarized in Table 9 are not only the result of the Biases inherent in the analytical models used to forecast the LOC pressures. There are biases that are introduced by the parameters that are used in these analytical models. The corrosion features geometric characteristics are uncertain and the material properties are similarly uncertain. There is even some variability that is introduced by the pipeline geometric characteristics; the diameter and wall thickness. All of this uncertainty should be taken into account when forecasts are developed for LOC pressures; this indicates the need for an analytical process that is founded on probabilistic methods.

This field test contained some surprises. The pipeline was extremely 'robust' after 22 years of continuous service. Even though corroded and with inevitable defects, it was able to sustain in excess of 6,000 psi before it lost containment.

The pipeline LOC pressure was reasonably well predicted by the analytical models based on the input that was provided to these models. However, the extent of corrosion based on the in-line data was not found in the failure section. In addition, the pipeline did not fail where it was predicted to fail by any of the LOC analytical models. Even though there was significant corrosion in segments of the pipeline that were retrieved (up to 33% to 45% in the non-failed retrieved segments), the pipeline failed at a section where there was an unexpected and undetected flaw (inclusion, lamination) and a lower tensile strength.

Even though the First Round LOC pressures were based on a relatively crude corrosion projection model, the LOC pressure Bias was very close to that developed based on results from the in-line instrumentation in the Second Round. This is not an accident because the crude corrosion model was partly based on the analysis of results from in-line instrumentation on other pipelines. Information from in-line instrumentation can provide useful information for pipelines that have not or can not be instrumented.

Table 9: Summary of LOC Biases from three rounds of predictions

Method / Round	#1	#2	#3
B31G	1.40	1.39	1.28-1.45
DNV	0.97	0.90	0.81-0.91
ABS	1.79	1.84	1.21-1.38
RAM PIPE	1.19	1.02	0.98-0.98

ACKNOWLEDGMENTS

The authors would like to acknowledge the support provided by the POP project sponsors and for their permission to publish these results. The POP project sponsors included: the American Bureau of Shipping, the California State Lands Commission, the U.S. Department of Transportation, Nuevo Energy Inc., Chevron Petroleum Technology, Co., Natural Resources Canada, Shell International Exploration, the U.S.

Minerals Management Service, ROSEN USA and ROSEN Technology & Research Center.

The authors would also like to acknowledge the efforts of Winmar Consulting Services, Inc. as the project manager and director, ROSEN Pipeline Inspection for performing the in-line instrumentation and analyzing the data, and Stress Engineering Services Inc. for performing the laboratory tests to characterize the geometric and material properties of the retrieved segments of the pipeline.

The authors would like to acknowledge the analytical and computational assistance provided by University of California Berkeley Graduate Student Researchers Angus McLelland, Elizabeth Schreiber and Ziad Nakat.

REFERENCES

- [1] Kvernfold, O., Johnson, R., and Helgersen, T., 1992, "Assessment of Internal Pipeline Corrosion", *Proceedings International Conference on Offshore Mechanics and Arctic Engineering*, Vol. 4, American Society of Mechanical Engineers, New York, NY, pp 100-107.
- [2] Bea, R. G., Smith, C., and Valdes, V., 1999, "Requalification and Maintenance of Marine Pipeline Infrastructure," *Journal of Infrastructure Systems*, American Society of Civil Engineers, Herndon, VA, pp 89-96.
- [3] Advanced Mechanics & Engineering Ltd., 1995, *PARLOC 94: The Update of Loss of Containment Data for Offshore Pipelines*, Heath and Safety Executive – Offshore Technology Report, OTH 95 468, , London, UK.
- [4] Bjorney, O.H., Cramer, E.H., and Sigurdson, G., 1997, "Probabilistic Calibrated Design Equation for Burst Strength Assessment o Corroded Pipes," *Proceedings of Seventh International Offshore and Polar Engineering Conference*, International Society of Offshore and Polar Engineers, Golden, CO., pp 189-196.
- [5] Kiefner, J.F., Vieth, P.H., and Roytman, I., 1996, *Continued Validation of RSTRENG, Final Report*, Line Pipe Research Supervisory Committee Pipeline Research Committee, PRC International, Worthington, OH.
- [6] Bjornoy, O.H., and Marley, M.J., 2001, "Assessment of Corroded Pipelines: Passt, Present and Future," *Proceedings International Offshore and Polar Engineering Conference*, Vol. II, International Society of Offshore and Polar Engineers, Golden, CO., pp 93-101.
- [7] Stephens, D.R., and Francini, R.B., 2000, "A Review and Evaluation of Remaining Strength Criteria for Corrosion Defects in Transmission Pipelines," *Proceedings of ETCE/OMAE 2000 Joint Conference*, American Society of Mechanical Engineering, New York, NY., pp 1-11.
- [8] Bjornoy, O.H., Sigurdsson, G., and Marley, M.J., 2001, "Background and Development of DNV-RP-F101 Corroded Pipelines," *Proceedings International Offshore and Polar Engineering Conference*, Vol. II, International Society of Offshore and Polar Engineers, Golden, CO., pp 102-109.
- [9] Collberg, L., Mork, K.H., and Marley, M.J., 2001, "Inherent Safety Level in Different Pressure Containment Criteria," *Proceedings Eleventh International Offshore and Polar Engineering Conference*, International Society of Offshore and Polar Engineers, Golden, CO.

[10] American Society of Mechanical Engineers (ASME), 1986, *Manual for Determining the Remaining Strength of Corroded Pipelines*, ASM B31G, ASME, New York, NY.

[11] Det Norske Veritas (DNV), 2000, *Recommended Practice for Corroded Pipelines*, RP F-101, Oslo, Norway.

[12] American Bureau of Shipping (ABS), 2001, *Guideline for Building and Classing Subsea Pipeline Systems and Risers*, ABS Plaza, Houston, TX.

[13] Bea, R. G., 2000, "Reliability, Corrosion, & Burst Pressure Capacities of Pipelines," *Proceedings International Conference on Offshore Mechanics & Arctic Engineering*, OMAE2000-6112, American Society of Mechanical Engineers, New York, NY, pp 1-11.

[14] MSL Engineering Ltd., 2000, *Appraisal and Development of Pipeline Defect Assessment Methodologies*, Report to US Minerals Management Service, Herndon, VA.

[15] Bea, R.G. and Mclelland, A., 2001, *POP Performance of Offshore Pipelines Project Spring 2001 Report*, Report to Joint Industry Project, Berkeley, CA.

[16] Bea, R.G. and Xu, T., 1999, "Evaluation of Biases and Uncertainties in Reliability Based Pipeline Requalification Guidelines," *Proceedings Pipeline Requalification Workshop*, Offshore Mechanics and Arctic Engineering Conference, St. Johns, Newfoundland, American Society of Mechanical Engineers, New York, NY.

[17] Bai, Y., Xu, T., and Bea, R. G., 1997, "Reliability Based Design and Requalification Criteria for Longitudinally Corroded Pipelines," *Proceedings International Conference on Offshore and Polar Engineering*, Vol. II, International Society of Offshore and Polar Engineers, Golden, CO, pp 23-33.

[18] Stress Engineering Services Inc., 2001, *Pipe Survey and Coupon Tests*, Report to Winmar Consulting Services, Houston, TX.

APPENDIX A – SUMMARY OF BURST PRESSURE ANALYTICAL MODELS

ASME B-31G

$$P' = 1.1P \left[\frac{1 - \frac{2}{3} \left(\frac{d}{t} \right)}{1 - \frac{2}{3} \left(\frac{d}{t \sqrt{A^2 + 1}} \right)} \right]$$

$$A = 0.893 \left(\frac{L_m}{\sqrt{Dt}} \right) \leq 4$$

P' = safe maximum pressure for the corroded area $\leq P$

Lm = measured longitudinal extent of the corroded area, inches

D = nominal outside diameter of the pipe, inches

t = nominal wall thickness of the pipe, inches

d = measured depth of the corroded area

P = the greater of either the established MAOP or P = SMYS*2t*F/D

(F = design factor, usually equal to .72, = 1.0 for Pb analyses)

DNV RP-F101

$$P_f = \frac{2 \cdot t \cdot UTS (1 - (d/t))}{(D - t) \left(1 - \frac{(d/t)}{Q} \right)}$$

$$Q = \sqrt{1 + .31 \left(\frac{L}{\sqrt{D \cdot t}} \right)^2}$$

Pf = failure pressure of the corroded pipe

t = uncorroded, measured, pipe wall thickness

d = depth of corroded region

D = nominal outside diameter

L = length of corroded region

Q = length correction factor

UTS = ultimate tensile strength

ABS 2001

$$P_b = \eta \text{ SMYS } (t - t_c) / R_o$$

R_o = (D - t) / 2

SMYS - specified minimum yield strength

η - utilization factor = 1.0

t - pipe nominal wall thickness

t_c - pipe corrosion thickness

D - pipe nominal outer diameter

RAM PIPE

$$P_{bd} = \frac{3.2 \cdot t_{nom} \cdot \text{SMYS}}{D_o \cdot \text{SCF}}$$

$$P_{bd} = \frac{2.4 \cdot t_{nom} \cdot \text{SMTS}}{D_o \cdot \text{SCF}}$$

$$\text{SCF} = 1 + 2 \cdot (d/R)^{.5}$$

P_{bd} = burst pressure

t_{nom} = pipe wall nominal thickness

D_o = mean pipeline diameter (D-t)

SMYS = Specified Minimum Yield Strength

SMTS = Specified Minimum Tensile Strength

SCF = Stress Concentration Factor

d = t_c = depth of corrosion

R = D_o/2

OMAE 2002/S&R-28195

RELIABILITY BASED DESIGN CRITERIA FOR INSTALLATION OF PIPELINES IN THE BAY OF CAMPECHE, MEXICO: PART 1

Robert Bea and Tao Xu

University of California
Berkeley, CA 94720-1712
bea@ce.berkeley.edu

Ernesto Heredia-Zavoni, Leonel Lara, and Rommel Burbano

Instituto Mexicano Del Petroleo
Del. Gustavo A Madero 07730, Mexico, DF
eheredia@www.imp.mx

ABSTRACT

Studies have been performed to propose reliability based design criteria for the installation of pipelines in the Bay of Campeche, Mexico. This paper summarizes the reliability formulations that were used to develop Allowable Stress Design and Load and Resistance Factor Design guidelines for Ultimate Limit State conditions, background on the target reliabilities that were used in the development, and the methods that were used to characterize the demands (loads, displacements) induced in pipelines during their installation. This paper summarizes data that was gathered during the installation of pipelines in the Bay of Campeche to help define the Biases (actual stresses / calculated stresses) associated with the analytical model used to predict installation demands. These results are compared with those published previously based on other field and laboratory tests. A companion paper details the analyses of pipeline Ultimate Limit State capacities and the Biases associated with these capacities.

INTRODUCTION

The design criteria and guideline formulations summarized in this paper are conditional on the following premises:

- The pipelines will be fabricated, installed, operated, and maintained according to current API [1], DNV [2], and ASTM [3] guidelines.
- The pipelines will be installed in water depths less than 100 m. The pipelines will be installed using conventional

lay barges using S-lay techniques. The pipelines will have diameter to thickness ratios of 20 to 80.

- The installation design analytical models used in this study were based in so far as possible on analytical procedures that are founded on fundamental physics, materials, and mechanics principles. Due to the calm weather conditions during the pipeline installation period in the Bay of Campeche, the installation design analytical models address static induced stresses.
- The installation design analytical models used in this study were founded on in so far as possible on analytical procedures that result in unbiased (the analytical result equals the median – expected actual value) assessments of the pipeline demands and capacities.
- Physical test data and verified – calibrated analytical model data were used in so far as possible to characterize the uncertainties and variabilities associated with the pipeline demands and capacities.
- The uncertainties and variabilities associated with the pipeline demands and capacities were concordant with the uncertainties and variabilities associated with the background used to define the pipeline reliability goals.

DESIGN FORMULATIONS

The Allowable Stress Design (ASD) allowable stress factor (f) was based on the following Lognormal demand – capacity formulation:

$$f = [(B_{S50} / B_{R50}) \exp(\beta \sigma)]^{-1} = [B_{SR50} \exp(\beta \sigma)]^{-1}$$

where B_{S50} is the median Bias (actual value / nominal value) in the pipeline demands (pressures, induced stresses or strains), B_{R50} is the median Bias in the pipeline capacities (failure stresses or strains), β is the pipeline Safety Index (desired level of safety), and σ is the total uncertainty in the pipeline demands and capacities (standard deviation of their logarithms).

$$\sigma = (\sigma_{\ln S}^2 + \sigma_{\ln R}^2)^{0.5}$$

The Load and Resistance Factor (LRFD) load factors (γ) and resistance factors (ϕ) was founded on the following formulations:

$$\gamma = B_{S50} \exp(K \beta \sigma_S)$$

$$\phi = B_{R50} \exp(-K \beta \sigma_R)$$

The splitting coefficient, K, was determined from:

$$K = (\sigma_{\ln S}^2 + \sigma_{\ln R}^2)^{0.5} / (\sigma_{\ln S} + \sigma_{\ln R})$$

For the anticipated range of uncertainties in the installation demands ($\sigma_{\ln S} \leq 0.1$ to 0.2) and pipeline capacities ($\sigma_{\ln R} \leq 0.1$), the splitting coefficient was taken as $K = 0.70$.

The primary criteria development challenges are quantifying the required safety (β), the uncertainties in pipeline installation demands and capacities (σ), and the median Biases in the pipeline or riser demands and capacities (B_{50}).

In development of the design formulations, it is important to discriminate between pipeline 'segments' and 'systems'. A pipeline system can be decomposed into a sub-system of series segments. Paired pipeline segment strengths and capacities have been shown to be strongly positively correlated [4,5]. In addition, due to the expected larger uncertainties associated with the pipeline demands compared with the pipeline capacities, high failure mode correlation can be expected. For these reasons, in development of these criteria it was evaluated that the probability of failure of the pipeline system during laying operations will be determined by the probability of failure of the most likely to fail element along the length of the pipeline of concern (stinger over-bend zone to sag-bend –sea floor touchdown zone).

INSTALLATION SAFETY INDICES

A present-value, minimum installation cost economics approach was used to characterize the probability of failure (Pfo) based on the exposure period or life (L) as:

$$Pfo = 0.4348 / (CF / \Delta Ci) L$$

During the installation period, the costs associated with failure are far lower than during the operating period. In this development, based on information provided by PEMEX and IMP, it was evaluated that the costs associated with failure of the pipeline during the installation phase are 10% to 25% of those associated with the operating phase. The costs to reduce

the probability of failure by a factor of 10 were evaluated by to be the same as for the operating phase.

Based on previous experience with the installation of major pipelines in the Bay of Campeche, the exposure period of the pipeline during the installation phase was evaluated to be between 3 and 6 months (0.25 to 0.50 year). Given the use of a PVF for the long-life production phase of the pipeline of 10, these assumptions indicate that the optimum probability of failure during the installation period (PfoI) is related to the optimum probability of failure during the operating period (PfoO) as:

$$PfoI = 80 \text{ PfoO to } 400 \text{ PfoO}$$

Given these results, a conservative evaluation of the probabilities of failure during installation was developed as:

$$PfoI = 100 \text{ PfoO}$$

Based on the foregoing developments and the previously defined PfoO [6,7], Table 1 summarizes the annual probabilities of failure and Safety Indices associated with each of the three Safety and Serviceability Classifications (SSC) for design of pipelines and risers during installation.

Table 1. Serviceability Classifications and Probabilities of Failure (loss of stability), and Safety Indices for Pipeline Stability During Installation

SSC	Consequences of Failure	Probability of Failure (installation)	Safety Index (installation)
1	Very High	1 E-2	2.32
2	High	5 E-2	1.65
3	Moderate	1 E-1	1.28

For development of these criteria, a conservative target reliability value of $Pft = 1 \text{ E-2}$ per year (or per annum, pa) or annual Safety Index of $\beta = 2.32$ was used for all categories of pipelines and risers.

Vinnem [8] has addressed the unique issues associated with risk acceptance criteria for the installation phase of marine structures. Vinnem observes that the temporary installation phase is generally set an order of magnitude higher than the permanent phase due to the limited duration of the temporary phase. This development is consistent with the results developed by Vinnem. These target reliabilities also are consistent with those suggested in the DNV pipeline design guidelines [2] and by Sotberg, et al [9;10].

During the installation period, the pipeline can be subjected to two categories of hazards:

- those 'natural' (not accidental, everything done according to specifications) hazards that threaten the capacity or Ultimate Limit State (ULS) resistance of the pipeline, and
- those hazards that are associated with 'accidental' conditions (ALS) that arise generally due to human and organizational factors that result in 'errors' being made during the installation of the pipeline.

The probability of failure during the installation period can be expressed as (independent hazards):

$$P_{fi} = P_{f_{natural}} + P_{f_{accidental}}$$

Based on a target reliability value of $P_{ft} = 1 \text{ E-2}$ per year, and an equal allocation of reliability between the two categories of hazards, $P_{f_{natural}} = 5 \text{ E-3}$ pa and $P_{f_{accidental}} = 5 \text{ E-3}$ pa.

Two categories of natural installation hazards were addressed in development of these criteria:

- those associated with the installation processes that result in induced stresses and strains in the pipeline consisting of axial tension, bending or flexure, and radial compressive stresses – strains, and
- those associated with the temporary stability of the pipeline on the seafloor before it is trenched or buried.

The probability of failure due to natural hazards during the installation period can be expressed as (independent hazards):

$$P_{f_{natural}} = P_{f_{laying}} + P_{f_{stability}}$$

Based on a target reliability value of $P_{f_{natural}} = 5 \text{ E-3}$ pa, and an equal allocation of reliability between the two categories of hazards, $P_{f_{laying}} = 2.5 \text{ E-3}$ pa and $P_{f_{stability}} = 2.5 \text{ E-3}$ pa.

Three categories of accidental installation hazards (ALS) were addressed in development of these criteria:

1. those associated with accidental installation processes resulting in over-stressing the pipeline (e.g. excessive flexural stresses induced by improper stinger and supports positioning or loss of lay barge mooring or alignment),
2. those associated with objects dropped on the pipeline during installation, potentially resulting in propagating buckling, and
3. those associated with accidental loss of stability of the pipeline (e.g. pipeline not flooded before storm conditions).

The probability of failure to accidental hazards during the installation period can thus be expressed as (independent hazards):

$$P_{f_{accidental}} = P_{f_{acc \text{ laying}}} + P_{f_{prop \text{ buckling}}} + P_{f_{acc \text{ stability}}}$$

Based on a target reliability value of $P_{f_{accidental}} = 5 \text{ E-3}$ pa, and an equal allocation of reliability between the three categories of hazards, $P_{f_{acc \text{ laying}}} = 1.7 \text{ E-3}$ pa, $P_{f_{prop \text{ buckling}}} = 1.7 \text{ E-3}$ pa, and $P_{f_{acc \text{ stability}}} = 1.7 \text{ E-3}$ pa.

The ALS is comprised of two occurrences:

- occurrence of an accident sufficient to over-stress / strain the pipeline or result in its instability, and
- occurrence of a capacity in the pipeline that is insufficient to resist the imposed stresses / strains / forces.

For example, a propagating buckling failure that could occur during installation requires an accident - dropped object that results in a significant dent in the pipeline and a sufficiently high hydrostatic pressure to propagate the buckle in the pipeline.

In a probability framework, the probability of an accident caused failure can be expressed as follows:

$$P_{fai} = P_{fi} \cap P_A = [P_{fi} | A] [P_A]$$

P_{fai} is the probability of failure due to an accident of type i. P_{fi} is the probability of a failure given an accident involving the pipeline. P_A is the probability that such an accident occurs.

For installation conditions in the Gulf of Mexico, there is little data available on accidental failures. On experienced Gulf of Mexico pipeline installation contractor could only recall two instances in 30+ years when such failures were reported; it was noted that it is unusual that such occurrences are reported; rather they are repaired and the installation completed without further disruptions.

The 1994 PARLOC study developed data that provided some useful information on pipeline construction related incidents [11]. Of 401 incidents developed in the database on pipelines, 109 occurred during construction (about 25 %). Of 69 construction related incidents that occurred before hydrotesting or commissioning, 53 resulted in significant damage to the pipeline requiring repairs (80 % severe damage rate). Anchoring operations, dropped objects, and excessive forces (bending, tension in severe seas) were cited as the most frequent causes of these construction accidents.

The total frequency for incidents (401) were estimated to be in the range of 1.1 E-2 to 3.5 E-3 per year. Given that 25% of these were related to construction, the frequency of severe incidents would be 3 E-3 pa to 9 E-4 pa. Given an 80 % severe damage rate before commissioning and hydrotesting, these data indicate a severe damage accident rate during construction of 2.4 E-3 pa to 7.2 E-4 pa. This rate is consistent with the 1.7 E-3 pa identified by the economics based evaluation.

Use of a conservative annual Safety Index of $\beta = 2$ for the propagating buckling accidental limit state would equate to an annual probability of failure of $P_{fi} = 1 \text{ E-2}$ pa. Given the target reliability of $P_{fai} = 1.7 \text{ E-3}$ indicates a tolerable severe accident rate of $P_A = 1.7 \text{ E-1}$ per year; far in excess of the accident rates associated with installation operations in the North Sea. A very conservative annual Safety Index of $\beta = 2$ was used to develop the installation propagating buckling criteria and the other accidental limit states installation criteria.

VARIABILITIES & UNCERTAINTIES

Assessment of the variabilities and uncertainties is the most important part of the reliability based criteria development. In this development, three categories of uncertainties are delineated:

- Type 1 (aleatory) – natural, inherent, information insensitive
- Type 2 (epistemic) – model, parametric, state, information sensitive
- Type 3 – (accidental) human and organizational

Often, it is not possible to separate these uncertainties unambiguously; natural and model uncertainties are mixed and they are not easily separated. It is important to not account for the Type 1 uncertainties twice by including them separately and collectively in the Type 2 uncertainties.

In this development, model uncertainties are expressed with a random variable designated as 'Bias.' Bias (B_x) is the ratio of the true or actual value of the variable (x) to the predicted or nominal value of the variable. Results from laboratory, field, and sometimes numerical experiments are used to define the true or actual value of a variable. It is critical to ensure that these data do not incorporate Bias due to the type of instrumentation, experiment, numerical analysis, or data

analysis used. Emphasis was given to field experimental results first, then to laboratory results (hopefully verified with field data), and last to results from 'calibrated' numerical experiments.

The characteristics of the bias are expressed with a measure of the central tendency (e.g. median, B_{x50}), a measure of the variability (e.g. coefficient of variation, $COV = V_x$), and the type of distribution (Lognormal). The Type 1 uncertainties ($\sigma_{\ln X1}$) are added to the Type 2 uncertainties ($\sigma_{\ln X2}$) in quadrature as follows:

$$\sigma_{\ln X} = (\sigma_{\ln X1}^2 + \sigma_{\ln X2}^2)^{0.5}$$

LAY STRESS UNCERTAINTIES

Two categories of stresses induced in the pipeline during laying were addressed: 1) the local stresses in the pipe field joints caused by gaps in the concrete coating, and 2) the global stress in the over-bend and sag-bend area.

Stress Concentration Due to Weight Coating Joints

The stress / strain concentration in field joints due to the stiffening effect of the concrete coating is included as a multiplication factor on the global or nominal static stresses / strains (Strain Concentration Factor, SCF). The SCF is governed by geometrical and physical properties of the assembled pipeline section in which a natural variability occurs. In addition, model uncertainty is also involved due to the analytical models used to determine the SCFs.

Fig. 1 summarizes a statistical analysis of the Bias associated with the three analytical models used to predict the strain concentration factors for nominal strains in the range of 0.1 % to 0.25 % and concrete coating thicknesses of 40 mm and 80 mm [12-14]. The Lund et al model has a median Bias of 0.98 and a COV of 10 %. The Ness – Verley model has a median Bias of 1.01 and a COV of 5.1 %. The Igland parametric model has a median bias of 1.00 and a COV of 3.3%.

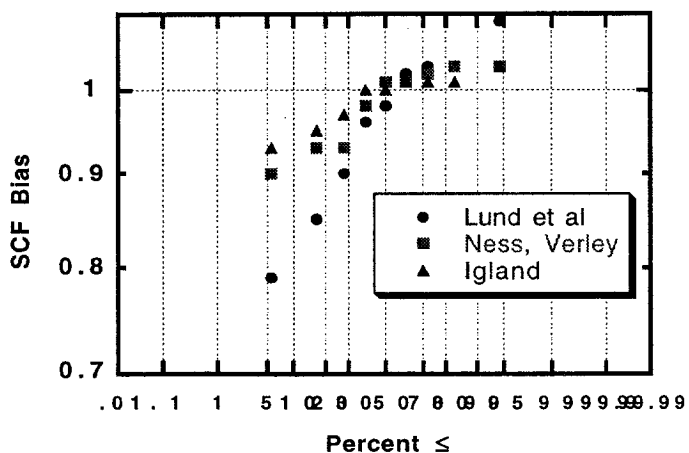


Fig. 1. Strain Concentration Factor Biases

Based on the experimental data, SCFs of 1.2 and 1.4 were specified in the installation design guidelines for 40 mm and 80 mm concrete thicknesses, respectively. The median Bias

and COV of the Bias of these SCFs are 1.0 and 3.3 %, respectively.

Computed Stresses

The lay barge parameters (roller positions, lay vessel trim, tensioner force) are usually assumed to be deterministic since the laying parameters are carefully controlled during installation. The pipe-support rollers on the stinger are positioned to ensure an optimal behavior of the pipeline on the over-bend (displacement controlled part of the pipeline).

Fig. 2 summarizes results from a static analysis of installation total (flexural and tension) global (no joint SCF) stresses in a 24-in diameter pipeline with a specific gravity of 1.2 in a water depth of 162 ft. The zero X-coordinate is at the end of the lay barge; the end of the pipe stinger is at X-coordinate = -125 ft. These results were developed by IMP using the OFFPIPE finite element analysis computer program [15,16]. The pipeline maximum laying stress is dominated by the flexural laying stresses in the over-bend area; the maximum sag-bend stress is about one-third of the maximum over-bend stress. The analyses indicate that about 90% of the total stress is caused by pipeline bending – flexure in the over-bend area.

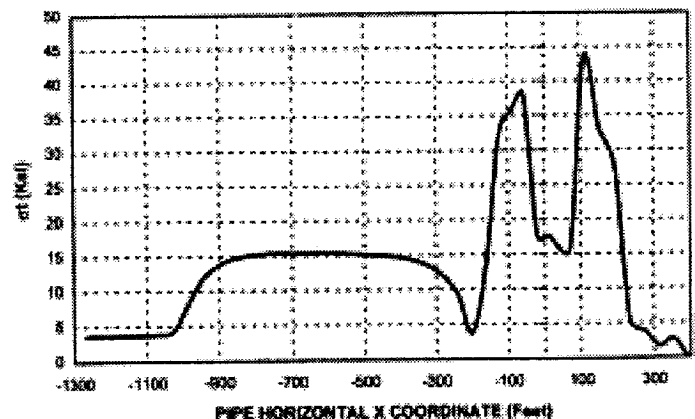


Fig. 2. Total stresses

Measured & Computed Stresses

In this study, a direct evaluation approach was used to determine the Bias and uncertainties associated with the global static stresses induced in the pipeline during laying operations. Field test data gathered during pipeline laying operations in the Bay of Campeche were compared with the analytical predicted data to develop the uncertainty measures (median Bias and COV of Bias).

Measurements of pipeline profiles during laying operations were used for a pipeline with the following characteristics:

- Diameter = 36 in
- Steel wall thickness = 0.75 in
- Pipeline segment length = 40 ft
- Weight coating thickness = 3.25 in
- Concrete density = 165 lb/ft³
- Water depth = 80 – 90 ft
- Rigid stinger length = 131 ft

During the pipeline laying operations, divers using depth gauges defined the vertical profile of the pipeline that was being laid by measuring the depth to each of the pipe joints [17]. At specified intervals during the laying operations (approximately 6 hours), the divers measured the depth of each joint on the over-bend and sag-bend. The tension on the pipeline was recorded. The weather was calm (wave heights less than 2 m). The measured pipeline tension during the lay operations varied between the 30,000 and 50,000 lbs. More than 60 pipeline profiles were gathered during this measurement program (Fig. 3).

Given the pipeline and lay barge stinger characteristics, the OFFPIPE analytical model [15] was used by IMP to determine the pipeline profile and associated tensile and flexural stresses [16,17].

The measured pipeline profiles were analyzed to determine the minimum radius of curvature in the over-bend and sag-bend. The radius of curvature was used to determine the maximum flexural strains; the strains were related to the stresses with the mean modulus of elasticity determined from

coupons of the pipeline steel. The flexural stresses were added to the measured tensile stresses (measured tensions divided by pipeline steel cross-sectional area) to determine the maximum total stresses in the over-bend and sag-bend area. These 'measured' maximum stresses were compared with those based on the analytical model to determine the Biases associated with the maximum global lay stresses.

Fig.4 summarizes the uncertainty evaluation results of the measured and predicted data for the over-bend of the pipeline during the installation. The median Bias and Bias COV are 1.0, 6.5 %, respectively. The data indicated comparable results for the sag-bend area.

The total uncertainty associated with global and local maximum static stresses during laying were evaluated to be 10% with a median Bias of 1.0. These values are comparable with those determined by Igland [14] and Igland and Moan [18] for static lay stress conditions. Comparable results also were developed by Bea, et al [19] from analyses of the measured and predicted stresses for the Zee Pipe conditions.

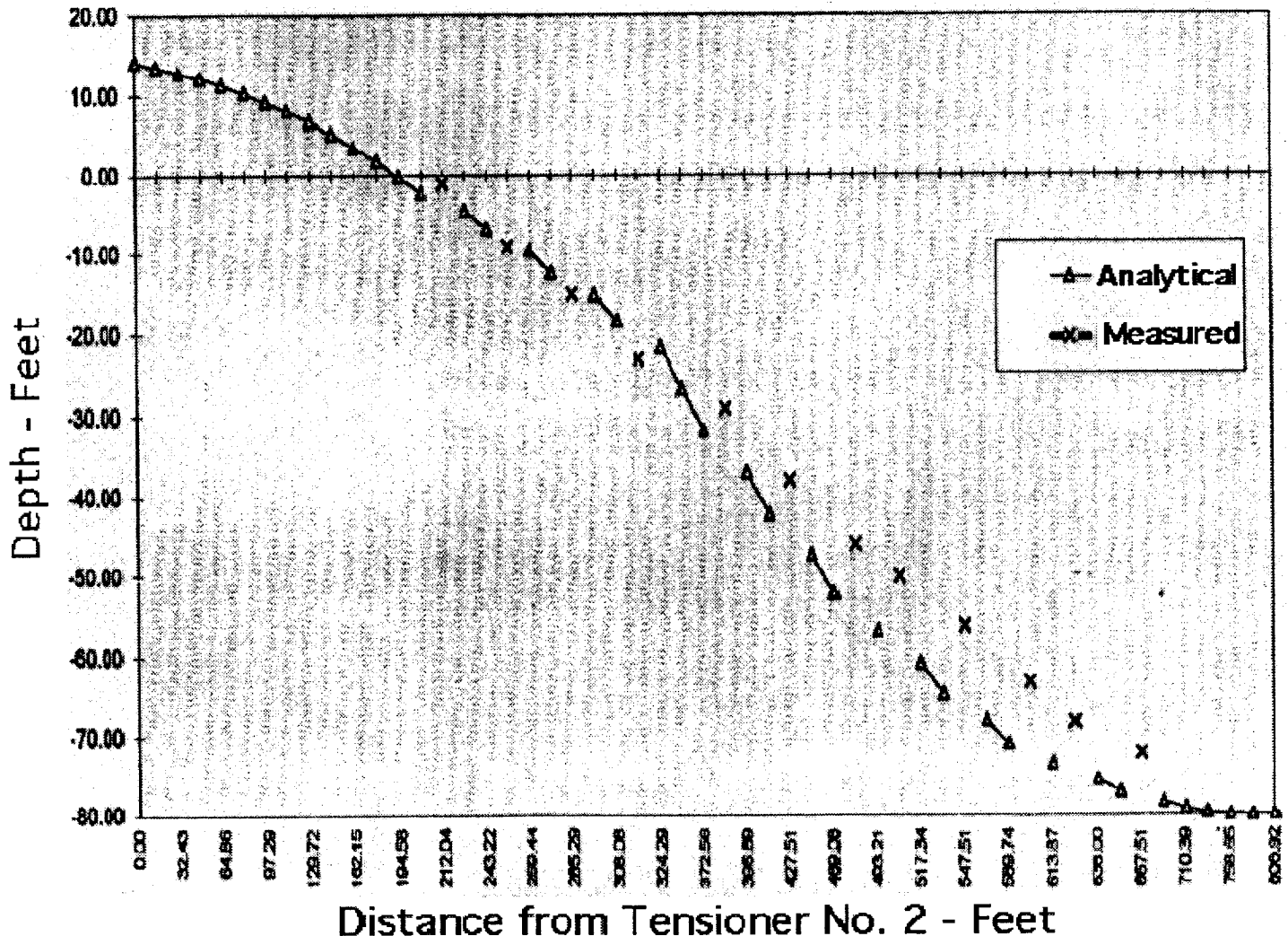


Fig. 3. Comparison of Measured and Predicted Pipeline Profiles During Laying

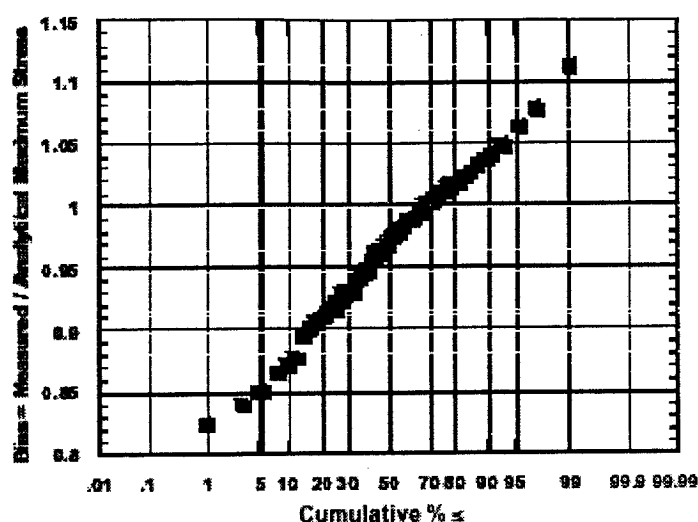


Fig 4. Global Lay Stress Bias in Over-bend

Table 2 summarizes the results of the uncertainties analyses for the Bay of Campeche installation conditions. The median Bias of 0.98 and COV of 2% for the accidental conditions associated with the collapse and propagating buckling loading states are based on the installation design guideline specified use of 10-year conditions (water depth) and a conservative value for the unit weight of water to determine the hydrostatic pressures.

Table 2. Summary of Installation Condition Biases and Uncertainties

Loading States (1)	Lay Stress Median Bias (2)	Lay Stress Annual COV (3)
Tension	1.0	0.10
Bending	1.0	0.10
Collapse	0.98	0.02
Propagating Buckling	0.98	0.02
Tension-Bending-Collapse	1.0	0.10

INSTALLATION CRITERIA SUMMARY

Tables 3 – 5 summarize the installation criteria that were developed based on the foregoing developments and on results of studies of pipeline capacities. Summary of the studies of pipelines capacities are the subject of the second part of this paper [20].

These tables identify the type of installation loading, the resulting demand and Ultimate Limit State capacity median bias and uncertainty, and the stress reduction factor (f), load factor (γ), and resistance factor (ϕ) associated with each type of installation loading.

The propagating buckling loading condition is identified as an accidental loading that is to be evaluated based on 10-year return period conditions (water depth).

The ASD combined stress reduction factors are generally close to 0.8. The LRFD loading factors are generally in the range of 1.0 to 1.2. The LRFD resistance factors are generally

in the range of 0.8 to 0.9. These values are very comparable with those contained in the DNV 2000 [2] guidelines. These values are also very comparable with those developed by Igland and Moan [18].

If the ASD and LRFD factors are close to those developed previously, then why should PEMEX and IMP undertake this work? After this work PEMEX and IMP engineers understand how the criteria were developed and most importantly, the limitations of these pipeline installation design guidelines [21]. This provides a firm foundation for continued development and application of these criteria in Mexico.

ACKNOWLEDGMENTS

The authors would like to express appreciation to Ing. Victor Valdez and Ing. Manuel Gorostieta from PEMEX for their leadership in development of these guidelines. Thanks also are due to Ing. Felipe Diaz for his support and assistance during this project.

Table 3. ASD Stress Reduction Factors

Installation Loadings	Demand/ Capacity Median Bias	Demand & Capacity Uncertainty COV	Pipelines & Risers ULS - f
Tension	0.85	0.15	0.83
Bending	0.85	0.15	0.83
Collapse	0.98	0.12	0.77
Propagating Buckling	0.98	0.12	0.80
Tension-Bending-Collapse	0.83	0.18	0.80

Table 4. LRFD Load Factors

Installation Loadings	Demand Median Bias	Demand Uncertainty COV	Pipelines & Risers LRFD - γ
Tension	1.00	0.10	1.14
Bending	1.00	0.10	1.14
Collapse	0.98	0.02	1.01
Propagating Buckling	0.98	0.02	1.01
Tension-Bending-Collapse	1.00	0.11	1.15

Table 5. LRFD Resistance Factors

Installation Capacities	Capacity Median Bias	Capacity Uncertainty COV	Pipelines & Risers LRFD - ϕ
Tension	1.00	0.08	0.88
Bending	1.00	0.11	0.84
Collapse	1.00	0.12	0.82
Propagating Buckling	1.00	0.12	0.85
Tension-Bending-Collapse	1.00	0.12	0.82

REFERENCES

- [1] American Petroleum Institute (API), 1999, *Design, Construction, Operation, and Maintenance of Offshore Hydrocarbon Pipelines*, API Recommended Practice 1111, Washington, DC.
- [2] Det Norske Veritas (DNV), 2000, *Submarine Pipeline Systems*, Offshore Standard OS-F-101, Hovik, Norway.
- [3] American Society for Testing and Materials (ASTM), 1998, *Metal-Arc-Welded Steel Pipe for Use with High-Pressure Transmission Systems*, New York, NY.
- [4] Bea, R.G., Smith, C., Smith, R., Rosenmoeller, J., and Beuker, T., 2002, "Real-Time Reliability Assessment & Management of Marine Pipelines," *Proceedings Offshore Mechanics and Arctic Engineering Conference, Pipeline Symposium*, OMAE02/PIPE 28322, Oslo, Norway, American Society of Mechanical Engineers, New York, NY.
- [5] Orisamololu, I.R., and Bea, R.G., 1999, "Reliability Considerations in the Development of Guidelines for the Requalification of Pipelines," *Proceedings International Workshop on Pipeline Requalification*, 18th Offshore Mechanics & Arctic Engineering Conference, Instituto Mexicano del Petroleo (Ed), Mexico, DF, pp 129-144.
- [6] Bea, R.G., Ramos, R., Hernandez, T., Valle, O., Valdes, V., and Maya, R., 1998, "Risk Assessment & Management Based Criteria for Design and Requalification of Pipelines and risers in the Bay of Campeche," *Proceedings Offshore Technology Conference*, OTC 8695, Society of Petroleum Engineers, Richardson, TX, pp 1 – 18.
- [7] Lara, L., Garcia, H., and Heredia-Zavoni, E., 1999, *Categorization of Pipelines in the Bay of Campeche for Risk Based Design and Assessment*, Subdirection de Ingenieria, Instituto Mexicano del Petroleo, Mexico, DF.
- [8] Vinnem, J.E., 1996, "Risk Acceptance Criteria for Temporary Phases," *Journal of Offshore Mechanics and Arctic Engineering*, Transactions of the ASME, Vol. 118, New York, NY, pp 230-237.
- [9] Sotberg, T., Moan, T., Bruschi, R., Jiao, G., and Mork, K.J., 1997, "The SUPERB Project: Recommended Target Safety Levels for Limit State Based Design of Offshore Pipelines," *Proceedings 16th International Conference on Offshore Mechanics and Arctic Engineering*, Vol. V, Pipeline Technology, American Society of Mechanical Engineers, New York, NY, pp 71-77.
- [10] Sotberg, T., Mork, K. J., Barbas, S., 1999, "ISO Standard Pipeline Transportation Systems: Reliability-Based Limit State Methods," *Proceedings International Offshore and Polar Engineering Conference*, Vol. IV, International Society of Offshore and Polar Engineers, Golden, CO, pp 325-330.
- [11] Advanced Mechanics & Engineering Ltd, 1995, *PARLOC 94: The Update of Loss of Containment Data for Offshore Pipelines*, OTC 95, 468, Health and Safety /Executive – Offshore Technology Report, London, UK.
- [12] Lund, S., et al, 1993, "Laying Criteria Versus Strain Concentration at Field Joints for Heavily Coated Pipelines," *Proceedings International Conference on Offshore Mechanics and Arctic Engineering*, American Society of Mechanical Engineers, New York, NY., pp 50 – 62.
- [13] Ness, O., and Verley, R., 1996, "Strain Concentrations in Pipelines with Concrete Coating," *International Journal of Offshore Mechanics and Arctic Engineering*, American Society of Mechanical Engineers, New York, NY, pp 123 – 131.
- [14] Igland, R.T., 1997, *Reliability Analysis of Pipelines During Laying, Considering Ultimate Strength Under Combined Loads*, Doctor of Engineering Thesis, Department of Marine Structures, The Norwegian University of Science and Technology, Trondheim, Norway.
- [15] Malahy, R.C., Jr., 1998, *OFFPIPE – Offshore Pipeline Analysis System*, Users Manual, Houston, TX.
- [16] Valle, O., Lara, L., Matias, J., Heredia-Zavoni, E., Diaz, F., 1998, *Transitory Criteria for Design and Evaluation of Submarine Pipelines in the Bay of Campeche, Risk Assessment and Management Based Allowable Stress Design and Load and Resistance Factor Design Stress Criteria and Guidelines for Design and Requalification of Pipelines and Risers*, Instituto Mexicano del Petroleo, Mexico, DF.
- [17] Lara, L., Matias, J., Heredia-Zavoni, E., *Report on Field Tests and Analyses of Pipeline Laying Operations*, Instituto Mexicano del Petroleo, Mexico, DF.
- [18] Igland, R. T., and Moan, T., 1998, "Reliability Analysis of Pipelines During Laying, Considering Ultimate Strength Under Combined Loads," *Proceedings Offshore Mechanics and Arctic Engineering Conference*, American Society of Mechanical Engineers, New York, NY., pp 1 – 8.
- [19] Bea, R. G., Xu, T., 2000, *RAM PIPE Project Phase 2 – Report 1, Installation Criteria & Guidelines*, Report to Petroleos Mexicanos and Instituto Mexicano del Petroleo, Marine Technology & Management Group, University of California at Berkeley.
- [20] Bea, R. G., Xu, T., Heredia-Zavoni, E., and Lara, L., 2002, "Reliability Based Design Criteria for Installation of Pipelines in the Bay of Campeche, Mexico: Part 2," *Proceedings of Offshore Mechanics and Arctic Engineering Conference*, OMAE02/S&R-28196, American Society of Mechanical Engineers, New York, NY.
- [21] PEMEX Exploration and Production and IMP, 1998, *Transitory Criteria for the Design and Evaluation of Submarine Pipelines in the Bay of Campeche*, First Edition, Instituto Mexicano del Petroleo, Mexico, DF.

OMAE 2002/S&R-28196

RELIABILITY BASED DESIGN CRITERIA FOR INSTALLATION OF PIPELINES IN THE BAY OF CAMPECHE, MEXICO: PART 2

Robert Bea and Tao Xu

University of California
Berkeley, CA 94720-1712
bea@ce.berkeley.edu

Ernesto Heredia-Zavoni, Leonel Lara, and Rommel Burbano

Instituto Mexicano Del Petroleo
Del. Gustavo A Madero 07730, Mexico, DF
eheredia@www.imp.mx

ABSTRACT

Studies have been performed to propose reliability based design criteria for the installation of pipelines in the Bay of Campeche, Mexico. This paper summarizes formulations that were used to characterize the important Ultimate Limit State capacities of the pipelines during the installation period (collapse, bending, tension, combined, and propagating buckling). A large database of laboratory and numerical analysis 'tests' (more than 2,000 results) to determine pipeline capacities was assembled to help evaluate the Biases (ratio of measured / predicted capacities) in the analytical methods used to determine pipeline capacities. Given the formulations, target reliabilities, and installation demand characterizations summarized in a companion paper (Part 1), installation design criteria were developed for both Working Stress Design and Load and Resistance Factor Design formats.

INTRODUCTION

Installation is one of the most severe conditions for pipeline design. Buckling and collapse under bending, tension, and external pressure is the major potential failure mode during pipeline installation. A comprehensive understanding of this mechanism as well as a rational assessment of the associated uncertainties is essential in the development of reliability based pipeline installation criteria.

Pipe failure under bending basically exhibits two modes: 1) maximum load effect failure (maximum bending moment/strain failure) and, 2) bifurcation failure. The maximum load effect failure is reached when the applied bending load effect exceeds the critical bending strain or

bending moment considering the increasing of the circumferential ovalization for increasing load. Bifurcation buckling refers to a change in the deformation pattern and thus also the moment capacity; it is caused by the development of local longitudinal wrinkles in the compressed region of the pipe section.

Bifurcation buckling may occur before the maximum strain is reached for high D/t ratios. For D/t ratios below 20 to 80, the maximum strain is generally reached before bifurcation [1]. For the pipelines installed in the Bay of Campeche, the relevant D/t ratios are usually below 40, this implies that the maximum load effect failure mode instead of the bifurcation mode is critical for the pipe buckling and collapse.

One of the parameters critical to buckling and collapse is the pipe section imperfection. The increase of ovalization under bending acts as a load-dependent imperfection and may be much larger than the pipe section initial ovality.

At very low D/t ratio, a pipe subjected to bending will collapse due to plastic yielding and the ovalization of the cross-section. At very high D/t ratios, local buckling occurs first. For immediate values D/t ratio (30 to 40), collapse occurs as a combination of ovalization and local buckling. Similarly, for pure external pressure at low D/t, collapse is initiated through yielding, where at high D/t it is initiated through buckling. For D/t ratio between 10 and 40, the failure mode of pipe under combined bending and external pressure is a combination of ovalization, yielding and local buckling.

The objective of the remaining parts of this paper is to review buckling/collapse capacity models and their abilities to simulate results from laboratory tests. The following Ultimate

Limit State (ULS) capacity installation loading conditions will be addressed in the remainder of this paper:

- Buckling under pure bending,
- Collapse under pure external pressure,
- Collapse under combined tension, and bending, and
- Propagating buckling.

Table 1 summarizes the ULS capacity formulations for single installation loading conditions that were adopted for the PEMEX / IMP criteria and guidelines [2]. Table 2 summarizes the ULS capacity formulations for combined installation loading conditions that were adopted for the PEMEX / IMP criteria and guidelines. Stain based design formulations also were developed during this study, but they are presented in this paper.

The extensive pipe test database developed during this study was evaluated primarily to characterize the Biases associated with the formulations that were adopted for the installation design. Bias was defined as the ratio of the test capacity to the capacity determined from the design capacity formulation. As appropriate for the characterization of Bias for a general installation design process, nominal pipe characteristics were used in the capacity formulations (e.g. pipe diameter, thickness, specified minimum yield or tensile strength). Application of the statistical characterizations of Bias that were developed based on comparisons of these formulations with laboratory test data to development of reliability based design criteria for installation of pipelines in the Bay of Campeche is given in a companion paper [3].

Results from the statistical analysis of Bias will be presented graphically as cumulative distribution plots of the Bias: the Bias for each test data point versus the cumulative percentage of values that are equal to or less than a given value. The Bias will be generally characterized with two parameters: the median Bias, B_{50} , and the Coefficient of Variation (COV) of the Bias, V_B . In most cases, the 'best fit' distribution proved to be a Lognormal distribution.

NOMENCLATURE

A	Nominal cross-sectional area of pipe
B	Bias (measured / nominal)
B_{50}	Median Bias (50-th percentile)
COV	Coefficient of variation
D	Nominal outside diameter of pipe
D_{max}	Maximum pipe diameter
D_{min}	Minimum pipe diameter
D_o	Mean nominal diameter of pipe (D-t)
DSAW	Double submerged arc welded
E	Young's elastic modulus
FEA	Finite element analysis
f_o	Ovality of pipe
K	Imperfection factor
L	Length of pipe
M	Applied external moment
M_p	Plastic moment capacity
M_u	Ultimate moment – bending capacity
P	Applied external pressure
P_b	Propagating buckling external pressure
P_c	Collapse pressure

P_E	Elastic collapse pressure
P_u	Ultimate collapse pressure
P_y	Yield collapse pressure
SMTS	Specified minimum tensile strength
SMYS	Specified minimum yield strength
t	Nominal thickness of pipe
T	Applied tensile force
T_u	Ultimate tensile capacity
ULS	Ultimate limit state
V_x	Coefficient of variation of variable x
ν	Poisson's ratio

BENDING

Test Data

Sherman [4,5] presented a review of tests on fabricated pipes with geometrical and material characteristics of cylindrical members in offshore structures. Uncertainties about the extrapolation of tubular test results to long pipes, as far as the plastic moment capacity is concerned, led to the testing programs of large-scale pipe beams [4, 6-8].

Jirsa et al [7] reported six tests of pipe under pure bending, with diameter varying from 10 to 20 in and D/t from 30 to 78. Sherman [4] presented experimental tests data on tubes under pure bending. The tubes had an outside diameter of 10.75-inches and D/t ratios from 18 to 102. Sherman concluded that the members with D/t of 35 or less can develop a fully plastic moment and sustain sufficient rotation to fully redistribute the moments in fixed end beams. This conclusion was demonstrated for pipe spans up to 22 diameters. In addition, Sherman concluded that tubes made by Electric Resistance Welded (ERW) could not develop the full plastic moment at as large a D/t as that proposed by Schilling.

Korol [8] performed a series of nine tests on single span circular hollow tubular beams with D/t ratios from 28.9 to 80.0. Korol concluded that the buckling strain was found to be inversely proportional to yield stress rose to an exponent factor between 0.5 and 1.0 for ductile materials that possess an essentially bilinear stress-strain curve and a small degree of strain hardening. This exponent factor tends to be 1.0 for elastic-perfectly plastic materials. For a high tangent modulus and small D/t pipe, it tends towards zero.

Sherman [5] reviewed six experimental research programs that contained tests on cylinders with unstiffened constant-moment regions. A total of 53 tests were included in the review. The test specimens were hot-formed seamless pipe; electric resistance welded tubes and fabricated pipes. The diameters ranged from 4 to 60 inches. However, in most cases the diameters were between 10 and 24 inches.

Two tests of the test series conducted by Sternmann et al (1989) for beam columns were included in the tests database development. These tests were for tubulars with nominal D/t ratio of 42, the outside diameter of 6.625 in and L/D of 24.9 and 17.3. These models were made from X-42 steel ERW pipe.

In addition, tests conducted by Kyriakides, et al [9], Fowler, et al [10] and Battelle [11] for longitudinal bending alone were included in the database.

Igland has provided an extensive database that contains results from 'numerical experiments' [12]. Nonlinear Finite Element Analysis (FEA) models of pipe sections were developed and calibrated with results from laboratory tests. Then the important random variables in the models were systematically varied throughout ranges indicated from statistical analyses of the variables to be appropriate.

Moment Capacity Formulations

Two design formulations were evaluated to determine the ULS moment capacity, M_u . The first was:

$$M_u = 1.13M_p \exp(-X) \quad (1)$$

$$M_p = (D_0 - t)^2 t \cdot SMYS \quad (2)$$

$$X = \frac{SMYS \cdot D_0}{E \cdot t} \quad (3)$$

The second formulation used was:

$$M_u = 1.1D_0^2 t \cdot SMYS \cdot \left(1 - 0.001 \frac{D_0}{t}\right) \quad (4)$$

Data Analysis

Fig. 1 and Fig. 2 summarize the statistical characteristics of the Biases developed by both of the analytical formulations. The results are presented as the Bias (ordinate) versus the cumulative likelihood of a value of the Bias being equal to or less than a given value (abscissa). The cumulative likelihood scale is distorted so that if the data plot on a straight line, then the data are well modeled by the assumed distribution. In this case, the vertical scale is Logarithmic and the 'best fit' distribution is Lognormal. Both models develop median Biases of $B_{50} = 1.0$ and COVs of the Biases of $V_B = 11\%$. The second model was used in development of the installation guidelines.

Statistical analyses of the numerical test data for pure bending of tubes provided by Igland [12] based on Eqn. 1 resulted in a median Bias of $B_{50} = 1.0$ and COV of the Bias was $V_B = 9.0\%$.

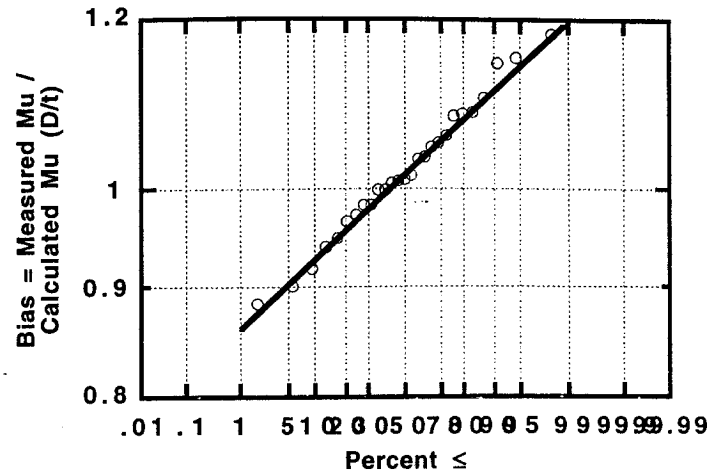


Fig. 2. Bias in calculated ultimate moments (Eqn. 4)

COLLAPSE

Test Data

Kyriakides, et al performed 33 tests on steel tubes with diameters ranging between 1.0-in and 1.5-in and lengths between 20 and 30 diameters [13, 14]. Commercially available drawn stainless steel 304 tubes were used in the experiments. The specimens were sealed at both ends and placed in a specially designed 1,0000 psi capacity pressure test facility. The maximum pressure recorded for each test was taken to represent the collapse pressure. Prior to tests, respective initial ovalities were measured. Typically the diameter variation around the circumference was measured at six to eight stations along the tube length. Variation of wall thickness around the circumference at the two ends was also measured. A longitudinal tensile coupon of width 0.25 in (6 mm) was machined out of each tube used to generate the tested specimens. Each experimental stress-strain curve was fitted with a three parameter Ramberg-Osgood expression. The yield stress as defined by the 0.2% strain offset and 0.5% strain offset were measured.

Fowler performed collapse tests under external pressure for 16 pipes with 16-in diameter [10]. Seamless and double submerged arc welded (DSAW) tubes were tested. The pipe length to diameter ratio was 7.0. For each type of tube, which generates the tested specimens, the following material testing was conducted: chemical analysis, longitudinal and circumferential tensile tests, and residual stress determined by the split ring method. Thickness variation and initial ovality was measured for each specimen prior to the collapse test. Ovalities were calculated based on the diameter difference between a 0-180 degree and a 90-270 degree line and also based on diameter difference between a 45-225 degree line and a 135-315 degree line. The reported ovality is the greater of the two. The tests were performed in a vessel with 30-in outside diameter and 2-in wall thickness. The specimens with both ends sealed were contained entirely within the test vessel. The vessel was pressurized up to the specimen catastrophic failure. For each specimen the maximum recorded pressure was

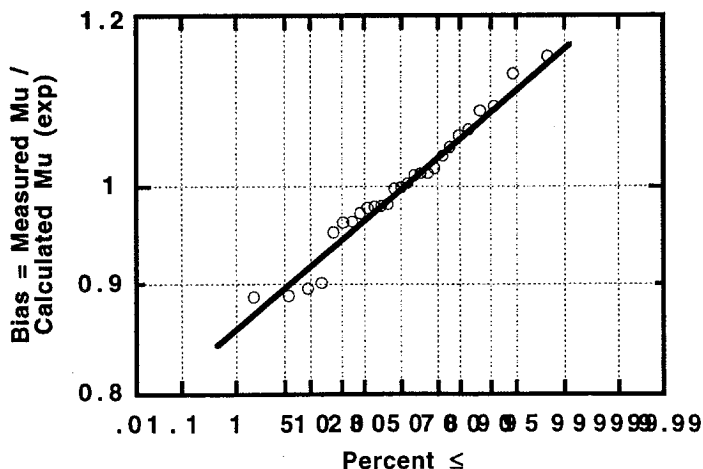


Fig. 1. Bias in calculated ultimate moments (Eqn. 1)

assumed as respective collapse pressure. For DSAW tubes the obtained collapse pressures presented considerable scatter.

Two different sets of pipeline test data were assembled during this study. The first database was founded on tests on fabricated pipelines: rolled plates welded longitudinally and circumferentially. The second database was founded on seamless pipelines.

Analysis of the test data indicated that the fabricated pipe specimens had a median ovality of $f_{50} = 1.0\%$ and a COV of the ovality of $V_f = 55\%$. Analysis of the test data indicated that the seamless pipe specimens had a median ovality of $f_{50} = 0.1\%$ and a COV of the ovality of $V_f = 90\%$.

Collapse Capacity Formulations

The fundamental analytical expression used for evaluation of pipeline net collapse pressure was:

$$P_c = 0.5 \left\{ P_y + P_e K - \left[(P_y + P_e K)^2 - 4 P_y P_e K \right]^{0.5} \right\} \quad (5)$$

This is the traditional 'Timoshenko Elastic' formulation. The terms in these expressions are as follows:

$$P_y = 2 \frac{SMYS \cdot t}{D} \quad (6)$$

$$P_e = \frac{2E}{1-\nu^2} \left(\frac{t}{D_0} \right)^3 \quad (7)$$

$$K = 1 + 3f_0 \left(\frac{D}{t} \right) \quad (8)$$

$$f_0 = \frac{D_{max} - D_{min}}{D_{max} + D_{min}} \quad (9)$$

A modification to the Timoshenko Elastic formulation was developed in which the yield collapse pressure, P_y , is replaced by an ultimate collapse pressure, P_u :

$$P_c = 0.5 \left\{ P_u + P_e K - \left[(P_u + P_e K)^2 - 4 P_u P_e K \right]^{0.5} \right\} \quad (10)$$

where:

$$P_u = 5.1 \frac{SMTS \cdot t}{D} \quad (11)$$

The 'Timoshenko Ultimate' formulation was based on an expression for P_u that represents a modification of the traditional yield pressure at collapse, P_y . This modification takes account of the additional pressure required to form four plastic hinge lines in the wall of the pipeline.

Generally, pipelines that have D/t greater than about 25 will be controlled by the elastic buckling pressure, P_e . Pipelines that have D/t less than about 25 will be controlled by the yield or ultimate collapse pressures, P_y or P_u .

Test Data Analysis

Fabricated Pipe

The tests on fabricated pipe specimens were used to evaluate the data based on the formulation identified as

Timoshenko Ultimate 4-hinge formulation (Eqn. 10). A statistical analysis of the results is summarized in Fig. 3. The median Bias is $B_{50} = 1.0$ and the COV of the Bias is $V_B = 31\%$.

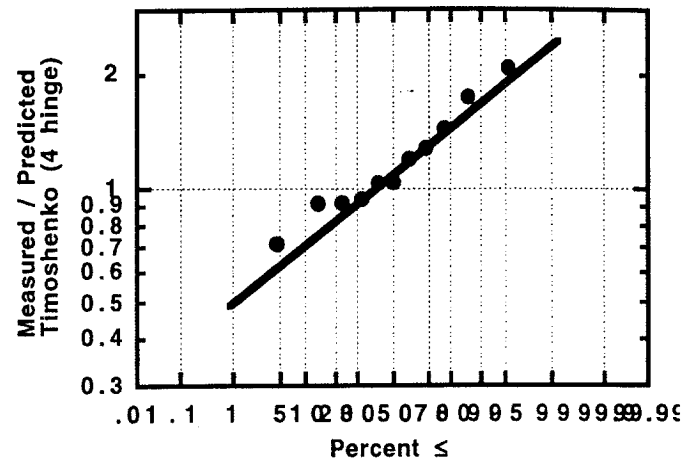


Fig. 3. Statistical analysis of Bias in 4-hinge Timoshenko Ultimate formulation

Seamless Pipe

A database of 74 tests on seamless pipeline test specimens was assembled during this project. The analyses were initially performed using the 4-hinge Timoshenko Ultimate formulation. The formulation substantially over-predicted the collapse pressures. The analyses were then performed using the Timoshenko Elastic formulation. The results are summarized in Fig. 4. The median Bias is $B_{50} = 1.0$ and the COV of the Bias is $V_B = 12\%$.

It is apparent that the residual stresses manufactured into seamless pipe have a deleterious effect on the collapse pressures. It has been proposed that heat treating be used to remove such stresses. If such treatment is used, the Biases determined based on these data would not be appropriate.

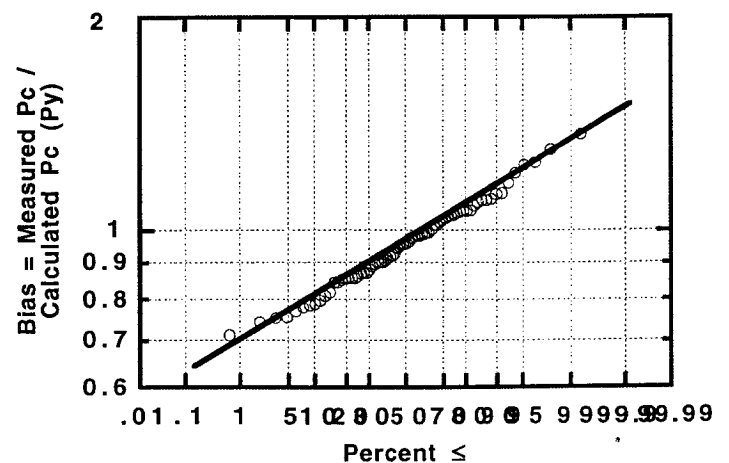


Fig. 4. Bias in Timoshenko Elastic formulation based on results from seamless pipe tests

BENDING, COLLAPSE, TENSION

Formulations for combined loading conditions are summarized in Table 2. These formulations are based on the individual loading condition formulations summarized in Table 1. Background on the test data that was incorporated into this study test database will be summarized in the following parts of this section together with the results of the analyses of Bias based on these data.

Bending & Collapse

Experimental data for tubes under external pressure and longitudinal bending are mainly from research on marine pipelines. Kyriakides et al [15] investigated the collapse of relatively thick walled pipes under combined external pressure and longitudinal bending. The experiments involved testing of drawn tubes stainless steel 304, with $D/t=17.3, 18.2, 24.5$ and 34.7 , nominal diameters of 1.25-in and 1.375-in and L/D ratios between 18 and 24. Material and geometric properties of each tested specimen were recorded prior to testing. Pressure-curvature interaction envelopes have been developed for two different load paths including external pressure followed by longitudinal bending, and longitudinal bending followed by external pressure. Kyriakides et al [15] concluded that the most severe condition is represented by external pressure followed by longitudinal bending. It was also concluded from the tests that the presence of initial ovality combined with inelastic effects led to limit load instabilities for the tubes tested. The collapse mechanism under combined external pressure and longitudinal bending was dependent on the load path, as discussed early. For high values of pressure, collapse followed the attainment of the limit moment. For lower values of pressure, bending beyond the limit moment was possible. For tested pipes, the collapse pressure at a given curvature for the pressure-bending loading path was significantly lower than that for the bending-pressure path.

Fowler [14] conducted combined pressure and bending tests on pipes with nominal outside diameter of 6.625-in and $L/D=8.0$. Initial ovalities were determined as described previously for external pressure loading. Six pipes were tested with pressure applied first followed by bending up to collapse and another six pipes with bending first and then pressure up to collapse. For the criteria development, only the former load path was considered.

Tests for combined external pressure with longitudinal bending were reported by Battelle [11], Yeh and Kyriakides [16], Johns and McConnell [17]. A total of 45 specimens with nominal D/t ratios of 16, 20, 30 and 40 were machined and smoothed to final diameter. Nominal outside diameters were between 1.316-in and 1.428-in. The specimens were made from DOM 1020 steel with yield stresses from 42 ksi to 80 ksi. The range of diameters taken at various angles around the specimens and at various points along the axis of the specimen varied within 0.0005 in which correspond to very small initial ovalities of less than 0.04%.

The Battelle specimens were subjected to bending moments through the use of four point bending fixtures. Pressure was applied to the end capped specimens by placing the bending fixtures in a pressure vessel. The pressure at

collapse for varying degrees of bending was then determined. Two different load paths have been used, pressure followed by bending and bending followed by pressure. The tests data was presented in terms of pressure, bending moment and longitudinal strain at collapse for each test specimen.

Application of the formulation for combined moment and external pressure capacities (Table 2) developed a median Bias of $B_{50} = 1.0$ and COV of the Bias of $V_B = 6\%$ (Fig. 5).

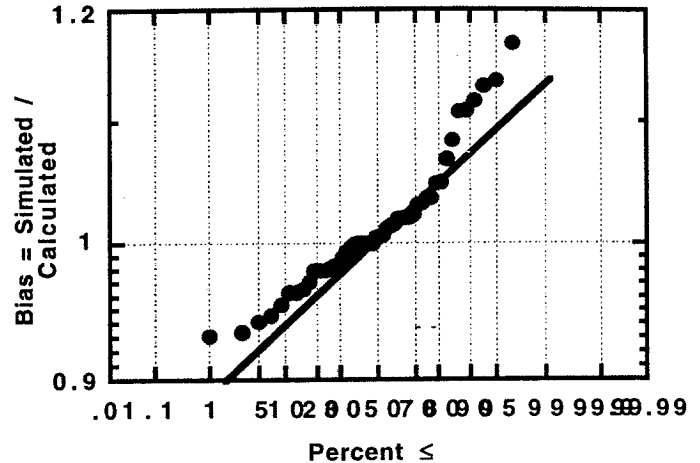


Fig. 5. Bias associated with moment – collapse pressure interaction formulation

Collapse Pressure & Tension

Most of the experimental data for tubes under external pressure combined with axial tension has originated from research on well casings. The experimental programs [18-20]. In addition, Kyriakides et al [15] and Fowler [14] conducted experimental programs on marine pipes under external pressure and axial tension.

Edwards, et al [18] detailed more than 200 tests on pipes subjected to external pressure and axial tension. The specimens had nominal outside diameter of 2-in, D/t between 11 and 22, and $L/D = 15.5$. The tube selected for the tests was seamless steel, with yield stress from 30 to 80 ksi. The specimens were grouped according to the steel grade and D/t ratio. For one set of experiments, the longitudinal yield stress was determined for each group by testing representative strips cut from tubes, and assuming as equal to the stress required to produce a total elongation of 0.5%. For another set of the experimental results, stress-strain curve were prepared and slit-ring tests performed to evaluate residual stresses. Simple open-end collapse strengths were determined for each group with no longitudinal load. For the combined loading tests, the desired tension load was applied first and held constant, while the pressure in the vessel was gradually raised until the specimen either collapsed or stretched. When the specimen had stretched 0.5% of its effective length, the conditions were recorded as "stretch failure". The test results showed that all cases of combined loads resulted in a low collapse strength than that obtained from the isolated external pressure mode. This reduction of collapse strength was more pronounced for thick-wall low

strength specimens than that of thin wall high strength specimens.

Kyogoku, et al [19] conducted experimental tests of full size commercial casings of 40 feet length produced by seamless mill. Hardness tests within wall thickness and slitting tests were carried out to check the presence of residual stresses. The experiments were conducted mainly using no cold rotary straightened casings, because this production technique is commonly applied to obtain high collapse strength casings. Specimens with D/t of 16.2, 20.4, 24.4, and L/D greater than 8, nominal outside diameters between 9.625 and 13.375 in and yield stresses from 89 to 125 ksi. Prior to testing, Kyogoku, et al measured the outside diameters by using an ovality gage and wall thickness by ultrasonic thickness meter. Collapse tests with axial tension were performed for each group. In the test under combined loading, an axial tension load was first applied and held constant while the external pressure was raised up to the collapse. The results confirmed that axial tension stress has no effect on collapse strength for elastic case. If the axial stress increases to the extent of the biaxial yield ranging defined by the Henckey-Von Mises maximum strain energy of distortion, the collapse strength is reduced depending on the axial tension stress.

Tamano, et al [20] conducted collapse tests of commercial casings under external pressure and axial tension. Specimens had D/t between 12 and 16, $L/D = 6.75$, nominal outside diameter of 7 in and yield stresses from 63.7 ksi to 133.4 ksi. Outside diameter and wall thickness were measured at every cross section spaced by one diameter length and at position of every 45 degree in each cross section by caliper and ultrasonic thickness-gage respectively. Residual stresses at the inside surface were determined by the slit-ring tests. Two loading paths were used to perform the experiments, axial load in proportion to external pressure and axial load followed by external pressure. It was confirmed that in the range of elastic collapse the axial tension stress has small effect on the collapse pressure.

Kyriakides, et al [15] conducted small diameter tubes tests. The tubes were of 304 stainless steel material, with D/t between 10 and 40, and L/D of 20. The thickness and diameter were measured at 5 to 10 sections along the specimen length prior to testing. For each tube from which specimens had been generated, stress-strain curves were obtained from axial tensile coupons. It was observed that for cold drawn tubes the anisotropy could be significant. Two different loading paths were used in the Kyriakides, et al tests, with the specimen either loaded by a given axial tension load followed by external pressure up to the collapse or by a certain external pressure and then axial tension. Collapse was characterized by a sudden drop of the pressure inside the test vessel. For the load path axial tension followed by external pressure, 45 specimens were tested. It was observed that for most of the specimens the collapse pattern appeared close to the maximum initial ovality section. Specimens of lower D/t values, tested under very high axial tensile loads, did not fail due to the experimental apparatus capability. The loads in these cases correspond to the highest at which the axial elongation reached the apparatus maximum possible value. Tests of a set of 7 tubes under load

path external pressure followed by axial tension were carried out to investigate the effects of the load path on the interaction curve. It was concluded that this effect was not significant.

Fowler [14] conducted experimental tests of 18 large-scale seamless pipes. With D/t ratios were between 22 and 26, $L/D=17.43$, and nominal outside diameter of 15 in, under combined external pressure and axial tension. Initial ovalities and thickness variation were measured prior to testing. Loading conditions represented by external pressure acting alone (3 tests), axial tension acting alone (3 tests), external pressure followed by axial tension (6 tests) and axial tension followed by external pressure (6 tests) were simulated. The specimens were assembled in the tests vessel and this vessel placed in an external load frame. End caps welded to the specimens and extended beyond the vessel were gripped to apply tension. Collapse results were presented in terms of maximum applied pressure and axial tension load for the combined loading conditions.

Fig. 6 summarizes the results of the Bias analysis of the laboratory test data (57 tests) on combined tension and external collapse pressure capacities of pipelines. These test specimens were all seamless pipe that diameter to thickness ratios of $D/t = 13$ to 38. The median Bias and COV of the Bias of the collapse pressure – tension formulation (Table 2) are $B_{50} = 1.0$ and $V_B = 8\%$, respectively.

Bending & Tension

The development of the pipe test database disclosed only a limited amount of experimental work on axial tension combined with longitudinal bending. Dyau et al [21] reported tests using tubes with a nominal $D/t = 24$ and 35. The loading condition was the bending of the tubes over a stiff, curved surface, in the presence of axial tension. This simulates the condition of a pipe that is bent over a reel. Dyau et al also conducted an analytical investigation for a condition that simulates the combined loading of a suspended length of pipe loaded primarily by gravity load. It was concluded that this loading condition has small effect on the ovalization of the cross section of the tube. It was also concluded that ovalization induced by combined bending and tension depended on the load path and tub geometry and material properties.

Wilhoit et al [22] performed tests of welded steel MT-1010/1020 tubes in combined bending and tension. The specimens' D/t ratios are between 36 and 83. Their L/D ratios and nominal outside diameters are 8.25-in and 20-in. For each D/t , one specimen was tested under pure bending. The other two initially loaded to prescribed axial load (25% or 50% of the axial load capacity) were tested under pressure. Based on the results, it was concluded that the curvature at which buckling occurs in the plastic range under axial tension decreases with D/t up to a point, but increase with the axial tension.

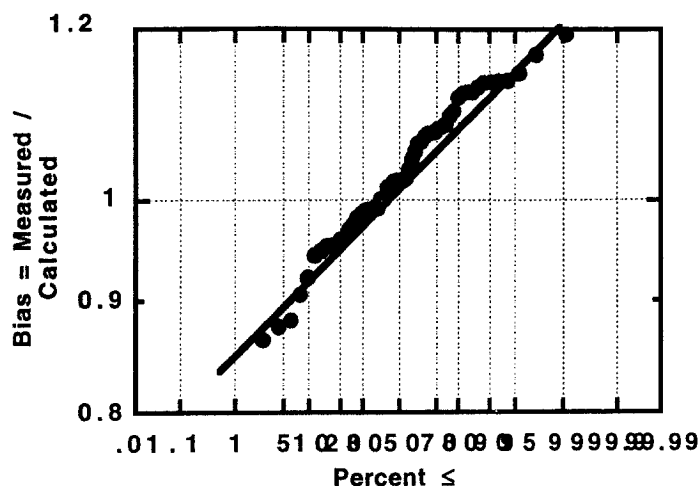


Fig. 6. Bias evaluation for the combined pressure-tension loading

Analysis of the available test data based on the proposed combined loading design formulation (Table 2) indicated a median Bias and COV of the Bias of $B_{50} = 1.0$ and $V_B = 6\%$, respectively (Fig. 7).

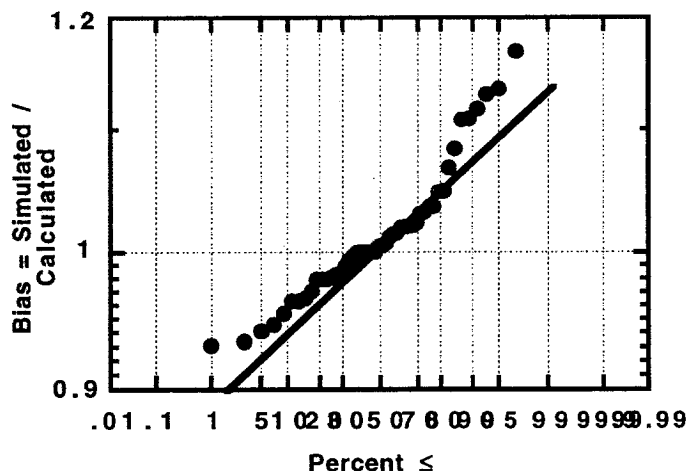


Fig. 7. Bias evaluation for the combined bending-tension loading

Bending, Collapse, Tension

No laboratory test data on combined bending, collapse, and tension loadings could be located and accessed during the development of the test database. The calibrated numerical finite element analysis (FEA) data developed by Igland [12] were used to evaluate the Bias characteristics associated with the proposed combined loading formulation (Table 2).

Fig. 8 summarizes results from the Bias analysis of the proposed formulation (Table 2) for interaction of pipeline tension, bending, and collapse pressure based on the FEA simulation data (127 simulations). The simulations covered a diameter to thickness range of $D/t = 15$ to 35, ovalities of 0.5 % to 0.35 %, X52, X60, and X77 pipe steel characteristics, and a range of residual and circumferential stress characteristics. The

median Bias is $B_{50} = 1.0$ and the COV of the Bias is $V_B = 8\%$, respectively

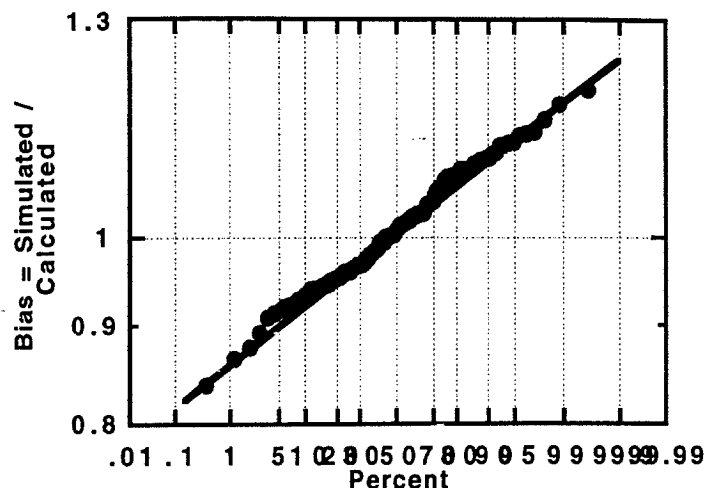


Fig. 8. Bias evaluation for the combined bending-tension - collapse pressure loading

COLLAPSE PRESSURE - PROPAGATING BUCKLING

Propagating buckling is an accidental limit state. The pipeline must be dented and then the external pressures must be sufficient so that the dent can be propagated at pressures lower than those required to collapse the un-dented pipeline. The formulation adopted for use in this study is given in Table 1.

Test data on propagation pressures for aluminum and steel tubes has been developed and analyzed by Estefen, et al [23]. Results from a statistical analysis of the Bias of the proposed formulation based on the data provided by Estefen, et al are summarized in Fig. 9. The median Bias is $B_{50} = 1.0$ and the coefficient of variation of the Bias is $V_B = 8\%$.

Test data on propagation pressures for steel tubes, prototype scale and small scale, have been published by Mesloh, et al [24], Johns, et al [25], and Langner [26]. The full-scale tests were conducted on 12-in diameter Grade X52 line pipe having D/t ratios of 25 and 66. Small-scale specimens with diameters of 2-in [24, 25] fabricated from electric welded mechanical tubing with d/t ratios ranging from 71 to 176 were tested [24,25]. The results from the 12-in diameter pipe specimens were comparable with the results from the 2-in diameter pipe specimens [24]. The data reported by Langner included tests on 6-in diameter Grade X-42 seamless pipe specimens that were 10-ft long. The results of the analysis of the Bias associated with the proposed propagating buckling formulation (Table 1) based on the tests on steel tubes are summarized in Fig. 10. The median Bias is $B_{50} = 1.05$ and the coefficient of variation of the Bias is indicated to be $V_B = 9\%$.

Fig. 11 summarizes results from analysis of Bias associated with the proposed formulation based on results from 12 tests of small scale (4-in diameter) pipelines fabricated from X-42 and X-65 steel reported by Kyriakides [27] and Kyriakides, et al [13, 15, 28]. The median bias is $B_{50} = 0.9$ and the COV of the Bias is $V_B = 12\%$.

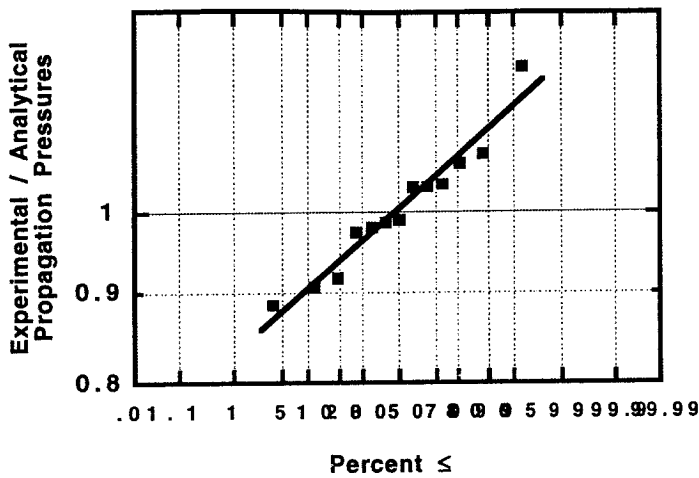


Fig. 9. Bias in predicted propagation pressures based on Estefen, et al [23] test data

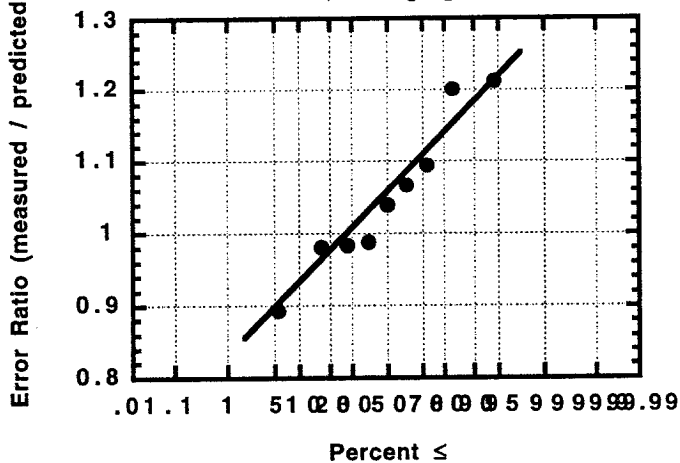


Fig. 10. Bias in predicted propagation pressures based on Mesloh, et al [24] and Langner [26]

Fig. 12 summarizes the test data on the effects of concrete weight coating on the collapse and propagating pressures as a function of the thickness of the weight coating to the steel thickness [24, 26]. The pipelines tested had diameter to thickness ratios in the range of 51 to 111. The concrete coating has the effect of increasing both the initiating or collapse pressure and the propagating pressure by substantial amounts. For a thickness ratio of 10, both the collapse and propagating pressures are increased by a factor of 2. As the thickness of the concrete coating relative to the pipeline wall thickness increases, there is a continued increase in the initiating and propagating pressures. The increase in the propagating pressures can be expressed as:

$$R_{pc} = (tc/ts) / 5 \quad (12)$$

where R_{pc} is the ratio of the propagating pressures with the concrete cover to the propagating pressures without the concrete cover, tc is the thickness of the concrete cover, and ts is the thickness of the pipeline steel.

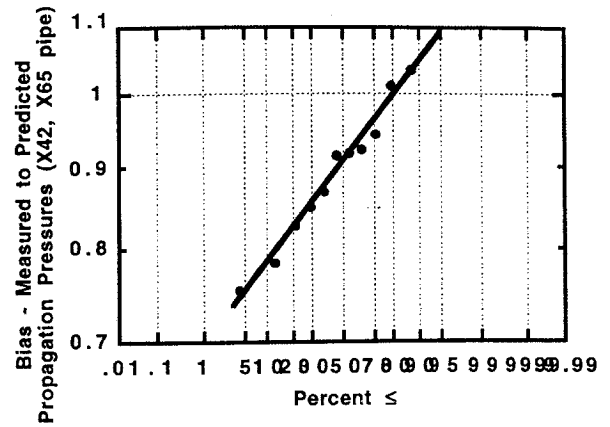


Fig. 11. Bias in predicted propagation pressures for X42 and X65 pipelines

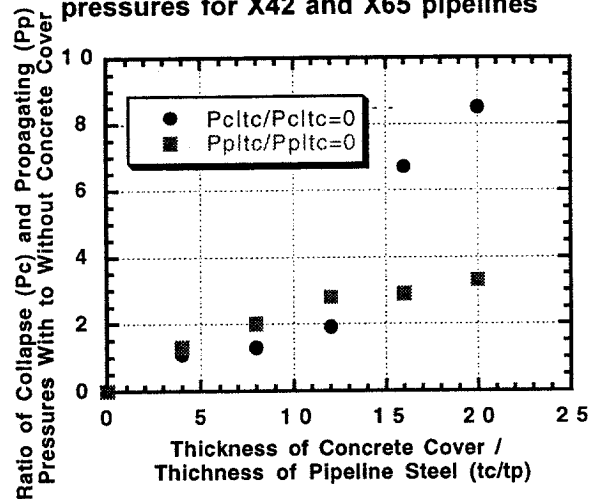


Fig. 12. Effect of concrete cover on collapse pressures and propagating pressures

SUMMARY

Laboratory test data has been used to characterize the Bias associated with the proposed pipeline installation design capacity formulations summarized in Tables 1 and 2. The resultant median Biases and COV of the Biases used in development of the reliability based installation design criteria are summarized in Table 3. Application of these Biases to development of Allowable Stress Design and Load and Resistance Design factors is summarized by Bea, et al [3] and has been translated into installation design guidelines by PEMEX and IMP [2].

ACKNOWLEDGMENTS

The authors would like to express appreciation to Ing. Victor Valdez and Ing. Manuel Gorostieta from PEMEX for their leadership in development of these guidelines. Thanks also are due to Ing. Felipe Díaz for his support and assistance in this project.

REFERENCES

- [1] Bai, Y., 2001, *Pipelines and Risers*, Elsevier Science Ltd., Kidlington, Oxford, UK, 520 p.
- [2] PEMEX Exploration and Production & IMP Mexican Institute of Petroleum, 1998, *Transitory Criteria for the Design and Evaluation of Submarine Pipelines in the Bay of Campeche*, First Edition, March, 1998, Mexico, DF.
- [3] Bea, R. G., Xu, T., Heredia-Zavoni, E., and Lara, L., 2002, "Reliability Based Design Criteria for Installation of Pipelines in the Bay of Campeche, Mexico: Part 1," *Proceedings of the Offshore Mechanics and Arctic Engineering Conference, Safety and Reliability Symposium*, OMAE2002/S&R-28195, American Society of Mechanical Engineers, New York, NY, pp 1-7.
- [4] Sherman D. R., 1986, "Inelastic Flexural Buckling of Cylinders" *Steel Structures: Recent Research Advances and Their Applications to Design*, M.N. Pavlovic (Ed.), Elsevier Applied Science Publishers, New York, NY. pp 339-357
- [5] Sherman D.R., 1984, *Supplemental Tests for Bending Capacity of Fabricated Pipes*, Report Dept. of Civil Engineering, University of Wisconsin-Milwaukee, WI, 153 p.
- [6] Schilling G.S., 1965, "Buckling Strength of Circular Tubes", *Journal of Structural Division*, Vol 91, American Society of Civil Engineers, Herndon, VA, pp 325-348.
- [7] Jirsa J.O., Lee F.H., Wilhoit Jr. J.C., and Merwin J.E., 1972, "Ovaling of Pipelines under Pure Bending", *Proceedings Offshore Technology Conference*, OTC 1569, Society of Petroleum Engineers, Richardson, TX.
- [8] Korol R. M., 1979, "Critical Buckling Strains of Round Tubes in Flexure", *International Journal of Mechanical Science*, Vol 21, New York, NY, pp 719-730.
- [9] Kyriakides S., Corona E., Babcock C. D., and Madhavan R., 1987, *Factors Affecting Pipe Collapse- Phase II*, Prepared for the American Gas Association PR-106-521, University of Texas at Austin EMRL Report No. 87/8, Austin, TX.
- [10] Fowler, J. R., 1990, *Pipe Collapse - Large Scale Tests*, Stress Engineering Services Inc., Report PR-201-818 to American Gas Association, Houston, TX.
- [11] Battelle Memorial Institute, 1970, *Buckling Strength of Offshore Pipelines*, Reports to Offshore Pipeline Group, Vols. I, II, and III, Columbus, OH.
- [12] Igland, R.T., 1997, *Reliability Analysis of Pipelines During Laying Considering Ultimate Strength Under Combined Loads*, Thesis, Department of Marine Structures, The Norwegian University of Science and Technology, Trondheim, Norway.
- [13] Kyriakides S. and Yeh, M.K., 1985, *Factors Affecting Pipe Collapse*, Report to American Gas Association (PRC) for project PR-106-404, University of Texas at Austin EMRL Report No. 85/1, Austin, TX.
- [14] Kyriakides, S., Yeh, M.K., and Roach, D., 1984, "On the Determination of the Propagation Pressure of Long Circular Tubes," *Journal of Pressure Vessel Technology*, Vol. 106, American Society of Mechanical Engineers, New York, pp 150-159.
- [15] Kyriakides S., Corona E., Babcock C.D., and Madhavan R., 1987, *Factors Affecting Pipe Collapse- Phase II*, Report to American Gas Association (PRC) for project PR-106-521, University of Texas at Austin. EMRL Report No. 87/8, Austin, TX.
- [16] Yeh, M. K., and Kyriakides, S., 1988, "Collapse of Deepwater Pipelines", *Journal of Energy Resource Technology*, Vol. 110, American Society of Mechanical Engineers, New York, NY, pp 1-11
- [17] Johns T. G., and McConnell, 1983, "Design of Pipelines to Resist Buckling at Depths of 1000 to 9000 Feet", *Proceedings 11th Pipeline Technology Conference*, Houston, TX.
- [18] Edwards S. H., and Miller C. P. (1939) "Discussion on the Effect of Combined Longitudinal Loading and External Pressure on the Strength of Oil-Well Casing", *Drilling and Production Practice*, American Petroleum Institute, Washington, DC, pp 483-502.
- [19] Kyogoku, T., Tokimasa, K., Nakanishi, H., and Okazawa, T., 1981, "Experimental Study on the Effect of Axial Tension Load on Collapse Strength of Oil Well Casing", *Proceedings of the 13th Offshore Technology Conference*, OTC Paper 4108, Society of Petroleum Engineers, Richardson, TX.
- [20] Tamano, T., Mimura, H., and Yanagimoto, S., 1982, "Examination of Commercial Casing Collapse Strength under Axial Loading", *Proceedings of the 1st Offshore Mechanics and Arctic Engineering Conference*, American Society of Mechanical Engineers, New York, NY, pp 113-118.
- [21] Dyaou J. Y. and Kyriakides S., 1991, "On the Response of Elastic Plastic Tubes under Combined Bending and Tension", *Proceedings of Offshore Mechanics and Arctic Engineering Conference*, Stavanger, American Society of Mechanical Engineers, New York, NY.
- [22] Wilhoit Jr J. C., and Merwin J. E., 1973, "Critical Plastic Buckling Parameters for Tubing in Bending under Axial Tension", *Proceedings Offshore Technology Conference*, OTC 1874, Society of Petroleum Engineers, Richardson, TX.
- [23] Estefen S. F., Souza, A. P. F., and Alves, T. M., 1995, "Comparison between Limit State Equations for Deepwater Pipelines under External Pressure and Longitudinal Bending", *Proceedings of the 16th Offshore Mechanics and Arctic Engineering*, Copenhagen, Denmark, American Society of Mechanical Engineers, New York, NY.
- [24] Mesloh, R., Johns, T.G., and Sorenson, J.E., 1976, "The Propagating Buckle," *Proceedings of the International Conference of Behaviour of Offshore Structures*, Vol. 1, Norwegian Institute of Technology, Trondheim, Norway, pp 787-797.
- [25] Johns, T.G., Mesloh, R.E., and Sorenson, J.E., 1976, "Propagating Buckle Arrestors for Offshore Pipelines," *Proceedings Offshore Technology Conference*, OTC 2680, Society of Petroleum Engineers, Richardson, TX, pp 1-10.
- [26] Langner, C.G., 1974, *Buckling and Hydrostatic Collapse Failure Characteristics of High-D/T Line Pipe*, Technical Progress Report No. 4-74, Pipeline Research and

Development Laboratory, Shell Development Company, Houston, TX, 144 p.

[27] Kyriakides, S., "Propagating Instabilities in Structures," *Advances in Applied Mechanics*, Vol. 30, Academic Press, Inc., New York, NY, pp 67-189.

[28] Kyriakides, S., Corona, E., Mafhaven, R., and Babcock, C. D., 1983, "Pipe Collapse under Combined Pressure, Bending and Tension Loads", *Proceedings Offshore Technology Conference*, OTC Paper 6104, Society of Petroleum Engineers, Richardson, TX, pp 541-550

Table 1. Individual Ultimate Limit State loading condition formulations

Loading States	Formulation	Formulation Factors
Longitudinal • Tension -Tu	$T_u = 1.1 \bullet SMYS \bullet A$	
Transverse • Bending - Mu	$M_u = 1.1 \bullet SMYS \bullet D^2 t \left(1 - 0.001 \frac{D}{t} \right)$	
• Collapse - Pc High ovality fabricated pipe ($f_{50} = 1\%$) Low ovality seamless pipe ($f_{50} = 0.1\%$)	$P_c = 0.5 \{ Pu' + Pe K - [(Pu' + Pe K)^2 - 4 Pu' Pe]^{0.5} \}$ $P_c = 0.5 \{ Pu + Pe K - [(Pu + Pe K)^2 - 4 Pu' Pe]^{0.5} \}$	$Pu' = 5.1 \text{ SMTS } (t / D)$ $Pe = 2 E (t / D)^3 / (1 - \nu^2)$ $K = 1 + 3 f (D / t)$ $f = (D_{\max} - D_{\min}) / (D_{\max} + D_{\min})$ $Pu = 2 \text{ SMTS } (t / D)$
• Propagating Buckling -Pp	$P_p = 39 \bullet SMYS \left(\frac{t}{D} \right)^{2.5}$	

Table 2. Combined Ultimate Limit State loading condition formulations

Loading States	Formulation
Tension & Bending Tu - Mu	$\left[\left(\frac{M}{M_u} \right)^2 + \left(\frac{T}{T_u} \right)^2 \right]^{0.5} \leq 1.0$
Tension & Collapse Tu - Pc	$\frac{P}{P_c} + \frac{T}{T_u} \leq 1.0$
Bending & Collapse Mu - Pc	$\left(\frac{P}{P_c} \right)^2 + \left(\frac{M}{M_u} \right)^2 \leq 1.0$
Tension, Bending & Collapse Tu - Mu - Pc	$\left[\left(\frac{M}{M_u} \right)^2 + \left(\frac{P}{P_c} \right)^2 + \left(\frac{T}{T_u} \right)^2 \right]^{0.5} \leq 1$

Table 3. Summary of Bias characteristics for pipeline installation formulation capacities

Loading States	Median Bias B_{50}	COV of Bias V_B
• Tension -Tu	1.0	0.08
• Bending - Mu	1.0	0.11
• Collapse- Pc fabricated pipe	1.0	0.31
seamless pipe	1.0	0.12
• Propagating buckling - Pp	1.0	0.12
Tu - Mu	1.0	0.06
Tu - Pc	1.0	0.08
Mu - Pc	1.0	0.06
Tu-Mu-Pc	1.0	0.08